SECTION I

RESEARCH IN PROGRESS

Nuclear Theory

H. McManus, G. Bertsch, J. Borysowicz, and P. Hauge

I. Unnatural Parity Excitations of Nuclei (McManus)

A fair number of clearly resolved, accurately measured, unnatural parity excitations have been observed in nuclei via proton inelastic scattering by the experimental group at MSU, and more will be forth coming. For many of these shell model asignments can be made with fair certainty, so there will be a statistically significant body of data to test the components of the nuclear force, non-central as well as central, responsible for these excitations. Preliminary calculations suggest that conventional forces related in some manner or another to the bound state interaction, do not account fully for these excitations. It is possible that two step, particularly (pd)(dp), which P. D. Kunz (Kunz, Colorado preprint) has shown can be important in pn reactions, and exchange currents (though these are estimated by Erickson to give ~30% effects only) play a role. Such limited π scattering data as exists also suggests that simple excitation is not adequate to explain these and the related charge exchange excitations. In this case only exchange currents might be expected to add to the lowest order amplitudes. It seems worth while to continue with a statistical analysis of data to see whether conventional interactions are adequate or not and to establish at least the order of magnitude of effects coming from two-step and exchange currents, as π-scattering data will be becoming available, and also electron scattering testing directly the nuclear configurations involved.

II. Giant Resonances (Bertsch)

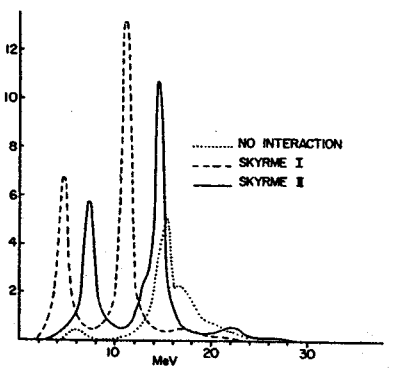

FIG. 1. Quadrupole strength in ^{208}Pb in units of 10^3/π fm^4/MeV. Dotted curve, with the free Green's function $G^{(0)}$; dashed and solid curves, for the Skyrme interactions with the diagonal G^{RPA}. Mesh spacing, 1 fm.

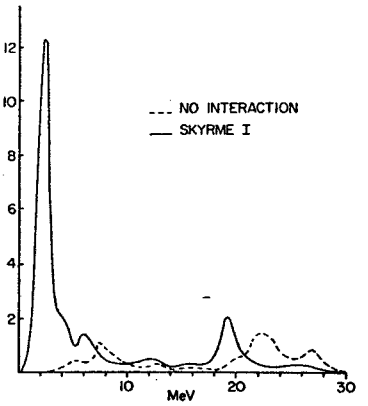

FIG. 2. Octupole strength in ^{208}Pb for Skyrme I interaction in units of 10^5/π fm^6/MeV. Dashed curve, with $G^{(0)}$; solid curve, with the diagonal G^{RPA}. Mesh spacing, 1 fm.

A new calculational scheme is developed for finding the nuclear response to a perturbation of arbitrary form and energy. The traditional method is to first determine the spectrum of the nucleus, and then use the eigenvectors to determine the response. Instead, we use the Green's function directly, solving by matrix inversion. To have matrices of low dimensionality, interactions and Green's functions are represented on a course mesh in configuration space. Skyrme-type interactions can be well described this way. Each curve (see figures) takes about 3-5 minutes of computer time to run, even though the number of configurations is typically 200. Obviously, this will be a useful tool to study core polarization, the effective particle-particle interactions, and imaginary part of the optical potential.

So far the method was applied to ^{208}Pb, and the following properties are found:

(1) The quadrupole strength has a low state and one identifiable as the giant quadrupole;

(2) Excitation with L 2 do not seem to have high energy collective parts;

(3) The giant dipole L=1, T=1 is too low unless the interaction has a strong momentum dependence.

III. Nuclear Mass Formulas (Borysowicz)

(a) Alternative methods other than one used originally by Gerace are investigated to fit the Garvey-Kelson mass formula. The experimental masses are weighted accordingly to the uncertainty in their determination. One method (modified steepest descent) is working well now.

(b) A method is developed to predict nuclear masses using a neighboring region of the mass table. In general the selection of the region is based on the specific position of the considered nucleus. For example only even-even nuclei may be used to predict even-even mass. Compared to the Garvey-Kelson method:

(1) the tedious fit to the whole mass table is avoided.
(2) estimation of the error should be more realistic.
(3) it can be applied to the regions which are too small to use Garvey-Kelson formula (for example Z>N region).

IV. Recoil Effects in Single-Nucleon Transfer Reactions (Hauge and Bertsch)

A formalism has been developed for approximately treating the recoil of the projectile in single-nucleon transfer reactions. We begin by considering a stripping reaction of the form

$$a+A\equiv(b+n)+A\rightarrow b+(n+A)\equiv b+B, \qquad (1)$$

where n is a nucleon that is transferred from the incident projectile a to form the final target B. The notation that we use is similar to Satchler's,[1] and the coordinates needed for specifying the interaction are shown in Fig. 1.

Following the procedure of earlier approximate recoil calculations,[2] we neglect the recoil of the target nucleus, translate the scattered wavefunction of the heavier projectile to a coordinate system centered about the lighter mass projectile, and make a plane-wave approximation to the translation operator. The reduced transition amplitude can then be written as:

$$T_{fi}(\theta)\sim\int d^3r\ \chi^-(\bar{R}_a,\bar{r})\chi^+(\bar{R}_b,\tfrac{A}{B}\bar{r})\int d^3r_1 e^{i\bar{r}_1\cdot\bar{Q}(r)}$$
$$\times[\psi_{\ell_2 m_2}(\bar{r}_2)V(\bar{r}_1)\psi_{\ell_1 m_1}(\bar{r}_1)] \qquad (2)$$

where χ^- and χ^+ are the scattered waves of the incoming and outgoing projectiles respectively, and $\bar{Q}(r)$ is proportional to the local momentum of the heavier projectile.[1]

In an earlier recoil calculation,[2] two further approximations were made, these being (1) approximating $\exp(i\bar{Q}\ \bar{r}_1)=1+i\bar{Q}\cdot\bar{r}_1$, and (2) approximating $\psi_{\ell_2 m_2}(\bar{r}_2)$ by an analytic function that is valid only for weakly bound wavefunctions. Neither of these approximations are made at present. Instead, we evaluate the inner integral of Eq. 2 exactly by using the expansion

$$\exp(i\bar{Q}\cdot\bar{r}_1)=4\pi\Sigma i^{\ell} j_{\ell}(Qr_1)Y^*_{\ell m}(\hat{Q})\ Y_{\ell m}(\hat{r}_1), \qquad (3)$$

and then rotating all functions in the integrand to a coordinate system where $\bar{r}$ is along the $\bar{z}$ axis. The details are given elsewhere.[3]

The theory is presently being applied to light-ion projectiles, and some tentative results have been obtained for three different experimental reactions.[4] In general, it is found that there is a noticeable change in shape between cross sections computed from the "local-energy approximation" in DWUCK and the "Recoil" theory presented here. We also find that although first-order recoil terms (i.e., terms arising from $\ell=1$ in Eq. (3) may be large, higher-order terms are comparatively much less important, and convergence is always easily obtained.

Our formalism can be generalized to multi-nucleon transfer reactions in a straight forward way, and we are presently investigating recoil effects in the three-neutron transfer reaction $^{13}C(^3He,^6He)^{10}C$.[5]

---

1. G. R. Satchler, in "Symposium on Heavy-Ion Reactions", Vol. 1, (Argonne National Laboratory, Argonne, Illinois, 1973), p. 145.
2. M. A. Nagarajan, Nucl. Phys. A196, 34(1972).
3. P. S. Hauge and G. Bertsch, to be published.
4. D. H. Youngblood, R. L. Kozub, J. C. Hiebert, and R. A. Kenefick, Nucl. Phys. A143, 512(1970) R. Doering, Michigan State University, private communication; S. S. Smith, G. Tibell, A. A. Cowley, D. A. Goldberg, H. G. Pugh, W. Reichart, and N. S. Wall, Nucl. Phys. A207, 273(1973).
5. E. Kashy, W. Benenson, I. D. Proctor, P. Hauge, and G. Bertsch, Phys. Rev. C7, 2251(1973).

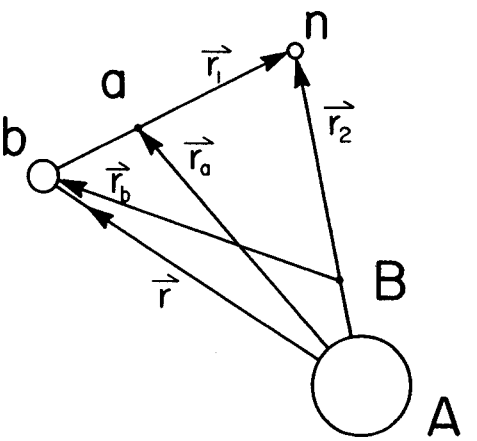

Fig. 1.--Diagram showing coordinates needed for the stripping reaction A(a,b)B where a=b+n and B=A+n.

V. Nuclear Densities from the Electron Scattering. (Borysowicz together with J. Hetherington)

Following the previous work (PR C7, 2295(73)) an attempt is made to remove further model assumptions, while determining nuclear densities. We would like to use a complete (infinite) set of model states and to take explicitly into account the fact that the density is known to be positive defined.

VI. Cluster Model of ^{16}O and Non-Central Interactions in Nuclear Transitions. (Bertsch)

Two projects are being pursued with graduate students. B. Poon is investigating the model of ^{16}O as $\alpha+^{12}C$, using a "realistic" α-α interaction and a model of ^{12}C as rigid triangle of 3α's. We

hope to get reasonable energies and transition rates for the α-like states in ^{16}O. G. Hamilton is using the inelastic scattering code DWBA70, which includes tensor, LS, and exchange interactions, to find nuclear transitions sensitive to the noncentral parts of the interaction. We constructed a realistic interaction by fitting the G-matrix of the Reid potential, and hope to systemize the theory of transition rates induced by the noncentral parts of the interaction. Love[1] has found that LS force plays a large role in certain transitions, and Wagner of this laboratory has found that the tensor force gives most of the cross section in a particular ^{208}Pb transition.

---

1. W. Love, Phys. Letters, 35B, 371(1971).

Reprints

1. Collective Contribution to Escape Width of Analog Resonances, N. Auerbach and G. Bertsch.
2. Effects of Operator Renormalization on Inelastic Scattering Calculations in ^{40}Ca, H. McManus, M. Dworzecka and G. R. Hammerstein.
3. Isospin Impurities in Nuclei, George F. Bertsch and Aram Mekjian (Rutgers University).
4. Shell-Model Study of ^{4}He with Realistic Forces, P. P. Szydlik (State University College, Plattsburgh, New York 12901) and J. R. Borysowicz and R. F. Wagner.
5. Errors on Charge Densities Determined from Electron Scattering, J. Borysowicz and J. H. Hetherington.
6. Three-Neutron Pickup Reaction on ^{13}C, E. Kashy, W. Benenson, I. D. Proctor, P. Hauge and G. Bertsch.
7. Effects of Complex Coupling in Inelastic Cross Sections, Assymetries and Spin Flip in the DWA, R. H. Howell and G. R. Hammerstein, Nucl. Phys. A192, 651(1972).

VII. Core Polarization in Inelastic Scattering

(H. McManus, J. Borysowicz, G. Hammerstein)

Effects of core polarization on the inelastic scattering of protons on nuclei is studied in detail. Both microscopic and collective descriptions are used. In the microscopic treatment we use formalism of effective operators. The calculations of pp' scattering from Ca, Ti, Yt, Zr and Pb isotopes has been done.

Electroexcitation and (p,p') Cross-Section

to Giant Resonances--Microscopic Theory Calculations

G. R. Hammerstein, H. McManus and A. Moalem

Electromagnetic transitions rates, longitudinal (e,e') form factors and (p,p') cross-sections for the Giant Dipole Resonance (GDR) and Giant Quadrupole Resonance (GQR) in ^{40}Ca are being calculated using a microscopic description of these processes. Both the GDR and GQR have been strongly excited by electron[1] and hadron[2] scattering, and have been interpreted within the frame work of phenomenological collective models.[3] These collective descriptions in their simplest form do not provide a link with nuclear structure. In addition another independent estimate of the cross-sections involved is important to supplement and confirm the interpretation made in previous studies.[1-3] The results for the GDR is summarized in the accompanying table.

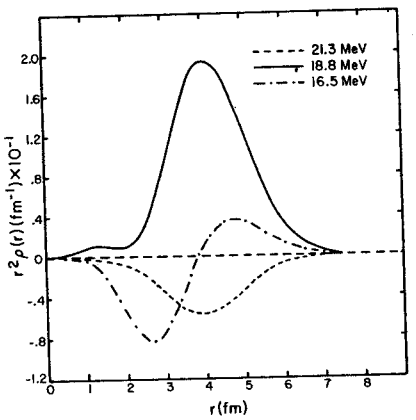

Fig. 1.--S=0 transition densities for $J^\pi = 1^-$, T=1 states in ^{40}Ca.

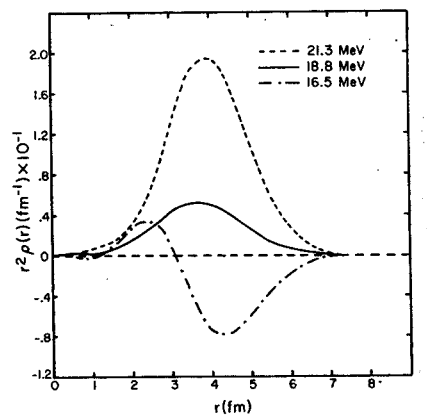

Fig. 2.--S=1 transition densities for $J^\pi = 1^-$, T=1 states in ^{40}Ca.

The model space contains eight 1p-1h excitations from the completely filled s-d shell to the f-p shell. The states which make up the resonance are admixtures of these 1p-1h states and fall in the region 9.5 to 21.3 MeV; each is built primarily on one 1p-1h pair (indicated in column 1

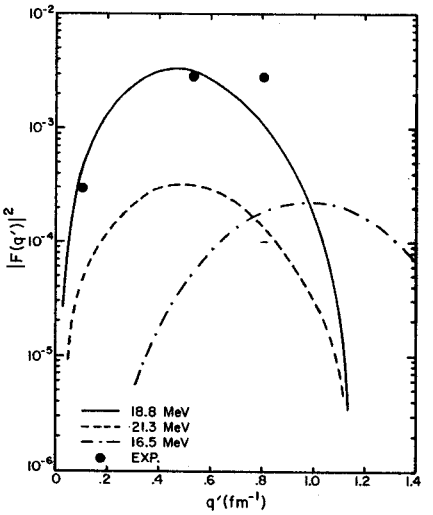

Fig. 3.--Form factors for $J^\pi = 1^-$, T=1 states in ^{40}Ca.

of the table) with the exception of the next to the highest (at 18.8 MeV) which is quite collective.

The transition densities to the two highest states are large, smooth and surface-peaked. For the 18.8 MeV state the S=0 density is three times stronger than the S=1, while for the 21.3 MeV state the reverse is true (see Figs. 1-2). The other states are rather weak and uninteresting for the present study except for the 16.5 MeV, whose S=0 density oscillates; a weak, surface-peaked first maximum goes over to a moderately strong second maximum located well inside the surface.

These features imply the following:

1) The 18.8 MeV state has about 90% of the electromagnetic transition strength and dominates the low momentum transfer electron scattering. The predicted value of the form factor agrees very well with the experimental values extracted for small momentum transfer.[1]

2) At higher momentum the main resonance peak should shift to lower energy and decrease in magnitude due to the fall off of the 18.8 MeV state form factor and increasing sampling of the 16.5 MeV state form factor. (See Fig. 3). However a peak at higher excitation should appear much more strongly, corresponding to transverse excitation of the 21.3 MeV state. Some indications of this can be found in Ref. 4.

3) Inelastic proton scattering is dominated by the 21.3 MeV and 18.8 MeV states. Unlike low momentum transfer (e,e') scattering, the S=1 transition density yields an appreciable contribution to the (p,p') cross-section. Thus the resonance peak taken with protons should be

TABLE I.--Columns 1 and 2 list the main 1p-1h configuration and excitation energy of each state. The B(E1) (in single particle units), and the square of form factors at two values of momentum transfer are given respectively in columns 3, 4, and 5. Columns 6 and 7 list the relative (p,p') cross-sections with RPA and TDA vectors provided by Kuo.[5]

	E (MeV)	B(E1) S.P.U	$\|F(q=.51fm^{-1})\|^2$	$\|F(q=1.03fm^{-1})\|^2$ x10^{-4}	$\sigma_i/\sigma_{Eot.}$ RPA	TDA
$d^{-1}_{5/2}\ f_{5/2}$	21.3	1.76	0.312 x10^{-3}	.215	36	20
$d^{-1}_{5/2}\ f_{7/2}$	18.8	19.10	3.130 x10^{-3}	.958	41	44
$d^{-1}_{5/2}\ p_{3/2}$	16.5	.005	0.047 x10^{-3}	2.22	4	4
$S^{-1}_{1/2}\ p_{1/2}$	14.9	.003	0.077 x10^{-5}	.053	6	5
$d^{-1}_{3/2}\ f_{5/2}$	14.1	.132	0.013 x10^{-3}	.053	3	2
$S^{-1}_{1/2}\ p_{3/2}$	13.0	.076	0.028 x10^{-3}	.049	2	2
$d^{-1}_{3/2}\ p_{1/2}$	12.1	.137	.014 x10^{-3}	.642	3	19
$d^{-1}_{5/2}\ p_{3/2}$	9.5	.005	.003 x10^{-3}	.041	5	4

somewhat higher in excitation energy than that observed in (e,e') scattering at low momentum transfer.

4) The calculated total cross-section with RPA or TDA vectors are the same. However, the relative strength of the various components are different.

5) The total integrated cross-section with RPA vectors is ~6 mb. This value is to be compared with ~3.3 mb obtained for the Jensen-Steinwedel model.[3] Similar calculations for the GQR are in progress.

1. K. Itoh, M. Oyamada, and Y. Torizuka, Phys. Ref. C2, 2181(1970); S. Fakuda and Y. Torizuka, Phys. Rev. Letters 29, 1109(1972), M. Nagao and Y. Torizuka, Phys. Rev. Letters 30, 1071(1973).

2. M. B. Lewis and F. E. Bertrand, Nucl. Phys. A196, 337(1972); M. B. Lewis, Phys. Rev. Letters 29, 1257(1972); A. Moalem, W. Benenson, and G. M. Crawley, Phys. Rev. Letters 31, 482(1973).

3. G. R. Satchler, Nucl. Phys. A195, 1(1972).

4. P. D. Zimmerman, A. R. Yearian and T. W. Donnelly, Phys. Rev. Letters 21, 1392(1968).

5. T. T. Kuo, private communication.

Calculation of Elastic π^--^{4}He Scattering in the Energy Region 50-300 MeV

K. E. Gilbert and J. H. Hetherington

The Los Alamos Meson Physics Facility (LAMPF) will soon make stable high flux pion beams available to nuclear physicists on a routine basis. Consequently, there has been considerable interest in recent years in the π-nucleus interaction. Attempts to calculate elastic π-nucleus scattering using the usual impulse approximation have had moderate success.[1,2,3] However, there still exist serious discrepancies between the theoretical elastic cross sections and existing data. As a result, many workers have questioned the validity of the simple impulse approximation, but so far there has been no systematic theoretical study of effects such as fermi motion, nuclear binding and the proper transformation of the π-nucleon scattering amplitude from the π-nucleon c.m. frame to the π-nucleus c.m. frame.

We have calculated elastic scattering of negatively charged pions from ^{4}He in the energy region 50-300 MeV. We treat the problems of fermi motion, nuclear binding and the π-nucleon scattering amplitude transformation exactly in a simple independent particle model. We have found that nuclear binding effects are very small except in the region of the (3,3) resonance where the elastic amplitude is reduced by 15%. A simple approximation has been developed that adequate describes the binding effects in the resonance region. Fermi motion and the π-nucleon scattering amplitude transformation are treated using techniques borrowed from 3-body theory. Preliminary results indicate that a proper treatment of these two effects considerably improves agreement with experiment.

We are also investigating the sensitivity of elastic π-nucleus scattering to different off-shell parameterizations of the π-nucleon scattering amplitude. In the simple impulse approximation, the effective on-shell π-nucleon force is independent of the off-shell parameterization. However, if fermi motion is taken into account, different off-shell parameterizations give different on-shell π-nucleon effective forces. This can be an important factor since elastic π-nucleus scattering is very sensitive to the on-shell part of the effective force.

1. H. K. Lee and H. McManus, Nucl. Phys. A167, 257(1971).

2. R. Mach, Nucl. Phys. A205, 56(1973).

3. R. H. Landau, S. C. Phatak and F. Tabakin (unpublished).

Nuclear Data Compilations: A=101,102 and 104

L. E. Samuelson,*+ R. R. Todd,**+ W. H. Kelly, Wm. C. McHarris and F. M. Bernthal

We have been revising the 1961 Nuclear Data Sheets for the mass chains A=101, 102 and 104.

The revision for A=101 has been completed and now appears as Nuclear Data Sheets 10, 47 (1973). The abstract of this compilation appears elsewhere in this report.

The A=102 compilation, nearing completion, contains information from approximately 60 publications. There are seven known nuclei for A=102. Only the ground state is known for ^{102}Cd, while the levels in ^{102}Mo are known only from a study of the ^{100}Mo(t,p)^{102}Mo reaction.

The relative positions of the ground and isomeric states of ^{102}Tc are unknown. No γ- rays have been observed from the decay of 5.38-s ^{102}Tc. The situation in ^{102}Rh is somewhat better. The decays of both the 207-d and 2.9-y activities have been extensively studied; however the relative positions of the ground and isomeric states are not known.

The levels of ^{102}Ru have received extensive study via β-decay, γ-decay, Coulomb excitation and the (α,2nγ) reaction. The levels of ^{102}Pd are known primarily from decay scheme studies of the 7.7-m ^{102}Ag isomer and the 12.9-m ^{102}Ag ground state. The placement of the ^{102}Ag isomer is uncertain and depends on indirect evidence.

Our revision of the 1961 Nuclear Data Sheets for A=104 is nearing completion with a projected finishing date of November, 1973. Information is included on eleven members of the A=104 mass-chain extending from ^{104}Zr to ^{104}Tc.

A variety of experiments, in addition to those associated with β-decay, have been performed on the A=104 nuclei. The members of the neutron excess wing, extending from ^{104}Zr to ^{104}Tc, have been studied in fission-fragment experiments, while neutron deficient ^{104}Sn has been studied sparingly with (HI,xn) reactions. Coulomb excitation experiments have been performed on the two stable isobars, ^{104}Ru and ^{104}Pd. In addition, (d,t) and (p,α) reaction experiments and a (p,p') experiment have been done on ^{104}Pd. The former yielded nuclear structure information while the latter yielded energy level placement to complement ^{104}Ag β-decay studies. The odd-odd nucleus ^{104}Rh has been studied extensively using a variety of methods that are associated with neutron capture by ^{103}Rh. A (d,p) experiment has determined some energy levels of ^{104}Rh.

The low-lying levels in the even-even members of the A=104 mass chain seem best described using a vibrational theory. Both ^{104}Ru and ^{104}Pd exhibit E2-enhanced ΔJ=1 γ-transitions between 2-phonon and 1-phonon vibrational states. The ^{104}Rh nucleus exhibits a quite complex level structure with a myriad of low-lying states (at least 44 levels with $J \leq 3$ exist below 1 MeV of excitation). Because the A=104 nuclei can have many active valence nucleons and have several energetically accessible shell-model orbitals, the odd-odd members are expected to exhibit complex level structure.

---

* Nuclear Information Research Associate, 1972-73.

+ Work supported by the National Science Foundation through the National Academy of Science-National Research Council.

** Nuclear Information Research Associate 1971-72. Now at the Department of Physics and Astronomy, Western Michigan University, Kalamazoo, Michigan 49001.

Calculations of the Matrix Elements Connecting Quasiparticle States in Even-Even and Odd-Odd Deformed Nuclei

T. L. Khoo and G. F. Bertsch

Unexpectedly large matrix elements between proton and neutron two quasiparticle states have recently been observed in ^{176,178}Hf.[1,2] We are currently performing calculations to account for these non-zero off-diagonal matrix elements. The single-particle Nilsson wave functions are expanded in a harmonic oscillation basis and the matrix elements between two particle states are then evaluated in terms of two-body matrix elements.[3] There are provisions in the computer program for using any two-body force, including tensor forces, which can be expressed in terms of matrix elements in the relative coordinates of the particles.

We have so far performed calculations for the $K=6^+$ states in ^{176}Hf using:

(a) a δ-interaction $H(\delta) = 4\pi g(\frac{\nu}{2\pi})^{3/2}(1-\alpha+\alpha\sigma_{\underline{1}}\cdot\sigma_{\underline{2}})$, with the force strengths $4\pi g(\frac{\nu}{2\pi})^{3/2} = 5.82$ MeV and $\alpha=0.146$ selected to reproduce the binding energy and the splitting of the Gallagher-Moskowski pairs in the neighboring odd-odd nuclei ^{174,176}Lu;

and (b) interaction matrix elements derived from a realistic (Reid) two-body force, including tensor components, in the Bruekner theory.[3]

The calculated off-diagonal matrix elements for the $K=6^+$ states in ^{176}Hf are shown in Table 1. The agreement with experiment is fair. Results for two neighboring odd-odd nuclei are given in Table 2. Calculations on other odd-odd cases are being performed to ascertain the suitability of the realistic interaction presently employed and to determine an appropriate effective interaction. Other even-even cases will also be investigated.

1. T. L. Khoo, J. C. Waddington, R. A. O'Neil Z. Preibisz, D. G. Burke, and M. W. Johns, Phys. Rev. Lett. 28, 1717(1972); T. L. Khoo, J. C. Waddington and M. W. Johns, to be published in Can. J. Phys.
2. R. G. Helmer and C. W. Reich, Nucl. Phys. A114, 649(1968).
3. G. F. Bertsch, The Practioner's Shell Model (North-Holland, Amsterdam), p. 92 and Chapter 4(1972).
4. J. O. Rasmussen, H. Massmann, T. E. Ward, P. E. Haustein and F. M. Bernthal, preprint (1973).

TABLE 1.--Off-diagonal matrix elements for $K=6^+$ states in ^{176}Hf.

Matrix Element[a]	δ-intrn	Realistic Intrn	Expt.
$\langle\frac{7}{2}n\frac{\bar{5}}{2}p\|V_{np}\|\frac{\bar{5}}{2}n\frac{7}{2}p\rangle_{1-}$	388	163	
$\langle\frac{5}{2}n\frac{\bar{5}}{2}p\|V_{np}\|\frac{\bar{7}}{2}n\frac{7}{2}p\rangle_{0-}$	-268	-92	
$\|\langle p_1p_2\|V\|n_1n_2\rangle_{K=6^+}\|$	299	115	209

[a] $|\langle p_1p_2|V|R_1n_2\rangle| = |(U_{n_1}V_{n_2}V_{p_1}U_{p_2} + V_{n_1}U_{n_2}U_{p_1}V_{p_2})$ $\times \langle n_1\bar{p}_1|V_{np}|\bar{n}_2p_2\rangle - (U_{n_1}V_{n_2}U_{p_1}V_{p_2} + V_{n_1}U_{n_2}V_{p_1}U_{p_2})$ $\times \langle n_1\bar{p}_2|V_{np}|\bar{n}_2p_1\rangle|$ (Ref. 4). The U's and V's are the usual BCS amplitudes; the bar over a subscript denotes the time-reversed orbital.

TABLE 2a.--Splittings of Gallagher-Moszkowski pairs.

Nucleus	Configuration		K^{π}		Splitting		
	Proton	Neutron	$\Sigma=0$	$\Sigma=1$	δ	Realistic	Expt.
^{174}Lu	7/2(404)↓	3/2(521)↑	5^-	2^-	72	41	90
		1/2(521)↓	3^-	4^-	77	121	80
		3/2(512)↓	6^-	1^-	99	35	110
^{176}Lu	7/2(404)↓	7/2(514)↓	0^-	7^-	-395	147	-240
		1/2(510)↑	4^-	3^-	89	117	118

TABLE 2b.--Contributions of n-p residual interaction to the binding energy.

Nucleus	ground state spin	n-p interaction		
		δ	Realistic	Expt.
^{174}Lu	1^-	-432	-309	-421
^{176}Lu	3^-	-367	-305	-473

Realistic Two-Body Matrix Elements for the (sd) - Shell

Sven Maripuu and Gale I. Harris*

The present calculations employ the Sussex matrix elements[1] to derive an effective interaction in the sd-shell model space. The relative harmonic oscillator matrix elements given in Ref. 1 are transformed from LS- to jj- coupling. The Brody-Mosinsky transformation has been performed for b=1.7 fm, presumably the appropriate oscillator length parameter for the (sd)-shell. The two-body matrix elements thus obtained are considered to correspond to the "bare" reaction matrix elements. In order to be used in a small model space they have to be corrected for space truncation effects. We have used perturbation theory up to second order to calculate 3p-1h, $2\hbar\omega$ and 4p-2h corrections. Energy denominators up to $2\hbar\omega$ excitations have been included. The energy denominators have the same oscillator size parameter as the one used in the calculation of the unperturbed matrix elements. We have taken the single-particle energies or one-body interactions from the experimental spectrum of ^{17}O. This approach has also been used by Kuo and Brown.[2] The calculation is thus performed without free parameters.

The two-body matrix elements obtained with the above described method are summarized in Table I. The different columns of Table I show the unperturbed interaction, V, the different perturbative corrections, V_{3p-1h}, V_{4p-2h}, V_{2p}, and the effective interaction, V_{eff}, respectively. The effective interaction, V_{eff}, is taken as the sum of the unperturbed interaction and the different corrections.

Excitation energies in A=18-22 nuclei have been calculated in full 0s-1d model space by using the present two-body matrix elements (and the experimental ^{17}O single particle binding energies). The construction of many-body Hamiltonians and diagonalization of the energy matrices has been performed with the codes described by French, Halbert, McGrory and Wong.[3]

The spectra of ^{18}F and ^{18}O are shown in Figs. 1 and 2. The energy scales used in Figs. 1 and 2 indicate binding energy with respect to ^{16}O. The agreement between experiment and theory is good except for the $J^\pi T=1^+0$ ground state of ^{18}F which is predicted somewhat too high. The calculated and experimental spectra for A=19-22 nuclei (not shown) are all well predicted. The calculated spectra are very similar to those obtained with the Kuo-Brown interaction although a different procedure has been followed. (A detailed comparison has been left out since the Kuo-Brown matrix elements contained some small errors[4]).

In Fig. 3 we have plotted the ground state binding energies for A=19-22 nuclei. For each mass number we have normalized the spectrum to the binding energy of the ground state with lowest isospin. Included are also some levels close to the experimental (or predicted) ground states. It can be concluded from Fig. 4 that for most cases the predicted isospin splitting is somewhat smaller than the observed one. Larger discrepancies are found for the binding energies of ^{21}O and ^{22}O.[5] In general, we also found that the absolute ground state binding energies turned out to be somewhat too large (interaction too attractive), indicating that better agreement would have been obtained with a somewhat smaller oscillator constant. However, it is not clear whether a physically reasonable size parameter will accomplish such an agreement. Furthermore, we find that the inclusion of the 4p-2h corrections greatly improves the isospin splitting. Higher order corrections might remove the remaining discrepancies provided the present model space is reasonable.

---

*Aerospace Research Laboratories, WPAFB, Ohio 45433

1. J. P. Elliott, A. D. Jackson, H. A. Mavromatis, E. A. Sanderson and B. Singh, Nucl. Phys. A121, 241(1968).

2. T.T.S. Kuo and G. E. Brown, Nucl. Phys. 85, 40(1966); T.T.S. Kuo, Nucl. Phys. A103, 71 (1967); G. E. Brown and T.T.S. Kuo, Nucl. Phys. A92, 481(1967); T.T.S. Kuo and G. E. Brown, Nucl. Phys. A114, 241(1968).

3. J. B. French, E. C. Halbert, J. B. McGrory and S.S.M. Wong, Advances in Nuclear Physics, Vol. 2 (Plenum Press, New York, 1970) p. 193.

4. T.T.S. Kuo, in The Structure of Low-Medium Mass Nuclei, edited by J. P. Davidson (University of Kansas, Lawrence, Kansas, 1972) p. 75.

5. A. G. Artukh, et al., Nucl. Phys. A192, 170 (1972).

TABLE 1.--The two-body matrix elements <ab; JT|V|cd; JT>, for the (1s0d)-shell together with the perturbative corrections. The numbers abcd represent $2J_a$, $2J_b$, $2J_c$ and $2J_d$, respectively. All matrix elements are calculated for the oscillator length parameter b=1.7 fm and are expressed in MeV.

a b c d	J T	V	V_{3p1h}	V_{4p-2h}	V_{2p}	V_{eff}
5 5 5 5	1 0	-0.113	-0.314	-0.134	-0.645	-1.206
	3 0	-0.769	+0.097	-0.033	-0.187	-0.892
	5 0	-2.990	-0.149	0	-0.388	-3.527
	0 1	-1.390	-0.587	-0.301	-0.298	-2.576
	2 1	-1.147	+0.099	-0.055	-0.123	-1.226
	4 1	-0.529	+0.336	0	-0.058	-0.251
1 1 1 1	1 0	-2.883	+0.159	-0.075	-0.440	-3.239
	0 1	-2.386	+0.244	-0.006	-0.160	-2.308
3 3 3 3	1 0	-0.043	-0.147	-0.047	-0.549	-0.786
	3 0	-1.861	+0.041	-0.108	-0.360	-2.288
	0 1	-0.034	-0.219	-0.228	-0.302	-0.783
	2 1	-0.297	+0.374	-0.039	-0.063	-0.025
5 1 5 1	2 0	-0.369	+0.060	-0.001	-0.400	-0.710
	3 0	-2.879	-0.285	-0.035	-0.500	-3.699
	2 3	-1.280	-0.027	-0.012	-0.098	-1.417
	3 1	-0.429	+0.455	0	-0.026	-0.000
5 3 5 3	1 0	-3.505	+0.109	-0.849	-0.529	-4.774
	2 0	-3.210	+0.064	-0.542	-0.429	-4.117
	3 0	-1.005	+0.241	-0.120	-0.239	-1.123
	4 0	-3.771	+0.199	0	-0.761	-4.333
	1 1	-0.551	+0.209	-0.003	-0.077	-0.422
	2 1	-0.465	+0.217	-0.025	-0.110	-0.383
	3 1	-0.555	+0.483	0	-0.026	-0.098
	4 1	-2.143	+0.433	0	-0.169	-1.879
1 3 1 3	1 0	-2.126	+0.045	-0.172	-0.386	-2.639
	2 0	-1.345	+0.212	-0.001	-0.522	-1.656
	1 1	-0.452	+0.528	-0.000	-0.015	+0.061
	2 1	-0.655	+0.369	-0.010	-0.125	-0.421
1 1 5 5	1 0	-0.246	-0.169	-0.014	-0.177	-0.606
	0 1	-0.768	-0.207	-0.038	-0.081	-1.904
3 3 5 5	1 0	+2.259	-0.558	-0.068	+0.180	+1.813
	3 0	+0.286	+0.177	-0.059	+0.050	+0.454
	0 1	-3.323	-0.409	-0.179	+0.010	-3.901
	2 1	-0.644	-0.196	-0.032	-0.023	-0.895
5 1 5 5	3 0	-1.005	-0.201	-0.034	-0.226	-1.466
	2 1	-0.601	-0.204	-0.025	-0.070	-0.900
5 3 5 5	1 0	+2.531	+0.004	+0.230	+0.215	+2.980
	3 0	+1.475	+0.220	+0.062	+0.097	+1.854
	2 1	-0.386	+0.049	-0.035	+0.017	-0.355
	4 1	-1.076	-0.252	0	-0.072	-1.400
1 3 5 5	1 0	-0.034	-0.299	+0.088	-0.200	-0.445
	2 1	-0.566	-0.242	-0.013	-0.054	-0.875
3 3 1 1	1 0	-0.408	+0.149	-0.022	+0.119	-0.162
	0 1	-0.627	-0.119	-0.032	-0.065	-0.843
5 3 1 1	1 0	+1.515	-0.191	+0.085	+0.213	+1.622
1 3 1 1	1 0	-0.653	+0.301	+0.090	-0.198	-0.460
5 1 3 3	3 0	+0.105	-0.066	-0.062	-0.110	+0.133
	2 1	-0.804	+0.078	-0.011	-0.037	-0.774
5 3 3 3	1 0	-0.253	+0.203	+0.065	-0.208	-0.193
	3 0	+1.477	+0.292	+0.114	+0.113	+1.996
	2 1	-0.834	-0.153	-0.026	-0.035	-1.048
1 3 3 3	1 0	+0.453	-0.071	+0.043	+0.250	+0.675
	2 1	-0.010	-0.094	-0.020	-0.060	-0.184
5 3 5 1	2 0	-1.243	+0.017	-0.018	-0.281	-1.525
	3 0	+0.809	+0.007	+0.065	+0.098	+0.979
	2 1	-0.161	+0.059	-0.016	-0.065	-0.183
	3 1	-0.047	-0.002	0	-0.011	-0.060
1 3 5 1	2 0	-2.392	+0.159	-0.001	-0.296	-2.530
	2 1	-1.531	-0.010	-0.005	-0.073	-1.619
1 3 5 3	1 0	-0.872	-0.012	-0.321	-0.005	-1.210
	2 0	-1.522	+0.303	-0.022	-0.345	-1.586
	1 1	-0.131	+0.040	+0.000	-0.003	-0.094
	2 1	-0.724	-0.050	-0.012	-0.014	-0.800

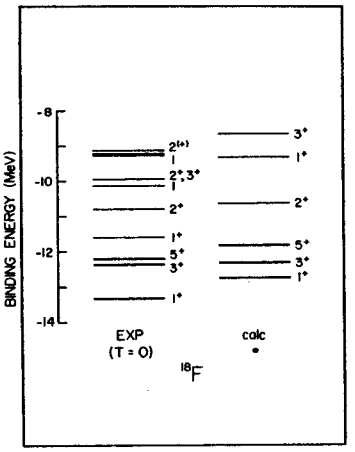

Figure 1

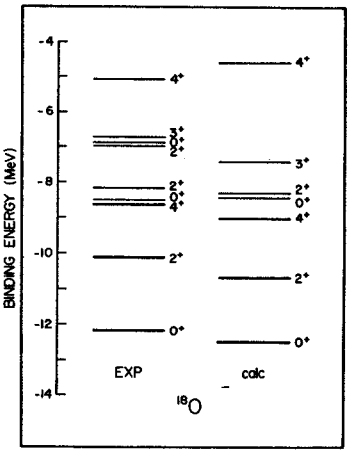

Figure 2

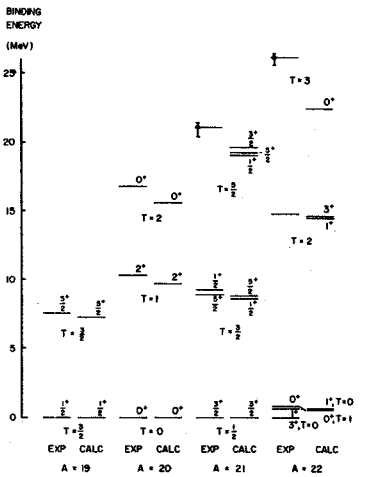

Figure 3

Shell Model Predictions for the Decay Schemes of "Exotic" Oxygen and Fluorine Isotopes

W. A. Lanford and B. H. Wildenthal

There is presently great interest in so called "exotic" light nuclei, that is nuclei far from the line of β-stability. It is now well established that the shell model calculations properly predict most of the features of light (s-d) shell nuclei.[1] In particular, the model predicts spin, parities and excitation energies very well. Recent work[2] has shown that the β-decay schemes can also be successfully predicted. It now seems appropriate to extend the established calculations to nuclei far from the line of β-stability and predict the spectra and β-decay schemes of these nuclei. It is already clear from the experience of the past year that if reasonably good predictions can be made for half-lives and β-decay branching ratios the experimentalist looking for new isotopes can tune their experimental equipment to take advantage of these predictions.

We have calculated wave functions for the oxygen and fluorine isotopes A=18-24. The β-decay half-lives and log (ft)-values have been predicted for the oxygen isotopes. At present we do not have calculations for the heavy Ne isotopes, so predictions of the β-decays of the flourine isotopes cannot be made.

The calculations assume these nuclides can be described by A-16 nucleons distributed over the $d_{5/2}$, $s_{1/2}$ and $d_{3/2}$ shell model orbital. These nucleons can occupy all the Pauli allowed configurations in this shell. The interaction between these nucleons is the same one which was used to describe the nuclei near β-stability with A=18-22.

The predicted excitation energies and β-decay schemes for this nuclei are shown in Fig. 1. The A=19 and 20 decay schemes are included here to show the quality of agreement between the calculation and experiment for cases where experimental information exists. Notice that the predicted excitation energies and β-decay log (ft) values are in excellent agreement.

Of the decay schemes for which there is no present experimental information, perhaps the most interesting are those for A=22 and A=24. Notice that for both these cases there is predicted to be a large gap between the ground state (0^+) and the first excited state (2^+). ^{22}O corresponds to closing the $d_{5/2}$ shell for neutrons; ^{24}O corresponds to closing the $s_{1/2}$ shell. The mass of ^{22}O has been recently reported by a group at Dubna[3] using the $^{232}Th(^{22}Ne,^{22}O)$ reaction. To measure the mass of ^{22}O it is necessary to extrapolate the continuous spectrum of ^{22}O particles down many MeV to the max energy of the spectrum. However if the first excited state of ^{22}O is at 3.22 MeV, the mass they deduced may be the mass as measured to the region of the spectrum where the density of states is reasonably high, i.e. several MeV above the ground state.

By using the calculated log (ft) values, half-lives for this isotope can be predicted. These half-life predictions are given in Table I along with the measured value where available.

1. E. C. Halbert, J. B. McGrory, B. H. Wildenthal and S. P. Pandya, Advances in Nuclear Science, Plenum Press, New York 1971.

2. W. A. Lanford and B. H. Wildenthal, Phys. Rev. C, 668(1973).

3. A. G. Artukh, G. F. Gridnev, V. L. Mikheev, V. V. Volkov and J. Wilczynski, Dubna report JINR-E7 6303 (1972).

TABLE I.--Predicted and Experimental Half-Lives of the Oxygen and Fluorine Isotopes.

Isotope	Calc. $t_{1/2}$	expt. $t_{1/2}$
F^{17}	56	66s
F^{18}	70m	110m
O^{19}	32s	29s
O^{20}	19s	14s
F^{20}	9.1s	11.s
O^{21}	1.2s	--
F^{21}	4.5s	4.5s
O^{22}	.15s	--
F^{22}	3.2s	4.0s
O^{23}	.11s	
O^{24}	.046s	

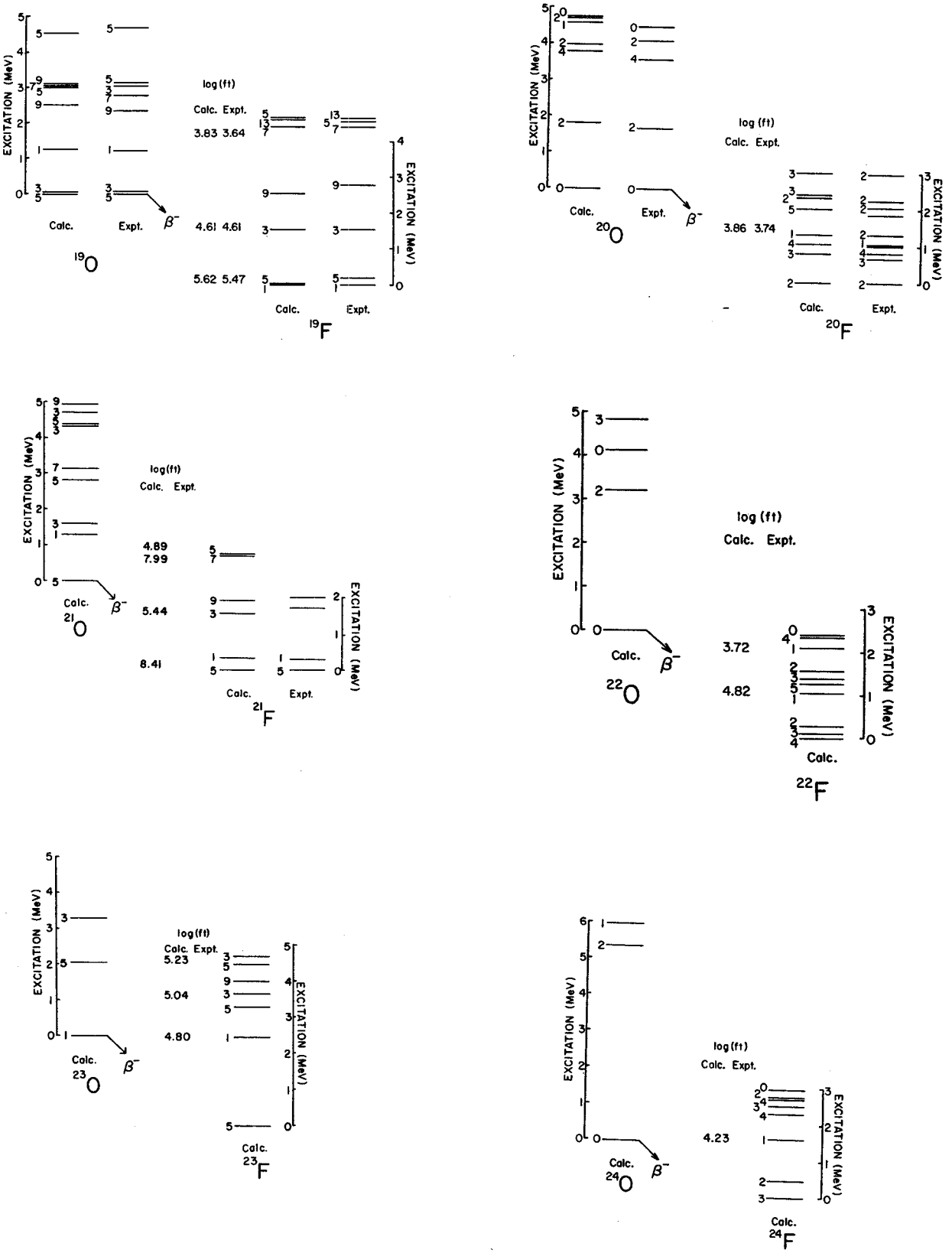

FIGURE CAPTION.--The calculated level schemes and ß-decay transition rates for the oxygen and flourine isotopes. The even nuclei have levels labeled by their spins (J); the odd nuclei have levels indicated by 2J.

Shell Model Study of Potassium and Argone Isotopes

S. Maripuu and A. O. Evwaraye*

Many successful shell model calculations exist up to date. Most of them, however, have been performed within one particular major shell. It seems to be less rewarding to perform calculations for nuclei in mass regions where the nulceon-nucleon interaction crosses a major shell. The phenomenological interactions are less known; the deduction of realistic interactions becomes more difficult due to ambiguities in determining the proper energy denominators. In addition there is the problem of spurious states.

The present investigation has been performed in order to try to study the interaction between nucleons in the upper part of the (sd)-shell and the lower part of the (fp)-shell. The calculations have been performed for K and Ar nuclei in different configuration spaces and with different two-body Hamiltonians.

For most spectra the configuration space includes up to two holes in $d_{5/2}$, $s_{1/2}$ and $d_{3/2}$ orbits, and no more than two particles in the $p_{3/2}$ shell. In some spectra we have also included 4-hole configurations.

Three different Hamiltonians have been used:

1. A realistic interaction, deduced from the Sussex matrix elements and corrected for space truncation effects. Perturbative corrections up to $2\hbar\omega$ have been included in 3p-1h, 4p-2h and 2p diagrams.

2. The modified surface delta interaction (MSDI).

3. The above mentioned realistic interaction modified such that the $d_{3/2}$-$f_{7/2}$ diagonal two-body matrix elements are treated as free parameters. There are altogether 258 of those two-body matrix elements. Eight of them have been fitted to 48 energy levels in A=38-47 nuclei.

We have calculated energy levels, spectroscopic factor for one-nucleon transfer reactions, magnetic moments, M1 transition strengths and log ft values for β-decay for A=38-47 nuclei. Most observables are in reasonably good agreement with predicted values. Some of the results are displayed in Figs. 1-3. In Fig. 1 the experimental spectrum of ^{42}K is compared with the predicted values from the three different two-body interactions. The same quantities for ^{46}K are shown in Fig. 2. The calculated spectroscopic factors for some (d,p)-reactions are compared with experimental results in Fig. 3.

Generally, the realistic interaction and the df-free parameter interaction are in better agreement than the MSDI. The MSDI seems to have trouble when a somewhat larger range of nuclei has to be covered with the same set of parameters.

Many results are as yet preliminary.

*Dept. of Physics, Antioch College, Yellow Springs, Ohio 45387.

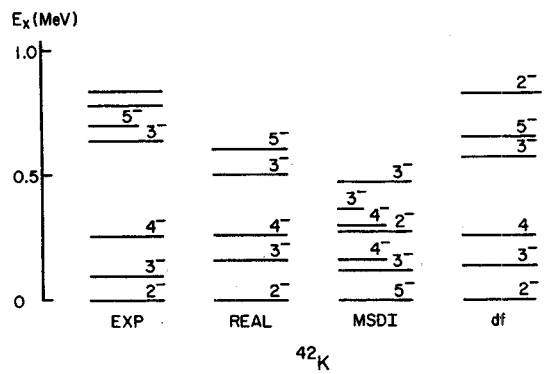

Fig. 1.--The experimental spectrum of ^{42}K as compared with three different predictions (see text).

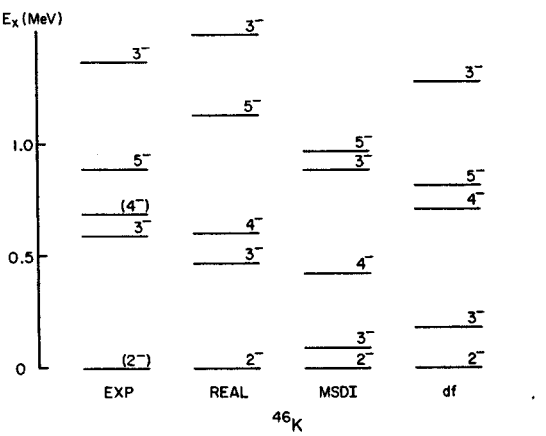

Fig. 2.--The experimental spectrum of ^{46}K as compared with three different predictions (see text).

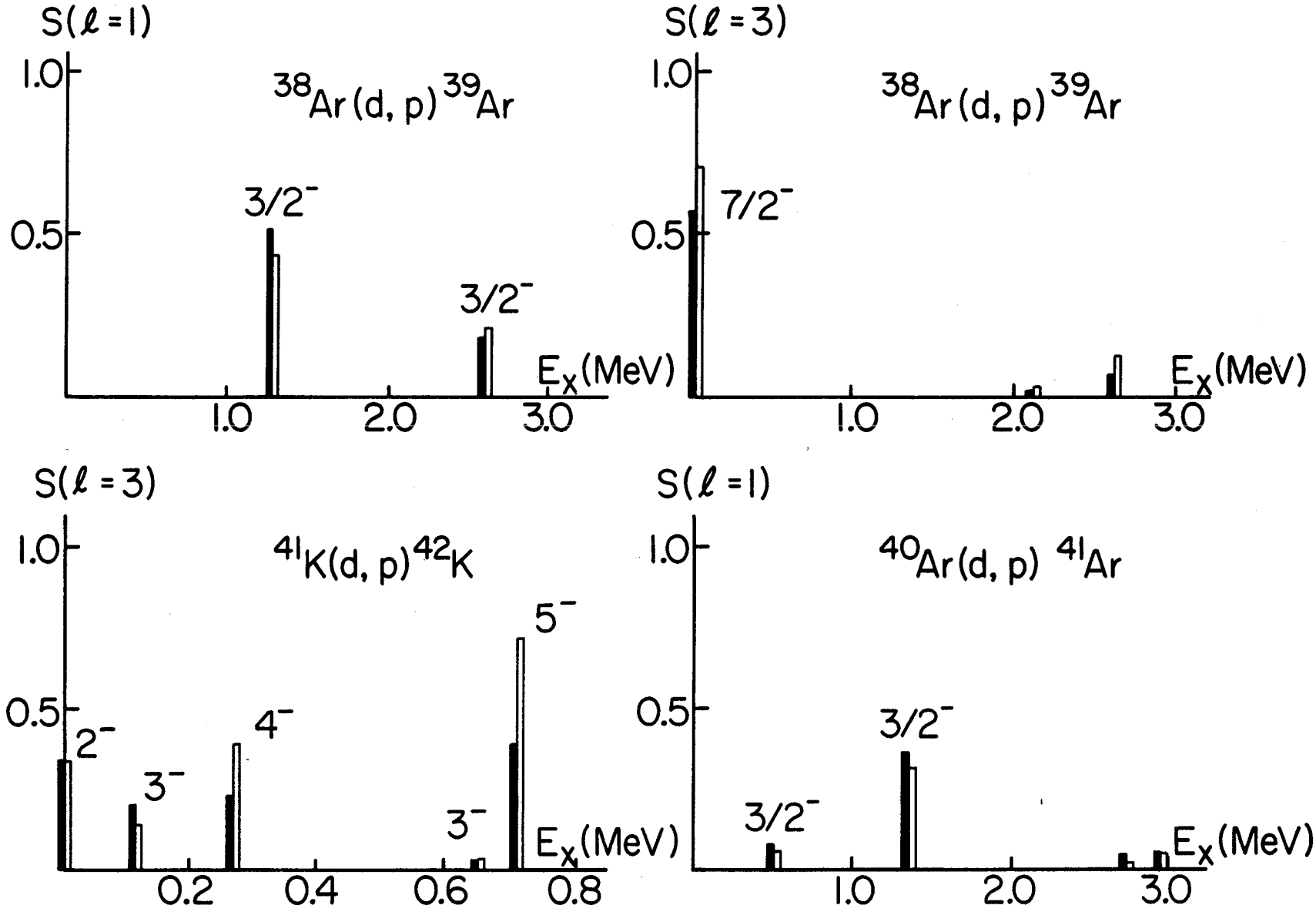

Fig. 3.--Spectroscopic factors for the ^{38}Ar(d,p)^{39}Ar (ℓ=1 and ℓ=3), ^{40}Ar(d,p)^{41}Ar (ℓ=3) and ^{41}K(p,d)^{42}K (ℓ=3) reactions. All predictions have been made with the realistic interaction.

Shell Model Calculations in the A=52-55 Nuclei

Paul S. Hauge and B. H. Wildenthal

Calculations are presently underway to find an effective interaction and basis space for nuclei in the A=52-55 mass region. Limitations in the computer code MULTISHELL[1] allow us to have at most four particles (or holes) in the $f_{7/2}$ shell, and we are therefore forced to carry out all of our calculations in hole formalism.

Several truncated spaces have been considered, and in each case we have determined the effective two-body matrix elements (2BME's) by performing a least-squares fitting to 61 experimental levels in the region. Originally, we included all basis configurations of up to four holes in the $f_{7/2}$ shell and all possible particle excitations to the $p_{3/2}$ orbit. However it was found that the number of basis states for such a truncated space was very small for the A=52 nuclei (5 or less for each JT pair), and increased rapidly with incrementing A, being usually greater than 100 for each JT pair in the A=55 nuclei. Therefore, we imposed a further restriction on the active space by allowing nomore than one particle in the $p_{3/2}$ shell. Table I displays the optimum 2BME's that were obtained from a six-parameter MSDI interaction (four potential parameters plus two single-hole energies), and a 21-parameter fitting where we allowed all relevant 2BME's to vary. The 2BME's that are left blank in the second fitting were not determined because of the limitation of only one particle in the $p_{3/2}$ shell. The r.m.s. deviation between experimental and theoretical levels was 0.55 MeV for the MSDI interaction, and this number was reduced to 0.33 MeV for the 21-parameter case.

In order to see how good our results were, we performed a third calculation on the same nuclei using only the $f_{7/2}$ shell configurations in our active space. It was found that several of the experimental levels well-described in our expanded $f_{7/2}$-$p_{3/2}$ space could not be described as simple $(f_{7/2})^n$ configurations. The r.m.s. deviation was also much higher. On the other hand, we have also found that a few of the experimental levels have definite $p_{1/2}$ or $f_{5/2}$ character, and so we are presently expanding our fitting procedure to allow at least one-particle excitation into both of these shells as well.

TABLE 1.--Effective 2BME's for the $f_{7/2}$-$p_{3/2}$ basis. The quantum numbers for the 2BME's are given in the first column, and the numbers abcd refer to $2J_a$, $2J_b$, $2J_c$ and $2J_d$ respectively. The numerical values of the 2BME's are then displayed in the second and third columns for the two fittings discussed in the text. The two single-hole energies, which were also treated as parameters, are given at the end of the table.

2BME's abcd-JT	6 PARAM MSDI	21 PARAM
7777-01	-2.561	-3.202
10	-2.944	-2.590
21	-0.853	-1.933
30	-2.459	-2.073
41	-0.584	-0.881
50	-2.437	-2.311
61	-0.449	-0.403
70	-2.739	-3.515
7773-21	-0.784	-0.68
30	-0.533	-1.05
41	-0.302	+0.07
50	-0.686	-1.02
7733-01	-1.585	-
10	-0.682	-
21	-0.347	-
30	-0.454	-
7373-20	-2.625	-1.813
21	-1.474	-2.391
30	-2.690	-1.994
31	-0.321	-1.527
40	-2.083	-2.096
41	-0.673	-0.592
50	-3.193	-2.421
51	-0.321	+0.012
7333-21	-0.510	-
30	-0.581	-
3333-01	-1.441	-
10	-2.551	-
21	-0.545	-
30	-2.551	-
S.H.E. ε_7	26.390	27.907
ε_3	24.070	23.907

1. J. B. French, E. C. Halbert, J. B. McGrory, and S.S.M. Wong, Advances in Nucl. Phys., Vol. 2., Plenum Press, New York, 1970, p. 193.

A Study of Giant Resonances by Inelastic Scattering

A. Moalem, W. Benenson and G. M. Crawley

Recent electron and proton inelastic scattering studies[1,2] have given evidence of a localization of the E2 strength in many nuclei at an excitation comparable to the giant dipole resonance (GDR) region. If the E2 strength is localized in a small region of excitation it should show up in inelastic ^{3}He scattering since this process favors collective states. However, the existing ^{3}He inelastic scattering data is very sparse and conflicting. One study[3] showed an enhanced region near the GDR on two heavy nuclei, the other[4] showed no enhancement in light and medium weight nuclei.

We undertook the study of inelastic ^{3}He scattering with the idea of checking very carefully whether the continuum region is in fact enhanced and if so whether the excitation can be proven to be E2. We used 70 MeV ^{3}He-particles and detected them in both the spectrograph (using a wire counter) and in a scattering chamber with silicon detectors. We studied 12 targets ranging throughout the periodic table from ^{16}O to ^{209}Bi. In every case we observed the enhancement of the continuum expected for the giant quadrupole resonance. Figure 1 shows some of the spectra obtained at 22°. We were unable to prove positively the E2 nature of the excitation. Angular distributions at this energy appear to be forward peaked and independent of L-transfer. Some results have been published.[5] The main conclusions can be stated as follows: (1) All spectra exhibit qualitatively the same characteristics as were observed in (e,e') and (p,p'). The width of the observed structure is considerably broader than the GDR and the main strength lies 2-3 MeV below it. (2) For lighter nuclei $A \leq 58$ the spectra exhibit a considerable amount of fine structure. For heavier nuclei the enhancement consists of a smooth single asymmetric bump. (3) The energy centroid of the structure appears to follow the rule predicted by the hydrodynamic model ($E \sim 60A^{-1/3}$) for an E2 state. (4) The cross section is A dependent increasing with increasing A. For heavier elements the magnitude exhausts the E2 sum rule limit. For light elements it is not possible to estimate the magnitude properly since the yield is spread out over so much of the continuum.

The fine structure of the giant resonance region in light nuclei is particularly interesting, and it is now the subject of further studies. The details of the structure can be compared with results from a variety of photonuclear and electro-excitation studies. ^{16}O is a very good example of this. The E2 strength observed in ^{12}C(α,γ) shows up as strong peaks in the data as can be seen in Fig. 2. Many of the E1 states show up as well but with less strength. It remains now to reproduce the structure with a calculation that takes into account both the GQR and the GDR.

Experimentally, we plan to study a similar excitation energy region in some of the same nuclei with 50 MeV α-particles to examine the isospin of the enhanced regions. If the proposed new state is of an isoscalar type it should be excited more strongly relative to the isovector GDR. An experiment investigating proton decays of the GQR in ^{40}Ca is already in progress.

---

1. S. Fukuda and Y. Torizuka, Phys. Rev. Letters 29, 1109(1972); M. Nagao and Y. Torizuka, Phys. Rev. Letters 30, 1071(1973).
2. M. B. Lewis and F. E. Bertrand, Nucl. Phys. A196, 337(1972).; M. B. Lewis, Phys. Rev. Letters 29, 1257(1972).
3. G. Chenevert, N. S. Chant, I. Halpern, C. Glashausser and D. L. Hendrie, Phys. Rev. Letters 27, 434(1971); G. Chenevert, Ph.D. Thesis, University of Washington, 1969 (unpublished).
4. R. J. Peterson, Nucl. Phys. A202, 557(1973).
5. A. Moalem, W. Benenson and G. M. Crawley, Phys. Rev. Letters, 31, 482(1973).

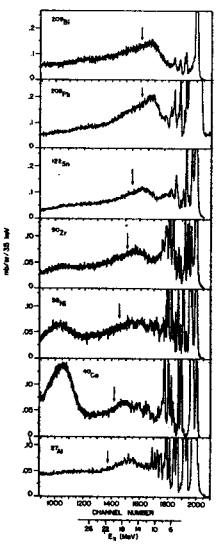

Fig. 1.

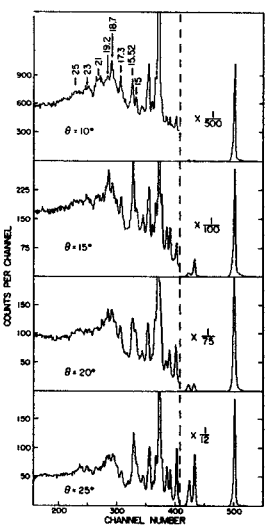

Fig. 2.

FIGURE 1.--Spectra from the (^{3}He,^{3}He') reaction on ^{27}Al, ^{40}Ca, ^{58}Ni, ^{90}Zr, ^{122}Sn, ^{208}Pb, and ^{209}Bi at 20°. The arrow indicates the position of the GDR as determined from photonuclear experiments. The broad peak near channel 1000 is due to elastic scattering from hydrogen.

FIGURE 2.--Spectra from the ^{16}O(^{3}He,^{3}He')^{16}O reaction. The position of known $J^\pi=1^-,2^+$ states in the GDR region are also indicated.

The $^{40}Ca(p,p')^{40}Ca$ Reaction at 35 MeV

J. Nolen, A. Moalem, T. Udagawa,* R. Gleitsmann, G. Hamilton, and H. McManus

A high resolution study of the $^{40}Ca(p,p')^{40}Ca$ reaction is in progress. This process was studied previously in this laboratory by Gruhn, et al.[1] but was limited to a resolution of 30 keV and several pairs of levels could not be resolved. These unresolved levels are the origin of our interest in this matter, and our objective is to obtain a reasonably complete picture of their nuclear structure. Also we attempt to solve some of the discrepancies noted in Ref. 1 between microscopic theory analyses and experiment. The new data, being recorded on nuclear emulsions in the split-pole magnetic spectrograph, are now in preliminary stages of analysis. A sample spectrum obtained at a scattering angle of 15° is shown in the figure. The experimental resolution is 4-4.5 keV, FWHM, which is adequate to resolve most of the states of interest up to about 10 MeV excitation energy.

The primary interest in the previous (p,p') calculation was in the states which were primarily of the $f_{7/2}$-particle, $d_{3/2}$-hole configuration. These states have spins 2^-, 3^-, 4^-, 5^- and isospin 0 and 1. The largest discrepancy in this analysis, which was in the 4^- T=0 and T=1 states is now seen to be at least partially due to contributions from previously unresolved nearby levels. The remaining discrepancy of about a factor of five in the 4^- T=0 and a factor of two in the 4^- T=1 level can possibly be removed by a modification of the tensor component of the nucleon-nucleon force used in the calculation.[2]

The role of multiple excitation is also being investigated for the 0_2^+ (3.35 MeV), 1_1^- (5.90 MeV), 2_1^- (6.03 MeV), 3_2^- (6.29 MeV) and 4_1^- (5.62 MeV) states. Simple coupling schemes which include the first excited 2_1^+ state and first octupole 3_1^- states are considered, i.e.,

$$0_1^+ \xrightarrow{0.1} 2_1^+ \xrightarrow{0.3} 0_2^+$$

and

$$0_1^+ \begin{matrix} \xrightarrow{0.1} \\ \xrightarrow[0.3]{} \end{matrix} \begin{matrix} 2_1^+ \\ 3_1^- \end{matrix} \xrightarrow[0.1]{0.3} I^- \qquad (I=1,2,3,4)$$

The deformation parameters which characterize the transition strengths are indicated and have been taken fron Ref. 3. Preliminary results show that multiple excitation is important for inelastic excitation of the 0_2^+ and 1_1^- levels (about 50% and 100% of the experimental cross-sections respectively). The calculations are being performed with the computer code JUPITOR.[4]

---

*Visitor at MSU during July, 1973. Permanent address--University of Texas, Austin, Texas.

1. C. R. Gruhn, T.Y.T. Kuo, C. J. Maggiore, H. McManus, F. Petrovich and B. M. Preedom, Phys. Rev. C6, 915(1972).
2. F. Petrovich and H. McManus, private communication.
3. J. R. MacDonald, D. H. Wilkinson, and D. E. Alburger, Phys. Rev. C3, 219(1971).
4. T. Tamura, ORNL-4152, unpublished.

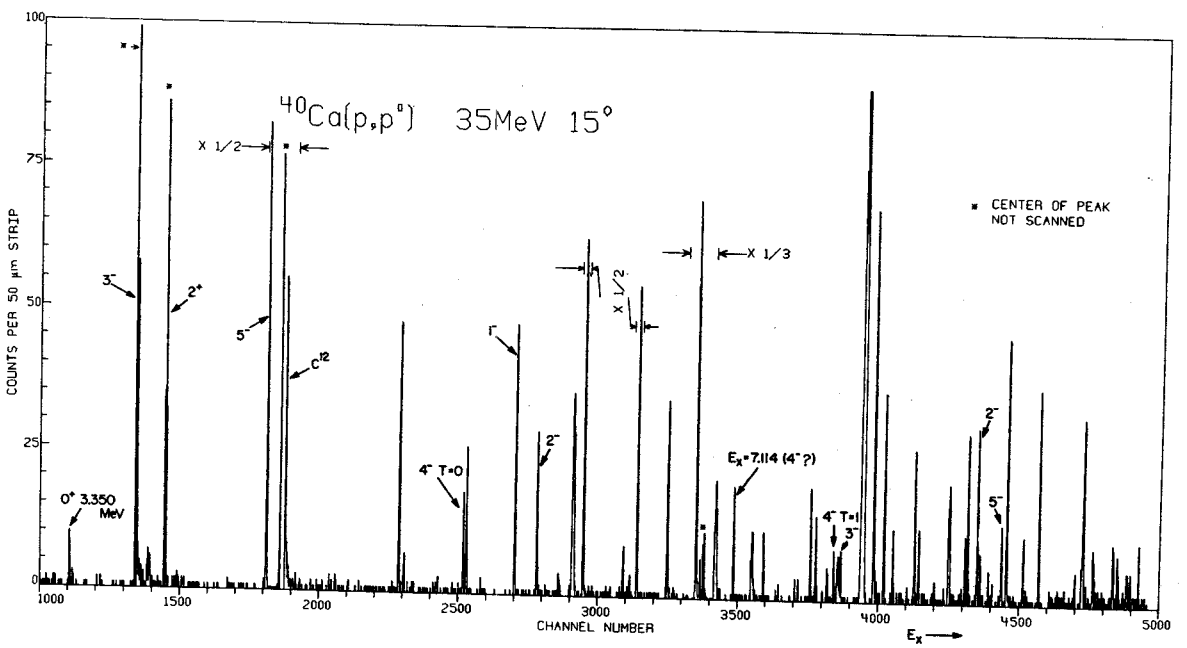

High Resolution Study of the Pb and Bi Isotopes

W. T. Wagner and G. M. Crawley

With the recent experimental improvements in energy resolution, many new and interesting levels can now be studied which were previously inaccessible at intermediate energies. Using ultra-high resolution proton inelastic scattering we are currently investigating the nuclei ^{207}Pb, ^{208}Pb, and ^{209}Bi. This study should allow extensive testing and possibly extension of the considerable theoretical work already carried out in this mass region.

Data has been taken on nuclear emulsions with a resolution of 5 to 8 keV (FWHM) at 35 MeV. The Michigan State University spectrometer-cyclotron high resolution system and an on-line resolution monitoring technique[1] were used. Angular distributions were taken from 10 to 100 degrees. Numerous levels were observed up to an excitation energy of 8 MeV and discrete states were seen up to about 7.5 MeV excitation. A typical spectrum is shown in Fig. 1. Data of 45 to 80 keV (FWHM) resolution was taken with a position sensitive proportional counter in the spectrometer to study the collective states with improved statistics and to normalize the plate data. Because of the necessity to scan in fine steps the plate scanning has proven to be a severe time limitation and thus far only the ^{208}Pb data is near completion.

Every spectrum recorded is dominated by the highly excited octupole level at 2.615 MeV of excitation as well as the first excited 2^+, 4^+, 5^-, and 6^+ levels. The preliminary results of the plate data analysis is shown in Fig. 2 for some of these states. The cross section in mb/sr is plotted against the center-of-momentum scattering angle. The solid line is a collective model fit to the data using the Becchetti-Greenlees optical model parameters.[2] The reduced transition probabilities obtained from these fits are in good agreement with values previously measured in low energy experiments but are consistently larger than the values determined in a 61 MeV (p,p') experiment.[3] This discrepancy is probably not due to exchange phenomena since the optical model parameters used in the collective model implicitly account for some exchange effects.

Microscopic model predictions for inelastic cross sections can be obtained without knowledge of the wave functions provided the nuclear transition density is known. The wealth of (e,e') data for ^{208}Pb provides this information for a number of different multipolarity transitions. Thus, without ambiquities in the nuclear motion a critical study of the nucleon-nucleon interaction can be made.

The dashed curves shown in Fig. 2 present microscopic model calculations using the Random Phase Approximation wave functions of Gillet, et al.[4] Both central and non-central forces were used and exchange was treated exactly in the calculations using the code DWBA70 of Schaeffer and Raynal. For each state these predictions underestimate the data. This is consistent with the anomalously small electromagnetic transition rates obtained with these wave functions. However, in the microscopic model poor agreement between the experimental and theoretical electromagnetic properties does not imply that the measured and predicted cross sections will be in poor agreement. The converse is also true. Hence, one "unique" aspect of the many wave functions for ^{208}Pb can be examined.

The third figure illustrates cross sections for some of the non-normal parity states which were observed. Spin and parity assignments were adopted from published results. The calculations were performed with the wave functions of True, et al.[5] and with central (dashed curves) and with central plus non-central forces (solid curves). For each case, the curves labeled D or D+E correspond to the direct or the direct-plus-exchange calculations, respectively. For the normal parity transitions the introduction of non-central forces provided little enhancement of the pure central result, perhaps 10 to 20 per cent. For the non-normal parity states the non-central forces are apparently the primary mediators of the excitations. The two 4^- states are interesting since each wave function is believed to be well known and is probably either a proton or a neutron configuration. Different portions of the non-central effective interaction can thus be probed. In each case the data is underestimated and the tensor force makes a much greater contribution to the cross section than the $\underline{L}\cdot\underline{S}$ force. Some knowledge of the small T=0 portion of the tensor interaction may be gained by this study. Coupled Channels calculations indicate that the two step processes via the highly excited 3^- or 2^+ levels is not important.

With this study of ^{208}Pb as a basis the ^{207}Pb and ^{209}Bi data should allow extension of the weak coupling and core polarization models to unstudied regions of excitation energy and multipolarity in the mass region.

---

1. H. G. Blosser, G. M. Crawley, R. deForest, E. Kashy, and B. H. Wildenthal, Nucl. Instr. and Methods 91, 61(1971).

2. F. D. Becchetti and G. W. Greenlees, Phys. Rev. 182, 1190(1969).

3. N. P. Mathur, Thesis, Univ. Delhi (1969).

4. V. Gillet, A. M. Green and E. A. Sanderson, Nucl. Phys. 88, 321(1966).

5. W. W. True, C. W. Ma and W. T. Pinkston. Phys. Rev. C3, 2421(1971).

Figure 1

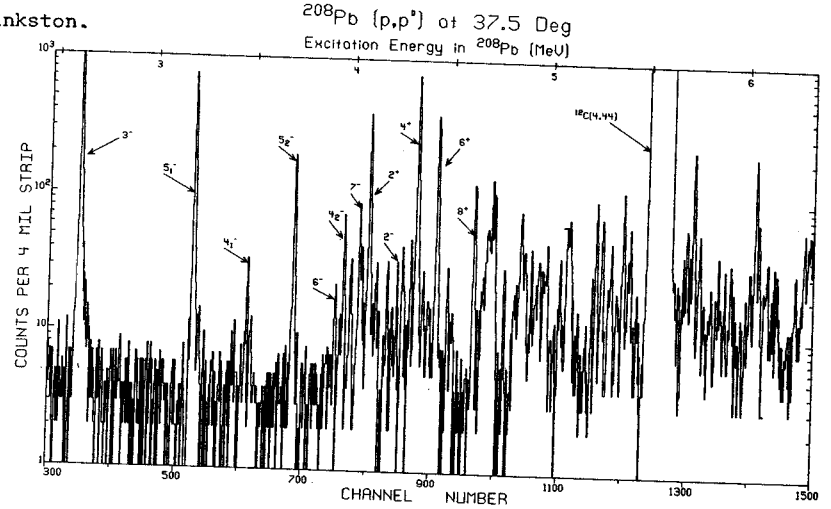

Figure 2

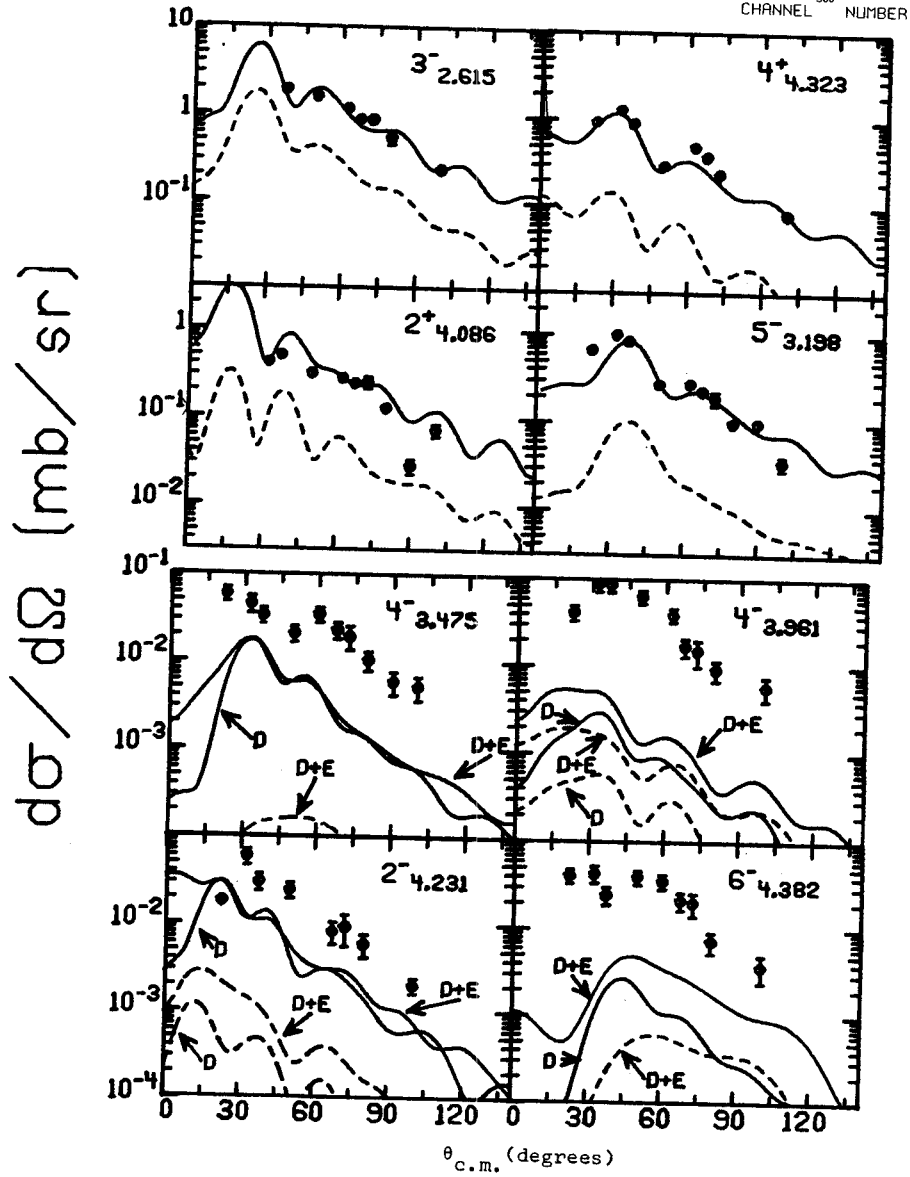

Figure 3

Collective States of Actinide Nuclei from Inelastic Proton Scattering*

J. S. Boyno, J. A. Nolen and Wm. C. McHarris

We have initiated a program to study the collective states of actinide nuclei via inelastic proton scattering. Previous work in this field,[1,2] done with 18 MeV deuterons, has shown that ground rotational bands, β- and γ-vibrations, and octupole vibrational states are all strongly excited in inelastic scattering, and that meaningful information about level energies, spins and parities can be extracted from such measurements. In addition, it has been shown[1,2] that B(Eλ) for the excitation of strong states can be obtained from cross section measurements.

Using the dispersion matched magnetic spectrograph system with the "resolution meter"[3] system, we should be able to produce very high resolution spectra with good peak intensities.

The first run in this program was performed with a thin ($\leq 100\ \mu g/cm^2$) ^{238}U target bombarded with 35 MeV protons from the MSU cyclotron. The resolution obtained was poor, ~25 keV FWHM. This was due to several experimental problems which developed in the use of the "resolution meter". We believe we have corrected these problems and we expect to greatly improve the resolution of these reactions in subsequent runs.

---

*Supported by USAEC and NSF.

1. Th. W. Elze and J. R. Huizenga, Nucl. Phys. A187, 595(1972).

2. J. S. Boyno, Th. W. Elze, J. R. Huizenga and C. E. Bemis, jr., Nucl. Phys. A209, 125(1973).

3. H. G. Blosser, G. M. Crawley, R. Deforest, E. Kashy and B. H. Wildenthal, Nucl. Inst. and Meth. 91, 61(1971).

A Search for $T=T_z+2$ Resonances in Heavy Nuclei

P. A. Smith, G. M. Crawley, T. L. Khoo and P. S. Miller

Prior to August, 1971, when Hoffmann, et al.[1] reported the observation of the T=23 state in ^{210}Po, double analog states, i.e. states with $T=T_z+2$, had not been seen except in light nuclei. To date no other double analog states have been found in heavy nuclei.

In light nuclei states with $T=T_z+2$ can be excited by direct reactions such as (p,t). However, the ratio of the cross sections for $T=T_z+2$ states to $T=T_z$ states in the same nucleus goes approximately as T^{-2}.[2] Thus in heavy nuclei, these direct reactions are greatly inhibited. It is more profitable to look for these states where T is large by isospin forbidden reactions such as $p+^{209}$Bi, where the statistical factors are more favorable. This reaction is made possible by isospin mixing with the high density of nearby $T=T_z+1$ states.

Hoffman, et al., recognized that the double analog state will preferentially decay in an allowed manner by the emission of two protons, as shown in the figure for ^{208}Bi. This suggests that one should look for enhancement in the summed coincidence spectrum as the bombarding energy is moved across the resonant energy.

In the previous experiment two E-veto telescopes were set up opposing each other and perpendicular to the beam. Enhancement is the summed coincidence spectrum was observed in the $E_1+E_2=24$ MeV energy region.

The reaction $p+^{209}$Bi to the T=23 state in ^{210}Po may not be the most favorable case because of the spin statistical factor. The reaction $p+^{207}$Pb to the double analog of ^{208}Tl in ^{208}Bi might be more favorable since the ground state spin of ^{207}Pb is 1/2 as compared to 9/2 for ^{209}Bi. The reactions ^{3}He + ^{205}Tl and ^{3}He + ^{207}Pb to these same states might be even easier to observe since the ratio of true proton coincidences to chance coincidences should be larger.

We have studied the reaction ^{207}Pb(p,2p) by looking for coincident protons in two ΔE-E-veto telescopes. This arrangement allows us to identify the protons, which was not done previously, and to eliminate the elastic protons from the chance spectrum. The number of elastically scattered protons is also kept to a minimum by placing each telescope 105° from the beam. The chances with this arrangement come primarily from the $(p,n\bar{p})$ reaction.

To check that the system is working correctly p-p scattering is observed using a Kapton[3] target. Time resolution of 3 ns. has been obtained.

No enhancement has been observed as yet. We set an upper limit on the cross section of 2μb/sr.[2] This upper limit is approximately 10 times larger than the cross section found by Hoffman, et al. Since the spin statistics are approximately forty times more favorable in our case, it is puzzling that we have not observed the resonance. More sensitivity is needed.

The telescope requirement prevents us from obtaining larger solid angles with solid state detectors. To overcome this difficulty we are building and testing two scintillator telescopes.

---

1. G. W. Hoffmann, G. J. Igo, C. A. Whitten, Jr., W. H. Dunlop, J. G. Kalleck, Phys. Rev. Letters, 28, 41(1972).

2. J. P. Schiffer, in Isospin in Nuclear Physics, edited by D. H. Wilkinson (North-Holland, Amsterdam, 1969), p. 667.

3. E. I. DuPont, DeNemours and Company.

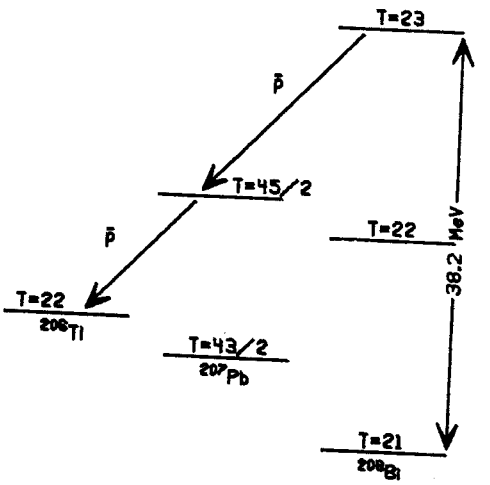

Neutron Time-of-Flight Program

J. G. Branson, R. R. Doering, A. Galonsky, and D. M. Patterson

A. Equipment Improvements

During the past year we have rearranged our neutron time-of-flight apparatus in order to cover a larger angular range with a longer flight path. At present we can go from 10° to 160° with a 5 meter flight path. Longer flight paths are available over a restricted angular range. A separate target station, followed by a 20° bending magnet, enables us to observe neutrons at 0°.

While doubling the neutron flight path improves our energy resolution by about a factor of two, it also reduces the solid angle by a factor of four. In order to compensate for this loss of overall efficiency, we have assembled a new neutron detector which has 4 1/2 times as much liquid scintillator as the old detector. The new detector consist of a 3 inch diameter by 1 1/2 inch thick glass encapsulated NE213 liquid scintilator coupled to a RCA 8575 photomultiplier tube via a short lucite light pipe. In tests with ^{60}Co gamma-rays, we deduced a time resolution of 0.3 nsec FWHM, for the new detector. The time resolution of the system while taking data is usually between 0.4 and 0.5 nsec, as measured by the width of the target gamma-ray peak.

A major improvement in operating efficiency has been obtained by motorizing the detector assembly so that the neutron detection angle may be controled from the data room. The detector is housed inside a steel naval gun barrel which is surrounded by boxes full of water. The entire detector assembly sits on a motorized air pad so that it may be floated and moved easily about the experimental area. The assembly is constrained to move in a fixed-radius arc about the target position by a 5 inch diameter aluminum pipe that pivots above the target. The signal and power cables for the detector are run through the pipe in order to avoid having cables on the floor that might impede the movement of the detector assembly. The gun barrel is constrained to point at the target by a pair of steel guy wires that also pivot above the target. The target angle and gun barrel orientation is monitored by TV camaras mounted on the aluminum pipe and the gun barrel, respectively. The scattering angle may be measured to better than 0.1°.

In the past, a major source of background has been due to small angle scattered beam striking the beam pipe after the target. This background has been reduced by about a factor of ten by placing a quadrupole triplet immediately after the target box in order to refocus the beam into a well shielded beam dump 8 meters from the target. In addition, the beam pipe between the target and beam dump has been electrically isolated so that the beam which does not reach the beam dump can be integrated. Thus the total integrated charge can be measured to an accuracy of better than a few per cent, independent of the target thickness.

B. (p,n) Isobaric Analog State Data

We have embarked on a program to measure differential cross sections of (p,n) reactions exciting the isobaric analog state of the target ground state. The objectives of the program are to determine the isospin dependent part of the nucleon-nucleon effective interaction, V_τ, and to determine the isospin-dependent part of the nucleon-nucleus optical potential. The targets chosen for this program are ^{48}Ca, ^{90}Zr, ^{120}Sn, and ^{208}Pb. These targets were chosen for their large neutron excess, their simple ground state shell model configurations, and because they span a large mass range. In order to study the energy dependence of the isospin-dependent interaction, data have been taken at proton bombarding energies of 25, 35, and 45 MeV. Figures 1 and 2 show typical neutron time-of-flight spectra obtained at 10° and 130°. The neutron energy resolution of the analog peaks vary from about 400 keV for ^{48}Ca to about 250 keV for ^{120}Sn. Low energy neutrons from previous beam bursts were eliminated by setting a sufficiently high energy threshold on the photomultiplier light output signal. The unlabeled arrows in the figures indicate the position of the target gamma-rays, which appear in the neutron spectra even though they are reduced by about a factor of 200 by our neutron-gamma pulse shape discriminator system. Figures 3 and 4 show the 25 and 35 MeV data. The 45 MeV data are not yet complete. The error bars indicated in the figures represent the uncertainties in the relative cross sections only. The uncertainty in the absolute cross sections is estimated to be about 10 to 20 per cent. Note that all of the data have a reasonable amount of structure, especially at back angles.

C. Macroscopic Analysis of the Data

We are in the process of trying to fit our 25 and 35 MeV data with Lane-model-consistent[1] DWBA macroscopic calculations. In the Lane model, the nucleon-nucleus optical potential may be written as

$$U(r) = -U_0(r)+4(\vec{t}\cdot\vec{T})/A^*U_1(r)+(\tfrac{1}{2}-t_3)U_c(r)$$

where U_0, U_1, and U_c are the isospin-independent, isospin-dependent, and Coulomb potentials, respectively; $\vec{t}$ and $\vec{T}$ are the isospin of the projectile and target, respectively; and A is the atomic number of the target nucleus. If the isospin of the target ground state has its minimum allowed value, then $T=T_z=\frac{1}{2}(N-Z)$ and the potentials for proton, neutron, and quasielastic

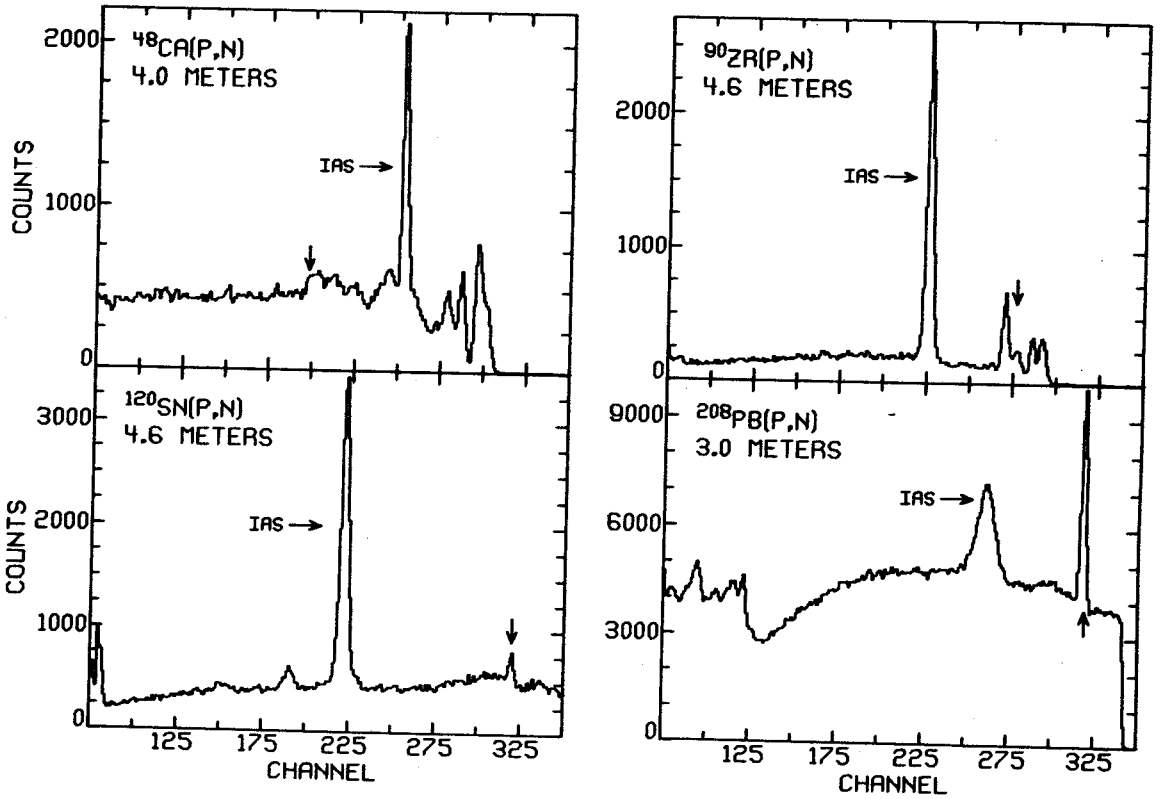

Fig. 1.--Neutron time-of-flight spectra obtained at 10° with E_p=25 MeV.

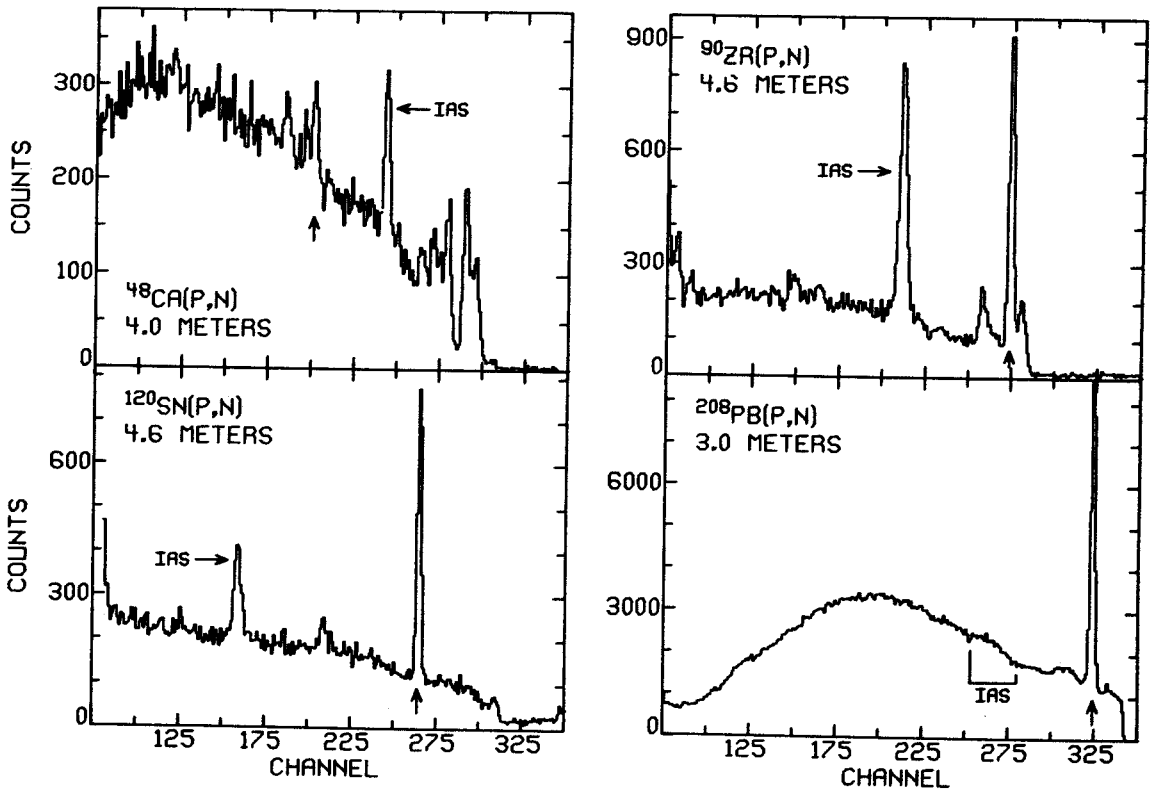

Fig. 2.--Neutron time-of-flight spectra obtained at 130° with E_p=25 MeV.

(p,n) scattering are

$$U_{pp}(r) = -U_0(r) - \frac{(N-Z)}{A} * U_1(r) + U_c(r)$$

$$U_{nn}(r) = -U_0(r) + \frac{(N-Z)}{A} * U_1(r)$$

$$U_{pn}(r) = 2\frac{\sqrt{N-Z}}{A} * U_1(r)$$

We have assumed that the Becchetti-Greenlees proton optical potentials[2] provide a reasonable parameterization of U_0 if the potential strength terms proportional to (N-Z)/A are omitted. U_1 has been parameterized similar to U_0, that is with a linear energy dependence. A non-linear least-square search program has been written, using a subroutine version of the DWBA program DWUCK[3], to optimize the parameters of U_1. We are currently in the process of doing global searches on all of our 25 and 35 MeV data. As an indication of the kind of agreement that can be obtained without searching, the dashed curves in figures 3 and 4 show the results of macroscopic DWBA calculations using the Becchetti-Greenlees best-fit proton and best-fit neutron parameters. The (p,n) form factor was obtained by summing the isospin-dependent strengths and averaging the geometry parameters of the proton and neutron potentials. It should be noted that these are not Lane model consistent calculations. The calculations do agree with our data surprisingly well, but there is still considerable room for improvement.

D. Microscopic Analysis of the Data

In the microscopic DWBA neglecting exchange, the transition amplitude for a reaction A(a,b)B may be written

$$T_{ba} = \int \chi_b^{(-)} \langle \psi_f | V_{eff} | \psi_i \rangle \chi_a^{(+)} d^3r$$

where the χ's are distorted waves generated in an appropriate optical potential, the ψ's are the wave functions of the states involved, and V_{eff} is the nucleon-nucleon effective interaction which induces the transition from the initial to the final state. We have chosen our targets for their simple ground state shell model configurations, so that the nuclear wave functions should not contribute much to the uncertainty of the calculations. In addition, the good overlap of the initial and final states in reactions exciting the isobaric analog of the target ground state tends to make the calculations insensitive to the fine details of the wave functions. Our macroscopic analysis of the data should provide us with good optical model parameters, so the distorted waves should not be much of a source of uncertainty either. Thus, the microscopic analysis of the data should provide a sensitive way to investigate V_{eff}. For central forces, V_{eff} may be written

$$V_{eff} = \sum_i (V_0(r) + V_\sigma(r)\sigma_i \cdot \sigma_p + V_\tau(r)\tau_i \cdot \tau_p + V_{\sigma\tau}(r) \sigma_i \cdot \sigma_p \, \tau_i \cdot \tau_p)$$

where the sum is over the valence nucleons. For the isobaric-analog-state transition, only the V_τ term contributes to the direct transition amplitude. Thus, our measurements should provide reasonably unambiguous information about the isospin part of the effective interaction. The solid curves in figures 3 and 4 were obtained from microscopic calculations using the DWBA program DWUCK. The Becchetti-Greenlees best-fit proton and best-fit neutron optical parameters were used to calculate the distorted waves. The nuclear wave functions were assumed to be $(f_{7/2})^8$ for ^{48}Ca and $(g_{9/2})^{10}$ for ^{90}Zr. V_τ (r) was assumed to have a Yukawan radial dependence with a range of 1.0F. The strength of V used in the calculations is 20 MeV for the 25 MeV calculations and 18 MeV for the 35 MeV calculations.

E. ^{40}Ar(p,n) to the Anti-Analog State

When the valence nucleons of a target are in more than one shell-model orbital, the isobaric analog state (IAS) is a linear combination of these orbitals. Then there is an orthogonal linear combination of the same orbitals called the anti-analog state (AAS). The (p,n) transition to the AAS is expected to be small and sensitive to the details of the wave functions and reaction mechanism because of the poor overlap between the target ground state and the AAS wave functions.

In(^{3}He,t) reactions to AAS in several nuclei, it was found that the angular distributions could not be fitted by the usual DWBA macroscopic analysis.[4] Microscopic computations[5] for ^{40}Ar(^{3}He,t)^{40}K(AAS) produced both an incorrect shape and a magnitude less than one-tenth that observed. It was then shown[6] that a reasonable fit could be obtained if the 2-step process (^{3}He,α)-(α,t) was included. Perhaps the composite nature of ^{3}He and t and the strength of (^{3}He,α) cross sections make the 2-step process more important in (^{3}He, t) reactions than in (p,n) reactions between the same states.

To test this possibility, we have measured the ^{40}Ar(p,n)^{40}K(AAS) differential cross section with 24 MeV protons. Figure 5 shows the time-of-flight spectrum obtained at 15° with a 11.5 meter flight path. Due to difficulties in determining the target thickness, we extracted the ratio of the AAS to the IAS cross sections. We then used the experimental values[6] obtained at the University of Colorado for the IAS with 22.8 MeV protons to normalize our AAS to IAS ratio. The results are shown in Figure 6. The curves in Figure 6 are the results of one-step microscopic calculations, including exchange,

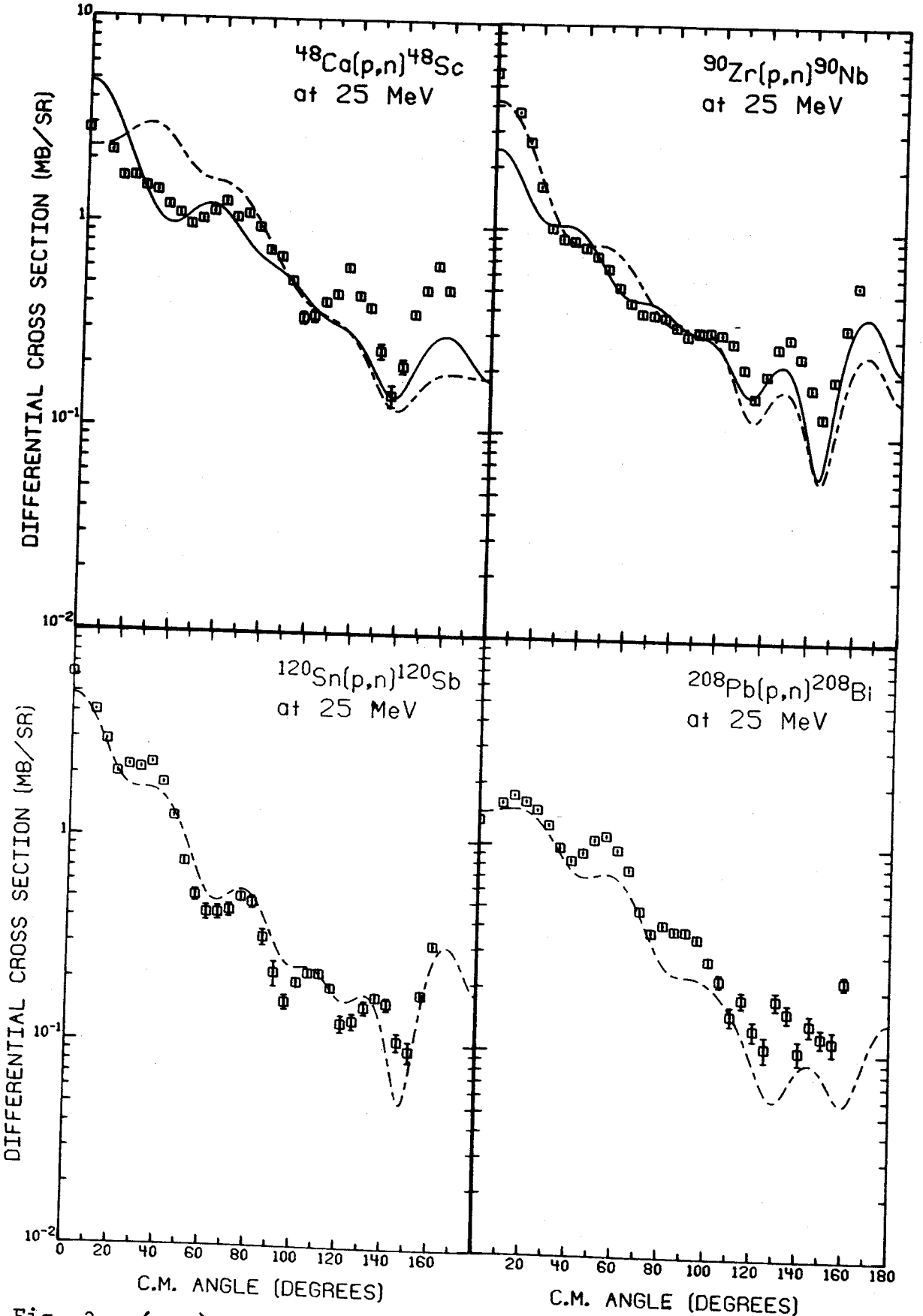

Fig. 3.--(p,n) angular distributions of the isobaric analog state for 25 MeV incident protons. The solid and dashed curves are the results of microscopic and macroscopic DWBA calculations, respectively, as described in the text.

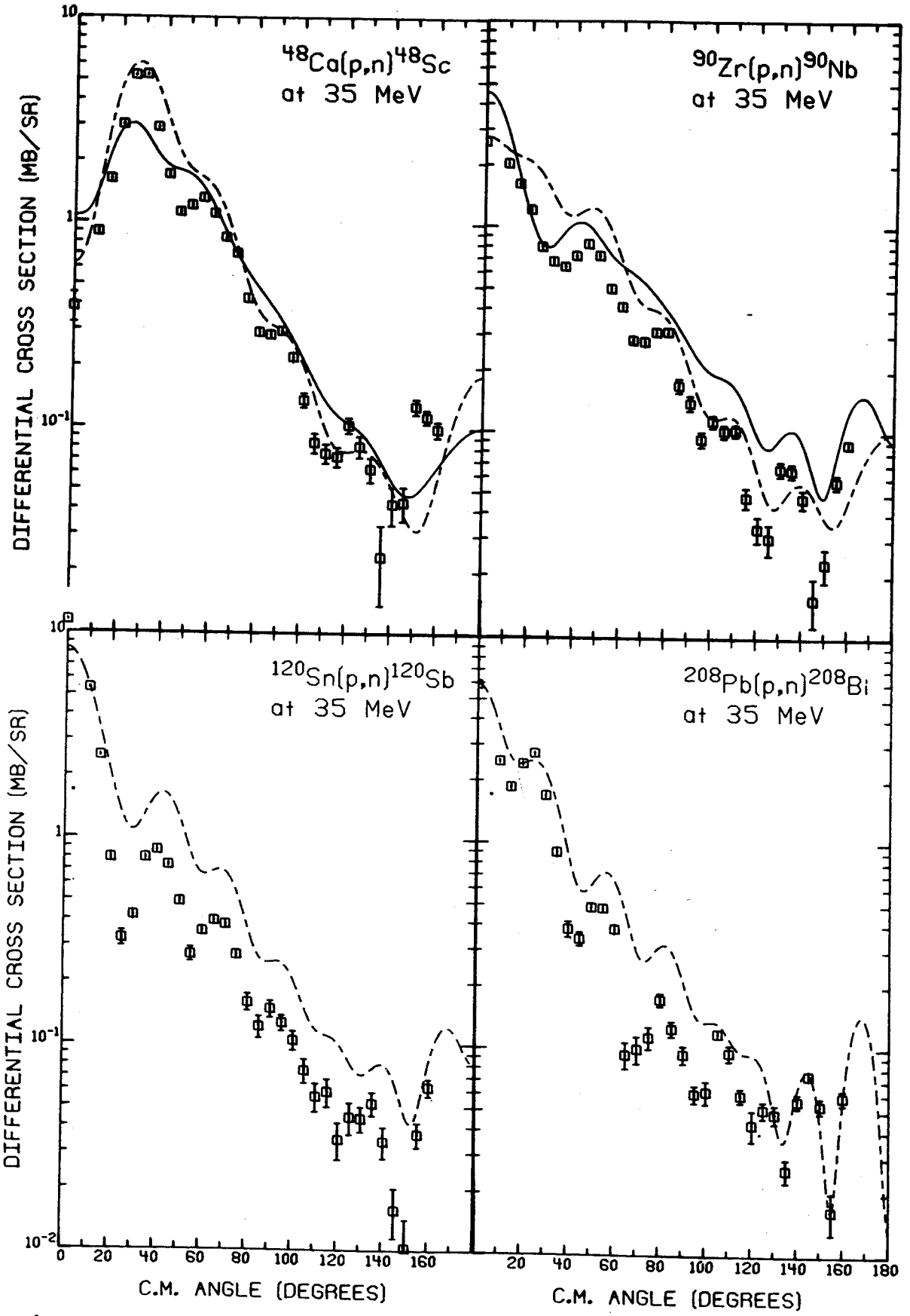

Fig. 4.--(p,n) angular distributions of the isobaric analog state for 35 MeV incident protons. The solid and dashed curves are the results of microscopic and macroscopic DWBA calculations, respectively, as described in the text.

that were done using the program DWBA-70 of Raynal and Schaeffer. We used the Becchetti-Greenlees best-fit optical parameters[2] for the distorted waves, a $(d^2_{3/2}f^2_{7/2})$ target wave function, and Yukawan effective interaction with a range of 1.0F and strengths as follows[7]: V_0=-30 MeV, V=6 MeV, V=20 MeV, and V=15 MeV.

Our conclusion is that there is no compelling need to include a 2-step reaction in order to obtain agreement with the data.

1. A. M. Lane, Phys. Rev. Lett. 8, 171(1962).
2. F. D. Becchetti and G. W. Greenlees, Phys. Rev. 182, 1190(1969).
3. P. D. Kunz, University of Colorado, Boulder, private communication.
4. R. A. Einrichs, R. Sherr, G. M. Crawley, and I. Proctor, Phys. Rev. Lett. 25, 829 (1970).
5. R. Schaeffer and G. F. Bertsch, Phys. Lett. 38B, 159(1972).
6. R. F. Bentley, J. D. Carlson, D. A. Lind, R. B. Perkins, and C. D. Zafiratos, Phys. Rev. Lett. 27, 1081(1971).
7. S. M. Austin, P. 285 in The Two-Body Force in Nuclei, ed. S. M. Austin and G. M. Crawley, Plenum Press, 1972.

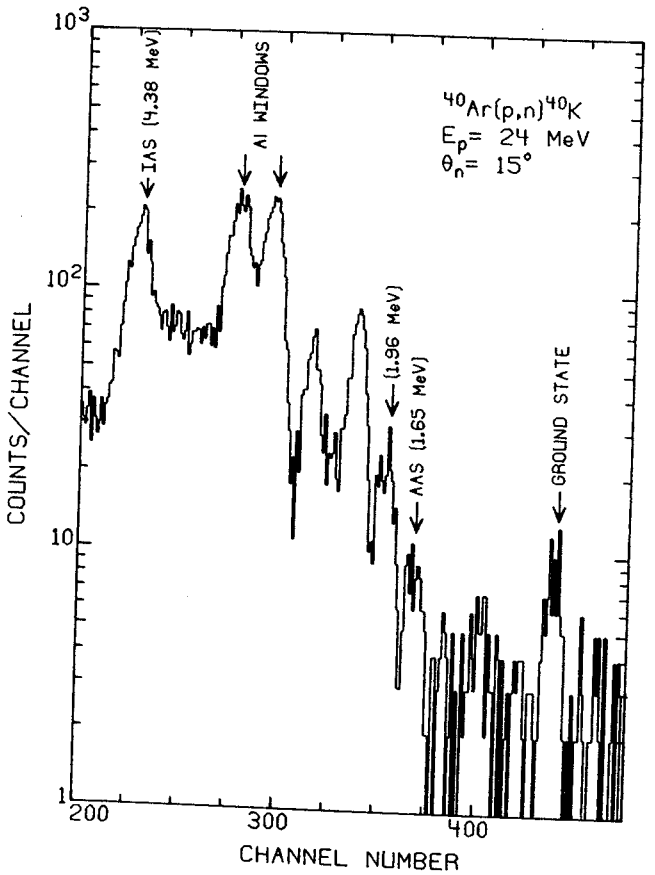

Fig. 5.--Neutron time-of-flight spectrum obtained at 15° for $^{40}Ar(p,n)$ with E_p=24 MeV. The neutron flight path was 11.5 meters.

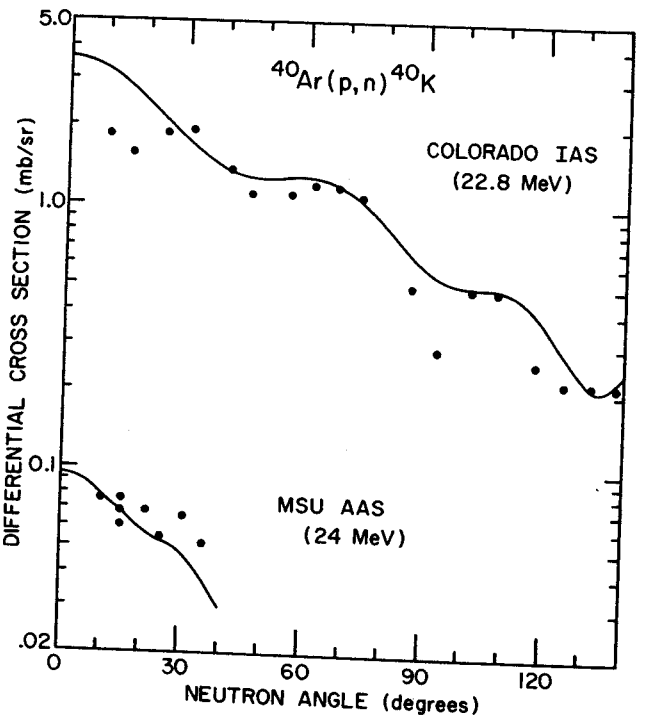

Fig. 6.--$^{40}Ar(p,n)^{40}K$ angular distributions of the isobaric analog state and the anti-analog state. The IAS data are from the University of Colorado and the AAS data are from MSU. The curves are the results of one-step microscopic DWBA calculations, including exchange, as described in the text.

Single Neutron Pickup on ^{14}C

S. Maripuu, G. M. Crawley and R. deMeijer*

The structure of ^{13}C was investigated by the pickup reaction $^{14}C(p,d)^{13}C$ at a proton bombarding energy of 35 MeV. While the levels in this nucleus have been studied by neutron stripping from ^{12}C practically no pickup information is presently available.

The target contained about 14 $\mu g/cm^2$ of ^{14}C and also impurities of ^{12}C, ^{16}O and ^{14}N. The deuterons were detected in a resistive-wire proportional counter placed in the focal plane of the magnetic spectrograph. The proportional counter was backed by a plastic scintillator which was used to identify the deuterons by a time of flight measurement. Since the counter was only 10 inches long, three separate runs were taken at each angle to study the spectrum of ^{13}C up to an excitation energy of 18 MeV. A proton monitor counter at 90° checked the condition of the target and checked the accuracy of the charge collection from run to run. The monitor counts were used to obtain angular distributions from 7° to 70°.

Angular distributions for eight states in ^{13}C are shown in Fig. 1 including the angular distribution for the isobaric analogue state ($J^\pi=3/2^-$ T=3/2) at 15.1 MeV. The angular distributions for the ground state ($J^\pi=1/2^-$) and 3.68 MeV ($J^\pi=3/2^-$) states are generally similar as expected since both are reached by a $\ell=1$ transfer but have slight differences especially forward of 20°. The angular distribution for the 3.09 MeV ($J^\pi=1/2^+$) is very strongly forward peaked, characteristic of $\ell=0$ transfer.

Distorted wave calculations were carried out using the code DWUCK72. Becchetti-Greenlees[1] proton optical parameters were used. Two sets of deuteron parameters were tried, the adiabatic model set[2] and parameters obtained by the Argonne group.[3] Some comparison of theoretical fits to the data are also shown in Fig. 1. Spectroscopic factors were extracted by comparing the fits from the adiabatic model with the experimental curves at the position of the forward maximum in the angular distribution. These spectroscopic factors normalized to the value 2.0 for the ground state are shown in the table together with values calculated by Cohen and Kurath[4] and by Maripuu and Hauge[5] and by True.[6]

The S-factors for the negative parity states of ^{13}C are in good agreement with shell-model predictions. The experimental C^2S value for the Ex=3.09 MeV $J^\pi=1/2^+$ state is considerably larger than the value predicted by True,[6] indicating the existence of a larger amount of S $1/2^2$ configuration in the ^{14}C ground state wave function than predicted by this model.

*Visitor from Florida State University.

1. F. D. Becchetti and G. W. Greenlees, Phys. Rev. 182, 1190(1969).
2. R. E. Johnson and P.J.R. Soper, Phys. Rev. C1, 976(1970); and G. R. Satchler, Phys. Rev. C4, 1485(1971).
3. J. P. Schiffer, G. E. Morrison, R. H. Siemssen and B. Zeidinan, Phys. Rev. 164, 1274(1967).
4. S. Cohen and D. Kurath, Nucl. Phys. A101, 1(1967).
5. P. Hauge and S. Maripuu, Phys. Rev. to be published, November 1973.
6. W. W. True, Phys. Rev. 130, 1530(1963).

TABLE I.--

	Experiment			Theory			
				Cohen & Kurath		Hauge & Maripuu	True
Ex (MeV)	J	T	C^2S	Ex (MeV)	C^2S	C^2S	C^2S
0.0	$\frac{1}{2}^-$	$\frac{1}{2}$	2.0	0.0	1.73	1.79	--
3.09	$\frac{1}{2}^+$	$\frac{1}{2}$	0.12	--	--	--	0.025
3.68	$\frac{3}{2}^-$	$\frac{1}{2}$	1.70	3.58	2.04	2.28	--
3.85	$\frac{5}{2}^+$	$\frac{1}{2}$	0.20	--	--	--	0.14
6.86	$\frac{5}{2}^+$	$\frac{1}{2}$	0.12	--	--	--	--
9.50	$(\frac{3}{2}^-)$	$\frac{1}{2}$	0.20	10.4	0.33	0.20	--
15.1	$\frac{3}{2}^-$	$\frac{3}{2}$	1.86	14.8	1.58	--	--

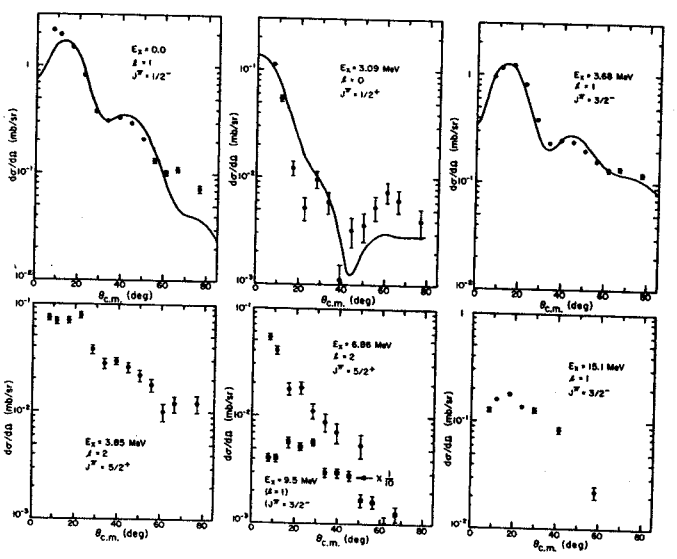

Fig. 1.--Angular distributions observed in the $^{14}C(p,d)^{13}C$ reaction at E_p=35 MeV. The solid curves are DWBA calculations.

Study of Sulfur Isotopes Via the (p,d) Reaction

A. Moalem, H. B. Wildenthal and D. Show

The (p,d) reaction on ^{32}S, ^{33}S and ^{34}S has been conducted as part of a systematic study of this reaction on nuclei in the sd shell region. Our objective in the present work is to obtain a reasonably complete understanding of the nuclear structure of levels in the Sulfur nuclei, including the region of the analog states, so as to allow more critical evaluation of recent shell model predictions.

The experiment was performed with a 35 MeV proton beam from the MSU sector focused cyclotron. Angular distributions were measured independently with a position sensitive wire proportional counter and nuclear emulsions in the focal plane of Enge-Split type spectrograph. We obtained a resolution of about 8 keV, FWHM, for the emulsion spectra. The data from the counter were limited to 50 keV resolution and were used to confirm the results obtained from the nuclear emulsions.

To this end data analysis for the $^{32,33}S(p,d)$ reaction is at very preliminary stages. For data for the $^{34}S(p,d)^{33}S$ reaction is near completion and the results are summarized in the accompanying table. A total number of thirty-seven levels have been resolved up through 7.5 MeV, essentially all of them known from previous studies. The excitation energy values obtained in the present work usually agree within the quoted errors with those obtained in Ge(Li) γ-ray studies of levels in ^{33}S. The spectroscopic factors appear to agree with those obtained in large space shell model calculations, for most of the strongly excited levels.

TABLE I.

E_x(keV)		ℓ	$100 \times C^2S^{\ell,j}$ Experiment	FPSDI
0		2	187	187
840	840.4±0.3	0	80	85
1966	1966.4±0.3	2	5	17
2313	2312.6±0.4	2	17	25
2867	2866.3±0.3	2	127	158
2935	2934.3±0.5	3	2	
2969	2968.7±0.4	(4)	1	
3220	3219.5±0.9	1	0.2	
3832	3830 ±2.	2	59	0
3935	3934 ±3.	2	2.5	13
4048	4047.6±1.	(4)	(0.8,0.4)	
4053*	4053 ±3.	0	0.3	10
4096	4093.8±1			
4147±3.5	4143 ±3.	(3,4)		
4211	4212 ±2.	---		
4380±6.	4377 ±5.	0	3	15
4425	4426 ±5.			
4733	4732 ±6.			
4747	4747 ±6.			
	4869 ±6.			
	4920 ±2.			
4947	4941 ±6.	3	5	
5182	5177 ±6	3	4	
	5210 ±6			
5273	5272 ±6			
5288±3.2	5287 ±6	flat		
5347	5340 ±6	2	3	
	5351 ±6			
5403	5399 ±6	flat		
5485	5475.4±1.4	0	46	40
	5599 ±5			
5619	5613 ±6	0	10	
5718±3.1	5715 ±6	flat		
5728±3.		4	(1.2,1.3)	
	5854 ±6			
5890				
5918*	5915 ±6	0	8.2	
	5982 ±6			
6364	6360 ±6	2	21	
6423±3.3	6428 ±2			
	6689 ±6			
	6892 ±6			
6907±6		2	35	18
6968	6965 ±6			
7194	7193 ±2			
7341	7344 ±12	2	41	40
	7420 ±2			
8100				

The $^{206}Pb(p,d)^{205}Pb$ Reaction

W. A. Lanford

There have recently become available shell model calculations of $^{206,205,204}Pb$ based on 2, 3 and 4 neutron holes in the lead ^{208}Pb core. These calculations have been very successful in predicting the spins, parities and excitation energies. Spectroscopic factors from the $^{207}Pb(p,d)^{206}Pb$ reaction[2] are also in excellent agreement. These calculations are based on the assumptions that (1) the six strong states excited in the $^{208}Pb(p,d)^{207}Pb$ reaction are single neutron hole states and (2) the low lying states in $^{206,205,204}Pb$ can be described as 2, 3 and 4 neutron holes distributed over these six neutron orbits. In order to make the analysis of the $^{206}Pb(p,d)^{205}Pb$ correspond to these assumptions, we have measured spectroscopic factors for transitions to states in ^{205}Pb relative to the strengths experimentally determined for the $^{208}Pb(p,d)^{207}Pb$ reaction. To distinguish these relative spectroscopic factors from absolute spectroscopic factors, we will denote them as C^2S. This use of relative C^2S is appropriate not only because they are the quantities predicted by most theories, but also because they can be evaluated to a few percent accuracy. That is by measuring the cross-sections for $^{206}Pb(p,d)$ relative to the cross-sections measured in $^{208}Pb(p,d)$ (not relative to DWBA as is usually done), one can avoid most for the uncertainties present in a DWBA analysis.

There is one simple test of these ideas which can be easily applied. The angular distributions measured on ^{206}Pb and ^{208}Pb targets must be the same, or clearly the procedure suggested above is inappropriate. Shown in Fig. 1 are $f_{7/2}$ angular distributions as measured on all four of the stable lead isotopes. Note that the curve is the same in all four cases and is simply an interpolation between the $^{208}Pb(p,d)$ data points. Clearly for all practical purposes, the angular distributions are the same. Similar plots for the other ℓ-values could also be shown.

These (p,d) reactions have been studied at 35 MeV using a combination of data taken with nuclear emulsions and with a position sensitive proportional counter in the focal plane of a spectrometer. Shown in Fig. 2 is a spectrum obtained using nuclear emulsions. The data taken with emulsions had resolution of about 15 keV (FWHM) while the data taken with the counter had about 45 keV resolution. The proportional counter data was used for states for which 45 keV resolution was sufficient and the plate data was used for other states. The proportional counter data has the advantages of better statistics and not having the uncertainty introduced by human scanners. On the other hand, the plate data has both better resolution and an accurately known calibration. Shown in Table I are the excitation energies and ℓ-values observed in the $^{206}Pb(p,d)^{205}Pb$ reaction along with information on ^{205}Pb from the literature.

Preliminary analysis of the data gives the spectroscopic factors given in Table II. Also shown are the predicted excitation energies and spectroscopic factors of McGrory, et al.[1] Note that there is generally good agreement.

1. J. B. McGrory, et al., Bull. Am. Phys. Soc. 17, 579(1972) and private communication.
2. W. A. Lanford and G. M. Crawley, submitted to Phys. Rev. C.
3. J. H. Hamilton, et al., Vanderbilt University, preprint.

TABLE I.--Comparison of the Excitation Energies from the $^{206}Pb(p,d)^{205}Pb$ Reaction with Results in the Literature.

Excitation Energy	ℓ-value	Nucl. Data Sheet Plus Hamilton, et al.[3]		J^π assumed for this analysis
.0006	1+3	$5/2^-$	0.0	$5/2^-$
		$1/2^-$	.0022	$1/2^-$
.262	1	$3/2^-$	.2628	$3/2^-$
.577	1	$3/2^-$	.5761	$3/2^-$
		$7/2^-$	.7034	$7/2^-$
.762	3	$5/2^-$	.7615	$5/2^-$
.802	(1)	(1/2,3/2$^-$)	.803	$1/2^-(3/2^-)$
		$9/2^-$	.9876	$9/2^-$
.997	(1)			$3/2^-(1/2^-)$
1.011	6	$13/2^+$	1.0137	$13/2^+$
1.042	3	$7/2^-$	1.044	$7/2^-$
		$5/2^-$	1.2647	$5/2^-$
1.373	1			$3/2^-(1/2^-)$
		$9/2^-$	1.4991	$9/2^-$
		(9/2$^-$,7/2$^-$)	1.5753	
1.583	3			$5/2^-(7/2)$
		$9/2^+$	1.5936	$9/2^+$
1.615	3	$7/2^-$	1.6144	$7/2^-$
		(11/2$^-$,9/2$^-$)	1.7050	
1.758	3		1.7564	$7/2^-$
		$9/2^+$	1.7585	$9/2^+$
		$7/2^-$	1.7643	$7/2^-$
		$7/2^-$	1.7758	$7/2^-$
2.352	1			
(2.521)	3	9/2$^-$,7/2	2.5214	
2.562		$9/2^+$	2.5651	
2.692	5			
2.795	0			
2.903	5			
3.933				
3933				
3999				
4013				
4050				
4.984				
5.095				
5.145				
5.174				

TABLE II.--Spectroscopic Factors for the $^{206}Pb(p,d)^{205}Pb$ Reactions Relative to the $^{208}Pb(p,d)^{207}Pb$ Reaction to the Single Neutron Hole States in ^{207}Pb. Also shown are the shell model predictions of McGrory, et al.

J^{π}	Excitation Expt.	Excitation Calc.	C^2S expt.	C^2S Calc.
$5/2^-$	0.0	.07	4.73	5.34
$1/2^-$	.002	0.0	.65	.94
$3/2^-$	.262	.21	3.00	3.36
$3/2^-$	.577	.75	.084	.04
$7/2^-$	.703	.91	0.0	0.0
$5/2^-$	.762	.88	.08	.19
1/2(3/2)	.803	.80	(.02)	.01
$9/2^-$	.988	1.06	0.0	0.0
$3/2^-(1/2)^-$	.997	1.02	.16	.23
$13/2^+$	1.011		11.52	
$7/2^-$	1.044	1.13	.54	.36
$5/2^-$	1.265	1.01	0.0	.01
3/2(1/2)	1.373	1.35	.008	.02
$9/2^-$	1.499	1.54	0.0	0.0
$(9/2^-,7/2^-)$	1.575		0.0	
			$C^2S(f_{1/2})=.06$	
$5/2^-(7/2^-)$	1.583	1.37		0.0
$9/2^+$	1.594		0.0	
$7/2^-$	1.615	1.58	1.04	.96
$11/2^-9/2^-$	1.705		0.0	
$7/2^-$	1.756	1.76	6.08	6.32

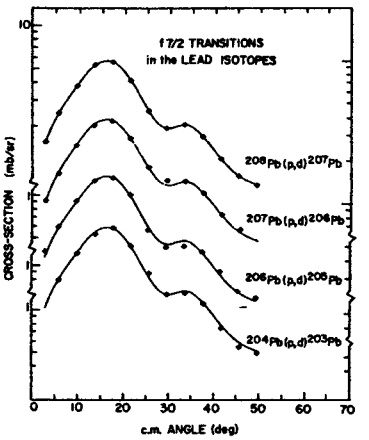

Fig. 1.--The $f_{7/2}$ angular distributions as measured on all four stable isotopes of lead. Note that the curve is the same in all four cases. The curve is simply the results of interpolating between the data points from the $^{208}Pb(p,d)^{207}Pb$ reaction.

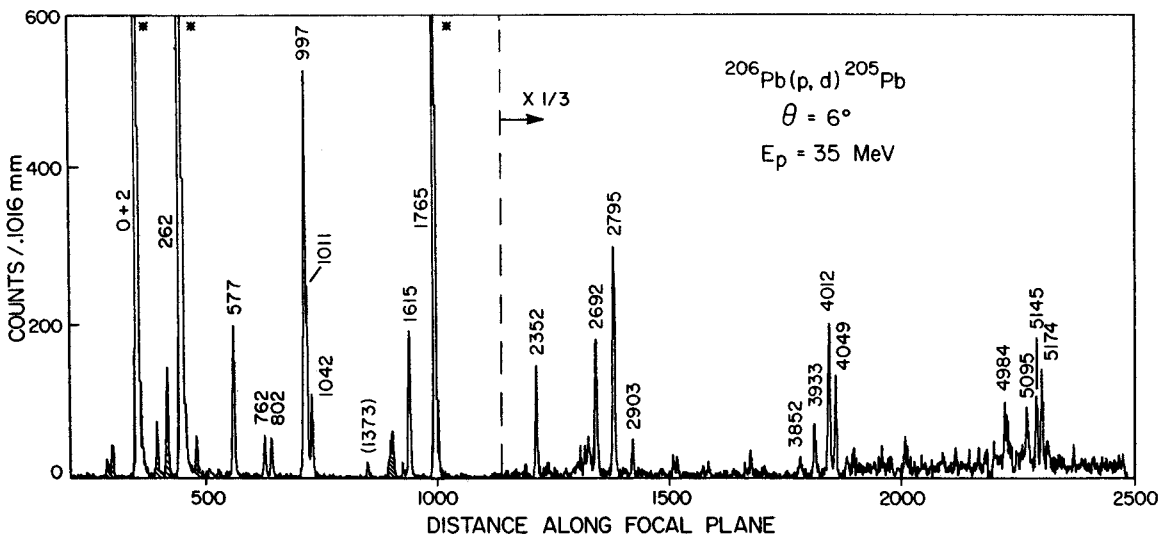

Fig. 2.--A spectrum of the $^{206}Pb(p,d)^{205}Pb$ reaction. The peaks are labeled with excitation energies in keV. The cross-hatched peaks are from impurities in the target. The peaks labeled with asterisks were too intense to scan and would go off the top of the scale.

Study of the (p,^{3}He) and (p,t) Reactions on ^{29}Si and ^{31}P

H. Nann, W. Benenson, and W. A. Lanford

The simultaneous investigation of the (p,^{3}He) and (p,t) reactions on target nuclei with isospin T=1/2 has two purposes. On one hand effects of a spin-isospin dependent interaction potential in the DWBA analysis of the two-nucleon transfer reactions can be studied. On the other hand, since the (p,^{3}He) reaction permits an S=0, T=1 and an S=1, T=0 spin-isospin transfer of a proton neutron pair, whereas the (p,t) reaction allows only an S=0, T=1 transfer of two neutrons, it is possible to test different parts of the wave functions of the target and the final nuclei.

We have begun the comparative measurements of these reactions on ^{29}Si and, till now to a lesser extent, on ^{31}P using the 40 MeV proton beam of the MSU Cyclotron. The reaction products were detected in a position sensitive proportional counter backed by a plastic scintillation counter on the focal plane of the split-pole magnetic spectrograph. The scintillation counter provides an energy signal and a time signal, both of which are used for particle identification. An overall energy resolution of about 30 keV was obtained.

We have measured angular distributions between 6° and 55° for mirror transitions to states up to 5 MeV excitation energy in the final nuclei. The transitions show nearly equally strength except the ground state transitions, the strengths of which are about one order of magnitude larger. We have tried to reproduce the experimental differential cross sections with microscopic DWBA calculations which employ spectroscopic amplitudes extracted from shell model wave functions of Wildenthal and McGrory.[1] In Fig. 1 we show as an example measured and calculated angular distributions of the (p,t) and (p,^{3}He) reactions on ^{29}Si for transitions to the first five states in the final nuclei. In all DWBA calculations the same sets of optical model parameters are used. The agreement between experiment and calculation for the shape of the angular distributions is generally quite satisfactory. The discrepancies in the ^{29}Si(p,t)^{27}Si angular distributions may point to some contributions from two step processes and not to inadequacies of the shell model wave functions used in the analysis. Each calculated angular distribution is independently normalized to the experimental data. Using the values $|D(S=0)|^2=0.72$ and $|D(S=1)|^2=0.30$ for the spin-isospin exchange terms in the stripping interaction[2] and a common normalization, corresponding to $D_o^2=18\cdot10^4$ MeV^{2}fm^3, one obtains the ratios σ_{exp}/σ_{th} which are given in Table 1. These relative magnitudes of the angular distributions produced in the (p,^{3}He) and the (p,t) reactions are affected not only by the details of the wave functions but also by the choosen values of D(S).

Our data indicate that the ratio $|D(S=1)|^2/|D(S=0)|^2$ used in the present analysis is too high in agreement with the results of Fleming, et al.[3] The detailed test of the shell model wave functions is still in progress.

1. B. H. Wildenthal and J. B. McGrory, Phys. Rev. C7, 714(1973).

2. J. C. Hardy and I. S. Towner, Phys. Lett. 25B, 98(1967).

3. D. G. Fleming, J. Cerny and N. K. Glendenning Phys. Rev. 165, 1153(1968).

TABLE 1.--Comparison of experimental and theoretical cross sections.

J^π	$E_x(^{27}Al)$ (MeV)	$E_x(^{27}Si)$ (MeV)	σ_{exp}/σ_{th} (p,^{3}He)	(p,t)
$5/2^+$	0.00	0.00	0.64	1.39
$1/2^+$	0.84	0.78	1.17	0.84
$3/2^+$	1.01	0.96	1.33	0.84
$7/2^+$	2.21	2.16	0.89	0.67
$5/2^+$	2.73	2.65	0.72	4.6

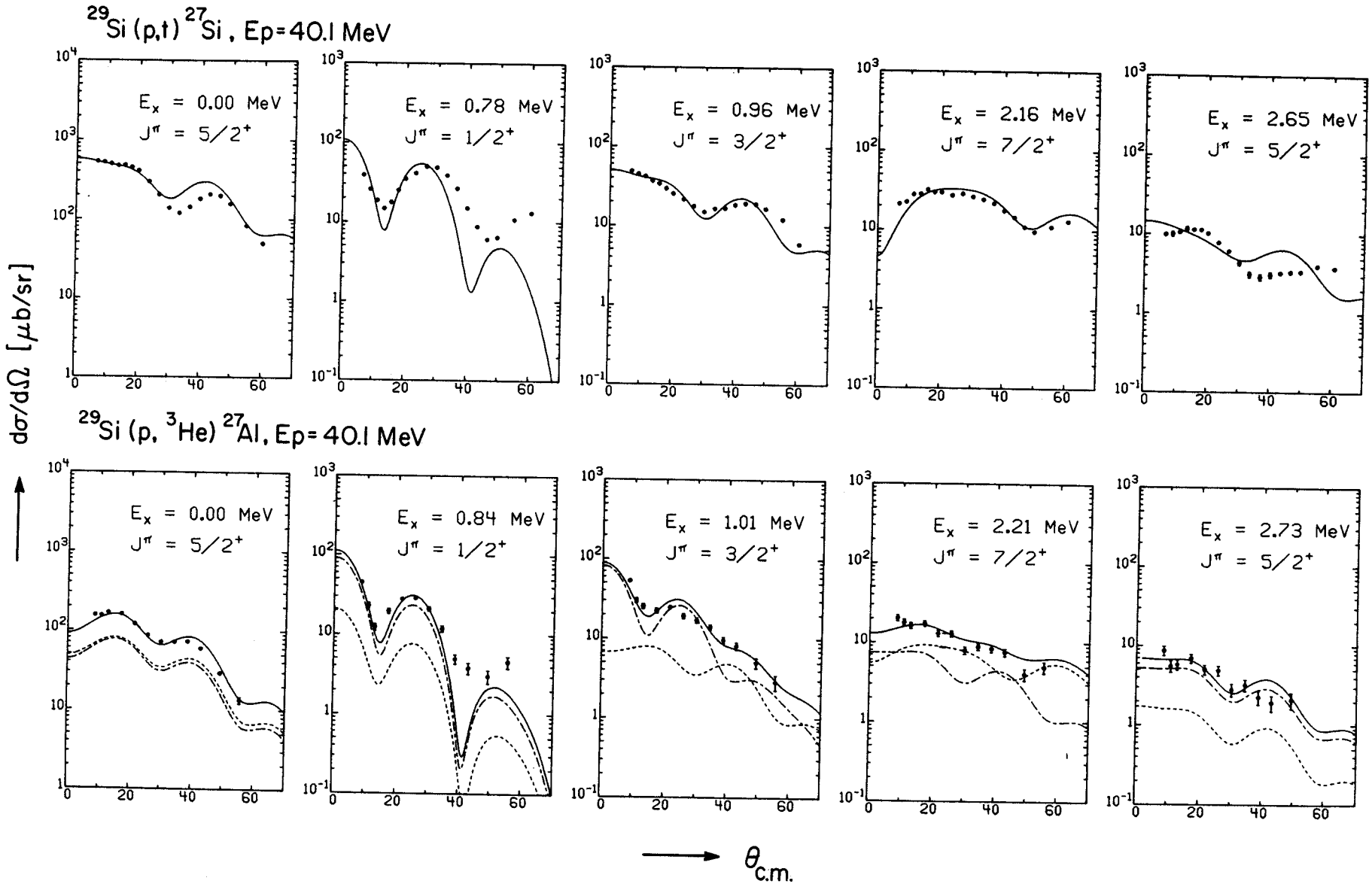

Fig. 1.--Angular distributions for the $^{29}Si(p,t)^{27}Si$ and $^{29}Si(p,^{3}He)^{27}Al$ reactions at E_p=40.1 MeV bombarding energy. For the $^{29}Si(p,^{3}He)^{27}Al$ reaction, displayed in the lower half, the contributions of the S=0, T=1 transfer (dotted curve) and the S=1, T=0 transfer (dashed-dotted curve) to the total differential cross section (full curve) are shown.

The Structure of ^{56}Ni via the ^{58}Ni(p,t)^{56}Ni Reaction

H. Nann and W. Benenson

The purpose of this investigation is to resolve some discrepancies in the energy levels and spin assignments of ^{56}Ni which occur in comparing results of previous studies of the ^{54}Fe(^{3}He,n)^{56}Ni reaction[1,2,3] and the ^{58}Ni(p,t)^{56}Ni reaction.[4,5] All these studies suffered from a lack of good energy resolution. As an example, in all (^{3}He,n) experiments a spin-parity of $J^{\pi}=0^{+}$ is uniquely assigned to the level at 3.95 MeV while a value of 4^{+} is found in the (p,t) reaction. Schneider, et al.[3] found a doublet at that energy and made spin assignments for the two levels.

We have measured angular distributions of the ^{58}Ni(p,t)^{56}Ni reaction at a bombarding energy of 40.3 MeV for the transitions to states up to 12 MeV excitation energy in ^{56}Ni. The triton spectra were recorded using either a position sensitive Si semiconductor detector or a position sensitive proportional counter in the focal plane of the split-pole magnetic spectrograph. An energy resolution of 8 and 25 keV, respectively, was obtained. Fig. 1 shows a triton spectrum taken with the proportional counter.

Besides the doublet at 3.95 MeV we found three other new doublets at 5.00, 5.33 and 5.99 MeV. The triton angular distributions for the transitions to the doublets at 3.95 and 5.00 MeV are displayed in Fig. 2. The angular distributions of the transitions to the 3.952 and 5.007 MeV states both exhibit a clear L=0 pattern; therefore these states have unambiguously the spin assignments $J^{\pi}=0^{+}$, the first assignment being in contradiction with that given by Schneider, et al.[3] From the L=4 pattern of the angular distribution of the 3.923 MeV transition a spin-parity of $J^{\pi}=4^{+}$ can be deduced. The 4.937 MeV state is probably an unnatural parity state with $J^{\pi}=3^{+}$. These assignments were deduced by comparing the shapes of the present angular distributions to those observed in the ^{56}Fe(p,t)^{55}Fe reaction for transitions to known 4^{+} and 3^{+} states, respectively.

Particular interest was directed to the transitions to $J^{\pi}=0^{+}$ states in ^{56}Ni, especially to T=2 states[6] around 10 MeV excitation energy. The analysis of this part is still in progress.

We presume from the strange shapes of some angular distributions that there are many unresolved levels in ^{56}Ni. Therefore further high resolution experiments on this reaction are being carried out using nuclear emulsions.

---

1. W. P. Alford, et al., Phys. Lett. 42B, 60(1972).
2. D. Evers, et al., Nucl. Phys. A198, 268(1972).
3. P. Schneider, et al., Z. Phys. 253, 30(1972).
4. W. G. Davies, et al., Phys. Lett. 27B, 363(1968).
5. G. Bruge and R. F. Leonard, Phys. Rev. C2, 2200(1970).
6. J. Cerny, Ann. Rev. Nucl. Sci. 18, 27(1968).

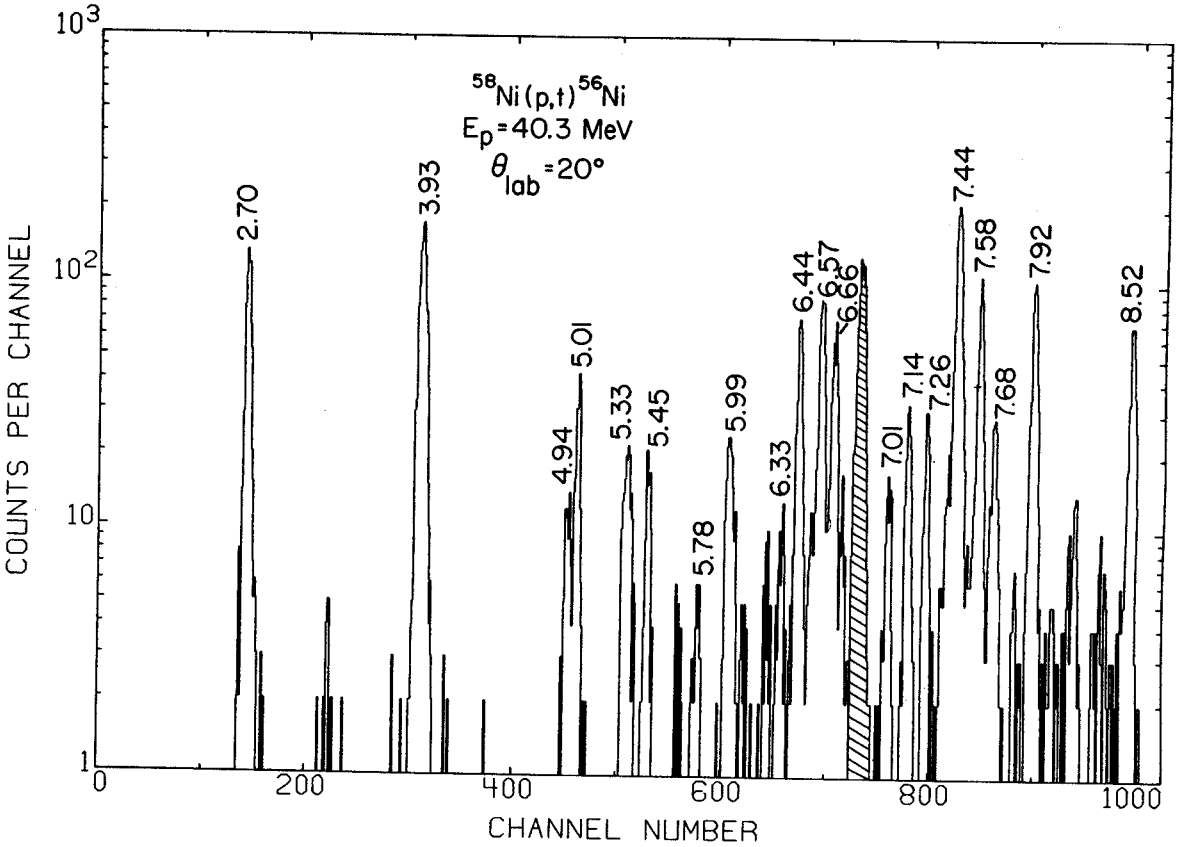

Fig. 1.--Spectrum of the ^{58}Ni(p,t)^{56}Ni reaction observed with a position sensitive proportional counter in the focal plane of the magnetic spectrograph.

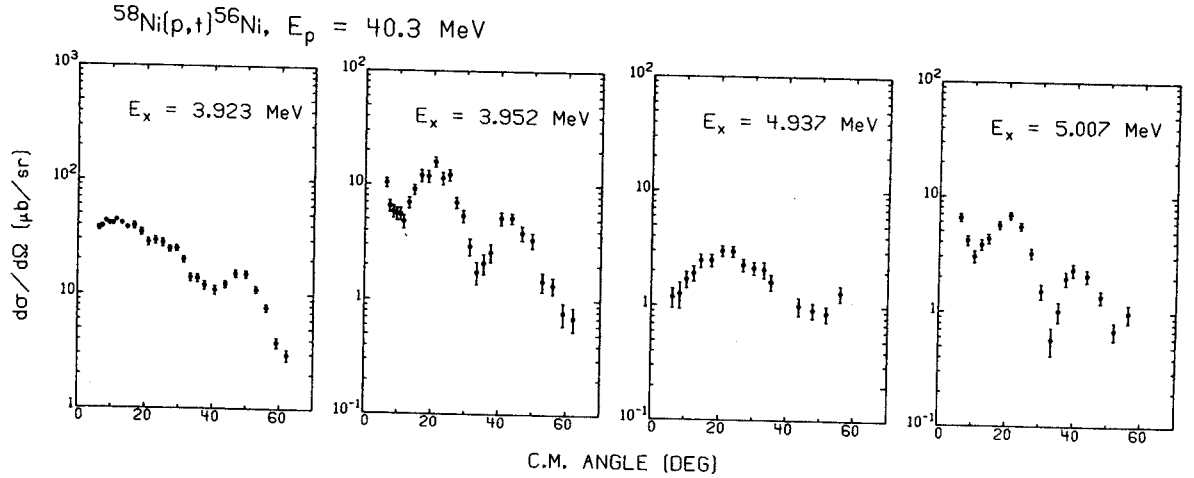

Fig. 2.--Angular distributions of the ^{58}Ni(p,t)^{56}Ni reaction to the states at 3.923, 3.952, 4.937 and 5.007 MeV in ^{56}Ni.

The (p,t) Reaction on ^{163}Dy*

J. S. Boyno, Wm. C. McHarris, R. A. Warner and R. W. Goles**

The study of odd-A rare-earth nuclei by the (p,t) reaction is continuing. The bulk of previous results dealt with levels in odd-Z nuclei.[1] Preliminary results of the $^{163,161}Dy(p,t)$ reactions which involve odd-N nuclei were also presented last year.[1] An effort was made to improve the spectra obtained from the $^{163}Dy(p,t)$ reaction, and although the resolution in the spectra shown in Fig. 1 is still not good enough to allow detailed analysis, certain features of the ^{161}Dy level scheme are now under investigation.

Angular distribution data, taken using a ~200 μgcm^{-2} target and a beam of 33 MeV protons from the MSU cyclotron, indicates tentatively that the very strong peak near channel 740 is an $\ell=0$ transition. One expects that the strongest $\ell=0$ transfer in this reaction would be the transition involving the $K^{\pi}=5/2^-$ ground state in ^{163}Dy with the $K^{\pi}=5/2^-$ excited state at 26 keV in ^{161}Dy. The absence, or extreme weakness, of the ground to ground transition, $5/2^- \rightarrow 5/2^+$ is not surprising as this involves a parity change with consequent change in structure.

With the high level density in both the target and final nucleus, the addition of coupled channel programs to the cyclotron soft ware library is welcomed. The many possibilities for direct and indirect population of the states in ^{161}Dy may require coupled channel analysis for explanation.

Work continues on this project with the fabrication of very thin (~100μgcm^{-2}) targets using the Th reduction method.[2] With the high resolution proton beam available from the MSU cyclotron, the thinner targets, in conjunction with the use of photographic plates, will enable us to obtain the 5-10 keV FWHM resolution necessary to separate the closely spaced ^{161}Dy levels.

---

*Supported by the USAEC and NSF.

**Present address: Battelle Northwest Laboratories, Richmond, Washington.

1. R. W. Goles, R. A. Warner and Wm. C. McHarris, MSU Cyclotron Annual Report (1972),52.

2. L. Westgaard and S. Bjornholm, Nucl. Inst. and Meth. 42, 77(1966).

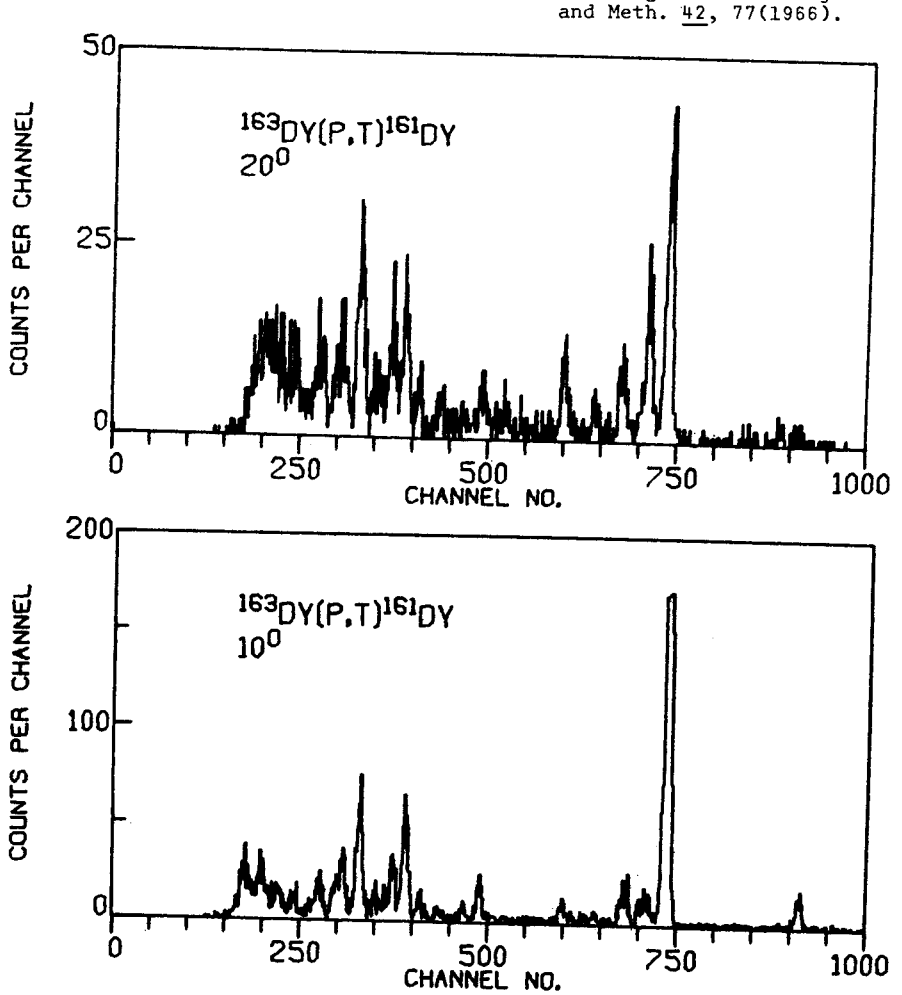

FIGURE 1.--$^{163}Dy(p,t)$ spectra taken at $\theta_l=10°$, 20°. These spectra were recorded using a wire counter in the focal plane of the spectrograph.

Exploration of Z>N Nuclei with the (^{3}He,^{6}He) and (p,^{6}He) Reactions

W. Benenson, E. Kashy, A. Moalem and H. Nann

In the past years the (^{3}He,^{6}He) reaction has been used for the study of exotic nuclei ranging from A=9 to A=55. Most of the solid targets which can be used for this type of investigation have now been bombarded. The last in this series was a study of ^{11}N using the ^{14}N(^{3}He,^{6}He) reaction. Our attention has therefore turned to three topics closely related to the previous (^{3}He,^{6}He) work. These are; (a) (^{3}He,^{6}He) on gas targets, (b) (^{3}He,^{6}He) on solid targets leading to non-exotic or "garden variety" nuclei, and (c) the (p,^{6}He) reaction. The general method diagrammed in Fig. 1 is applicable to all three topics.

Gas targets have properties which are not well matched to the spectrograph's capabilities. The main difficulties stem from the extended source defined by the collimator system. This difficulty was recently shown to be surmountable in a mass measurement of ^{34}Ar (J. C. Hardy, H. Schmeing, W. Benenson, G. M. Crawley, E. Kashy and H. Nann, to be published) performed in this laboratory and reported in this volume. In this experiment a gas cell with a narrow slit exit window was used. Focusing the optics of the spectrograph on this slit permitted an energy resolution of about 40 keV. This same technique is being applied to mass measurements of ^{33}Ar and ^{17}Ne and a remeasurement of the mass ^{29}S. A broad peak (1.5 MeV wide) corresponding to the ^{11}N ground state was observed with a solid melamine target. This experiment will be repeated with a ^{14}N gas target.

The (^{3}He,^{6}He) reaction is one of the very few reactions which have been used to study T_z=-1 nuclei. It can reveal different features of the final nucleus than does the more commonly used (p,n) and (^{3}He,t) reactions. The new levels in ^{10}C near 10 MeV shown in Fig. 2 below are examples of this. On the other hand ^{27}Al(^{3}He,^{6}He) and ^{9}Be(^{3}He,^{6}He) revealed no new features of ^{24}Al and ^{6}Be which have not been observed in ^{24}Mg(^{3}He,t) and ^{6}Li(^{3}He,t) reactions.

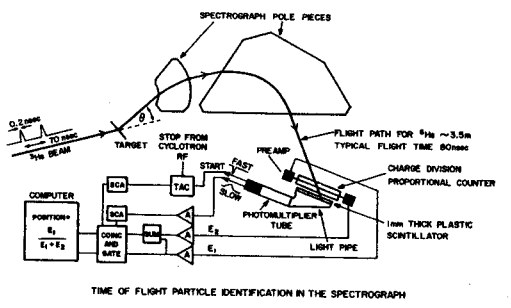

Fig. 1.--The apparatus for time of flight particle identification in the spectrograph.

The first runs on the (p,^{6}He) reaction took place recently. The reactions studied lead to well known non-exotic final nuclei. An example, ^{50}Ti(p,^{6}He), is shown in the Fig. 3. The cross section for this reaction was surprisingly large, approximately 50 nb/sr. This cross section is large enough to permit thin target experiments and therefore accurate mass measurements. The first nuclei to be studied will be ^{53}Co, ^{49}Mn and ^{45}V. These will be done at 45 MeV beam energy. Most of the other exotic nuclei which can be reached by (p,^{6}He) have Q-values so large and negative that special techniques will have to be used to detect the ^{6}He's even if the highest available beam energies (48-50 MeV) are used.

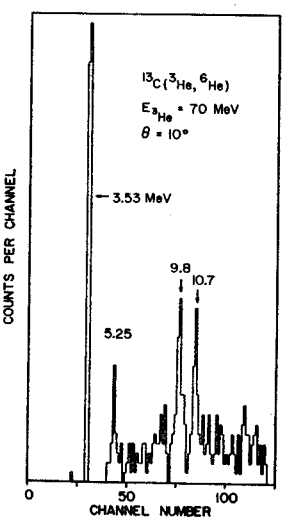

Fig. 2.--Spectrum from the ^{13}C(^{3}He,^{6}He)^{10}C reaction at 70 MeV.

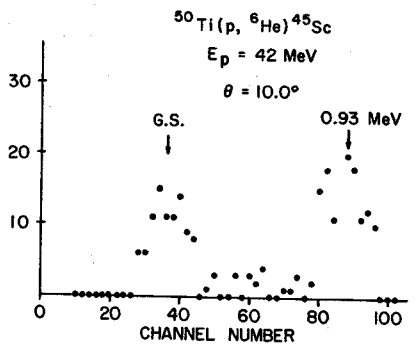

Fig. 3.--The first spectrum of the (p,^{6}He) reaction obtained in this laboratory.

The (^{3}He,^{7}Be) Reaction at 70 MeV

W. F. Steele, G. M. Crawley and S. Maripuu

The lifetime of the nucleus ^{44}Ar has been reported[1,2] but until now its mass and energy levels were unknown. During the past year, using the ^{48}Ca(^{3}He,^{7}Be)^{44}Ar reaction at 70 MeV ^{3}He bombarding energy, we have measured the mass of ^{44}Ar and the excitation energies of several of its excited states.

The ^{3}He beam was produced by the MSU variable energy sector focused cyclotron. The reaction products were analyzed by an Enge split-pole magnetic spectrograph.[3] Detection of ions in the focal plane of the spectrometer was accomplished by means of a system composed of a plastic scintillator photomultiplier unit behind a 25 cm single wire charge division gas proportional counter.[4] The counter measures both position along the focal plane and differential energy loss of an ion, while the scintillator is used to measure time-of-flight in the spectrograph.

^{7}Be spectra are complicated by those outgoing ^{7}Be ions which are in the .432 MeV particle stable first excited state. Thus each level in the residual nucleus produces in the ^{7}Be spectrum two peaks which are separated by about .4 MeV, the exact amount depending on the kinematical parameters. The experimental resolution (FWHM), due primarily to target thickness, of the spectrum measured at 7° laboratory angle (Fig. 1) is about 120 keV, which allows discernment of peak pairs, particularly those of impurities. Peak pairs corresponding to levels in ^{44}Ar occur as well.

Table I summarizes the mass excesses and excitation energies of levels identified as belonging to ^{44}Ar. Both the primary (^{7}Be .000) and secondary (^{7}Be .432) peaks corresponding to a given level have been used in calculating its entry. While levels above 4 MeV are observed, contaminant peaks make the assignment of excitation energies very difficult. The ground state mass excess differs from the Garvey-Kelson[5] prediction by about +500 keV which is about 10 times the average deviation found in their table. A new calculation by Borysowicz,[6] also listed in Table I, which uses more recent masses and which includes a weighting for the actual errors in the 1972 mass table,[7] is closer to our measured value for ^{44}Ar but still differs by about 350 keV.

Because of the ^{40}Ca impurity in the target, a comparison of the ^{40}Ca(^{3}He,^{7}Be)^{36}Ar and ^{48}Ca(^{3}He,^{7}Be)^{44}Ar reactions is possible. Unfortunately the ^{36}Ar ground state transition occurs in only a few spectra so the ratio of ^{36}Ar(0.0)/^{44}Ar(0.0) of approximately 10 is not well determined. The first excited state transition is measureable in more of our spectra and in this case the ratio ^{36}Ar(1.977)/^{44}Ar(.700) is roughly 16.

The ground state transition ratio is qualitatively in agreement with a shell model prediction. If one uses the shell model wavefunctions of Maripuu and Evwaraye[8] for the $J^\pi=0^+$ ground states of ^{36}Ar, ^{40}Ca, ^{44}Ar, and ^{48}Ca and assumes the (^{3}He,^{7}Be) reaction to proceed via α-particle pickup,[9] one obtains a ratio of 15 for the squared ratio of wave-function overlaps between the partitions ^{40}Ca→^{36}Ar + α and ^{48}Ca→^{44}Ar +α . For a more sophisticated calculation one must take into account the transformation coefficients describing the internal motion of the particles in the α-cluster as well as four-particle transfer fractional parentage coefficients. Such a calculation, however, would not at present be justified considering the large experimental cross-section uncertainty. The shell model[8] places the ^{44}Ar first excited state at 1.26 MeV. The measured value of .700 MeV is lower than not only the shell model value, but also lower than the excitation energies of the first excited states of all other known even-even argon isotopes.

In addition to using the (^{3}He,^{7}Be) reaction for mass measurements, the reaction mechanism itself is being studied.[10] To this end, detailed angular distributions are being measured. Displayed in the accompanying figure are angular distributions for the ^{24}Mg(^{3}He,^{7}Be)^{20}Ne reaction to the lowest 0^+, 2^+, and 4^+ states in ^{20}Ne. Their shapes appear to be distinctive: the 0^+ rises at forward angles while the 2^+ declines and the 4^+ has a broad forward hump falling off at extreme forward angles. All distributions have distinct diffraction structure and fall off sharply with increasing angle.

Future work on the (^{3}He,^{7}Be) reaction will include measuring cross sections for targets of mass greater than 90. It has been suggested[11] that while cross sections for (^{3}He,^{7}Be) reactions drop with increasing mass number, at some point the may reach a minimum and begin to rise. Also to be studied are the differences between the primary and secondary angular distributions for a given level, the shapes of which show qualitative rather than quantitative agreement.[12]

---

1. R. E. Larson and C. M. Gordon, Nucl. Phys. A133, 237(1969).
2. J. Hudis, E. Hageb, and P. Patzelt, Nucl. Phys. A151, 634(1970).
3. J. E. Spencer and H. A. Enge, Nucl. Inst. and Methods 49, 181(1967).
4. W. A. Lanford, W. Benenson, G. M. Crawley, E. Kashy, I. D. Proctor, and W. F. Steele, Bull. Am. Phys. Soc. 17, 895(1972).

5. G. T. Garvey and I. Kelson, Phys. Rev. Lett. 16, 197(1966); and G. T. Garvey, W. J. Gerace, R. L. Jaffe, I. Talmi, and I. Kelson, Rev. Mod. Phys. 41, S1(1969).

6. J. Borysowicz, Michigan State University, Private communication.

7. A. H. Wapstra and N. B. Gove, Nucl. Data Tables A9, 267(1971).

8. A. O. Evwaraye and S. Maripuu, Bull. Am. Phys. Soc. 18, 577(1973).

9. C. Détraz, H. H. Duhm, and H. Hafner, Nucl. Phys. A147, 488(1970).

10. W. F. Steele, G. M. Crawley, and S. Maripuu, MSU Cyclotron Lab. Annual Report, 4(1972).

11. C. D. Zafiratos, Univ. of Colorado, private communication.

12. W. F. Steele, G. M. Crawley and S. Maripuu, Bull. Am. Phys. Soc. 18, 134(1973).

TABLE I.--Energy levels of ^{44}Ar

Level	Mass Excess (MeV)	Excitation Energy in ^{44}Ar (MeV)
1	-32.27 ± .04[+]	0.00
2	-31.55 ± .04	0.70
3	-30.71 ± .09	1.55
4	-28.91 ± .18	3.34
5[*]	-27.56 ± .16	4.69

[+]Garvey-Kelson prediction for ground state mass excess -32.76 MeV

Borysowicz prediction for ground state mass excess -32.60 MeV

[*]The fifth level is included only tentatively.

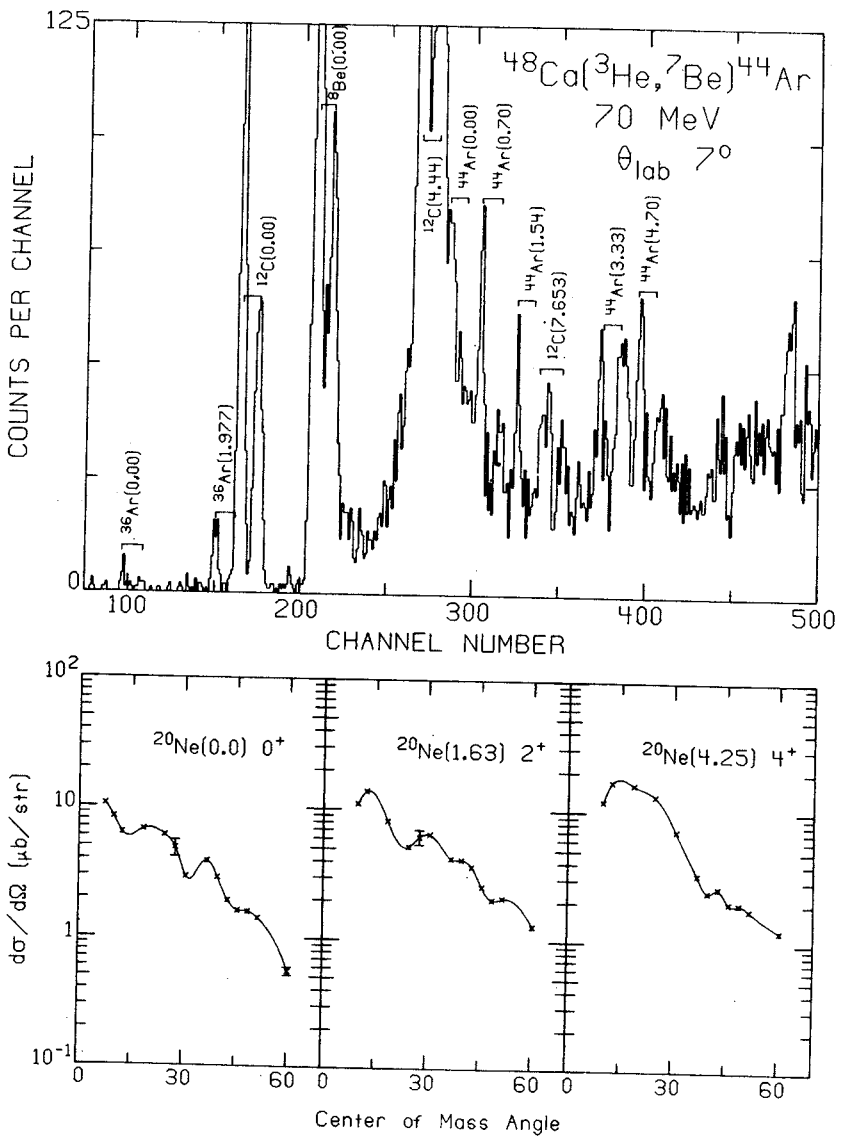

The $^{154}Sm(\alpha,^{6}He)^{152}Sm$ Reaction*

J. S. Boyno, W. Benenson, T. L. Khoo, Wm. C. McHarris and R. A. Warner

The investigation of the properties of the $(\alpha,^{6}He)$ reaction has begun here at MSU with the $^{154}Sm(\alpha,^{6}He)^{152}Sm$ reaction, chosen for the relatively large level spacing of ^{152}Sm states, and for the fact that these states have been investigated and identified in (p,t) reactions.[1]

The reaction was performed with 50 MeV α-particles obtained from the MSU cyclotron. A single-wire gas filled proportional counter was used and a plastic scintillator was placed behind the counter to give timing information. Time of flight information was used to separate all reaction products from the tritons and ^{6}He produced by the (α,t) and $(\alpha,^{6}He)$ reactions, respectively. The use of ΔE/E identification then separated the abundant tritons from the relatively rare ^{6}He particles. Resolution obtained was c. 40-50 keV FWHM which is quite good when one considers the energy width of the α-beam, the severe target loss problem and the poor dispersion of the ^{6}He ions.

Despite the large negative Q-value for this reaction (Q=-13.0 MeV), the momentum match of the α- and ^{6}He-particles is better than in (p,t). For this reason we are quite interested in obtaining complete angular distributions to see the features of the angular distribution for each ℓ-value.

Some of the results we have obtained are presented in Table 1. The presented cross sections for the $(\alpha,^{6}He)$ reaction are based on an estimate of the target thickness and should be taken only to within ±50%.

One is immediately struck by the near equality of the $I^{\pi}=0^{+}$ and 2^{+} cross sections in the $(\alpha,^{6}He)$ reaction. In contrast the $I^{\pi}=0^{+}$ states in the (p,t) are much stronger than the corresponding $I^{\pi}=2^{+}$ states. At θ=20° in the $(\alpha,^{6}He)$ reaction (not shown), the $I^{\pi}=2^{+}$ at 122 keV appears to be 1 1/2 times as strong as the ground state 0^{+}.

The absolute cross sections for the $(\alpha,^{6}He)$ reaction seem to be quite small and it will take some time before we have accumulated full angular distributions with sufficient statistics at each angle to perform a detailed analysis. These first experiments, however, appear quite different from (p,t) reaction results, and this difference may be useful in extracting spectroscopic data from two nucleon transfer reactions.

*Supported by USAEC and NSF.

1. W. McLatchie, W. Darcey and J. E. Kitching, Nucl. Phys. A159, 615(1970).

TABLE I.--Comparative Cross sections in ^{152}Sm

Level E (keV)[a]	$(d\sigma/d\Omega)^{a)}_{22.5^\circ}(p,t)$ (μb)	$(d\sigma/d\Omega)^{(\alpha,^{6}He)}_{8^\circ}$ (μb)	$(d\sigma/d\Omega)^{(\alpha,^{6}He)}_{14^\circ}$ (μb)	Identity[a]
0	510	50	15	0^{+}
122±10	34	35	16	2^{+}
370±10	37	6	3	4^{+}
694±10	100	14	5	0^{+}
819±10	40	17	3	2^{+}
1779±10	125	25	7	$(3,4^{-})$

[a] Taken from Ref. 1.

Mass and Energy Levels of ^{64}Ga

R.G.H. Robertson and W. Benenson

The mass of ^{64}Ge is of astrophysical interest, and has been measured[1] by determining the β^+ end point in coincidence with 427 keV γ-rays from an excited state in the daughter ^{64}Ga. Interpretation of the data rests on knowledge of the mass and level scheme of ^{64}Ga. Although ^{64}Ga has been extensively investigated by the (p,nγ) reaction, seemingly conflicting evidence has come from the threshold studies of Davids, et al.,[2] and from the n-γ and γ-γ coincidence studies of King[3] and Hansen, et al.[4]

In hopes of resolving the discrepancies and at the same time measuring the ground state mass of ^{64}Ga, the ^{64}Zn(^{3}He,t)^{64}Ga reaction has been examined at 37.6 MeV with the Enge spectrograph. Initial inspection of the spectra did not clarify the level scheme because the energy resolution was ~35 keV, the level density was high and it was not certain that the ground state was populated. Very recently, however, Hansen and her collaborators have obtained a high-resolution neutron time-of-flight spectrum of ^{64}Zn(p,n)^{64}Ga, and have settled most of the uncertainties in the ^{64}Ga spectrum. Careful fitting of the (^{3}He,t) peaks with the program SAMPO shows that a 9° and 12° the ground state is very weak compared to the 41 keV state, and that there is in fact excellent correspondence with the spectrum seen by Hansen. The level scheme has been extended to beyond the I.A.S. and a precise value for the mass of ^{64}Ga has been determined.

The spectrum of θ_{lab}=9° is shown in the figure, with energies in keV. Since the ground state is scarcely resolvable, the Q-value of the 323 keV level has been determined by comparison with the ^{27}Al(^{3}He,t)^{27}Si reaction. The 2646.8 keV level in ^{27}Si provides a calibration peak very close to the 323 keV state in ^{64}Ga. Mass measurements for ^{64}Ga are summarized below:

Mass Excess(MeV)	Error	Ref.
-58.934	0.030	5
-58.836	0.006	1
-58.819	0.008	Present

1. C. N. Davids and D. R. Goosman, Phys. Rev. C7, 122(1973).
2. C. N. Davids, D. L. Matthews and D. P. Whitmire, BAPS 17, 71(1972).
3. N.S.P. King, J. E. Draper and R. J. McDonald, BAPS 17, 908(1972).
4. L. F. Hansen, M. C. Gregory and F. S. Dietrich, BAPS 17, 605(19720.
5. A. H. Wapstra and N. B. Gove, Nucl. Data A9, 265(1971).

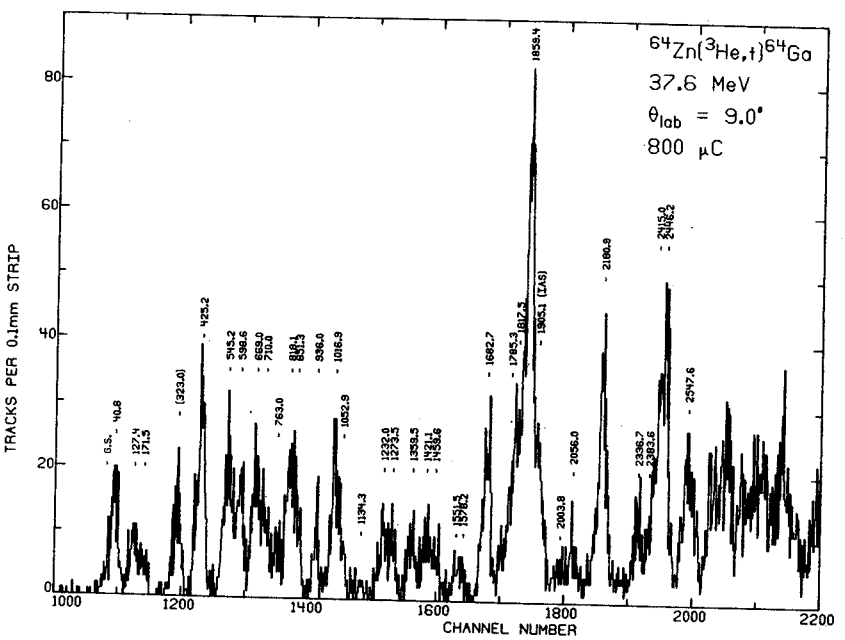

Decay of ^{65}Ge

R.G.H. Robertson and S. M. Austin

^{65}Ge is a very neutron-deficient isotope first identified in 1958 by Porile[1] by chemical separation of germanium from ^{64}Zn after α-particle bombardment. He measured a half-life of 1.5 min and observed 2 weak γ-rays of 0.67 and 1.72 MeV, but concluded that >95% of the decay went to the ground state of ^{65}Ga. No observation of ^{65}Ge, has been reported since. We recently carried out a search for the isotope ^{64}Ge,[2] and a byproduct of that work has been extensive new information on the decay of ^{65}Ge. Independent measurements of the ^{65}Ge decay have also been in progress in Amsterdam,[3] and the results are in excellent agreement with ours, and in disagreement with the early work of Porile.

The Ge activities were produced by the ^{64}Zn(^{3}He,xn) reactions on enriched ^{64}Zn targets at 50 MeV. Following a fast chemical separation of Ge from other activities by vacuum distillation of the tetrachloride, the γ-rays were observed with a Ge(Li) detector and multiscaled into 8 4K bins at 50 sec intervals.

The decay of the strongest line, 650 keV, is shown in Fig. 1. The good energy fit with levels seen[4] in ^{64}Zn(^{3}He,d)^{65}Ga and the rapid growth of the ^{65}Ga activity leads us to associate this and 8 other γ-rays with the decay of ^{65}Ge, although the measured half-life, 30.0±1.2 sec, is a factor of 3 shorter than Porile's result.[1]

Figure 2 shows the decay scheme from our work compared with the ^{64}Zn(^{3}He,d)^{65}Ga results. Absolute γ-ray intensities have been obtained by normalizing to the measured growth of daughter activity. In contrast to Porile, we find very little direct feed to the ground state, although normalization uncertainties would allow up to 25%. Nevertheless, allowed transitions to $1/2^-$ and $5/2^-$ states suggest $J^\pi = 3/2^-$ for ^{65}Ge.

These results are in excellent agreement with the subsequently published work of Jongsma, et al.,[3] except that they observed a large number of weaker γ-rays which were unable to see, but not the 1230 keV line which is concealed in their spectra by a ^{65}Ga contaminant. There is also an unexplained discrepancy in the intensity of the 1880 keV transition.

1. N. T. Porile, Phys. Rev. 112, 1954(1958).
2. R.G.H. Robertson and S. M. Austin, Phys. Rev. Lett. 29, 130(1972).
3. H. W. Johnsma, J. C. deLange, H. Verheul, F.W.N. deBoer and P.F.A. Goudsmit, Z. Physik, to be published.
4. M. G. Betigeri, H. H. Duhm, R. Santo, R. Stock, R. Bock, Nucl. Phys. A100, 416(1967).

Search for the (^{3}He,^{8}He) Reaction

R.G.H. Robertson, W. Benenson, D. Mueller and E. Kashy

We have spent about four days in the search for this 5-neutron pickup reaction with goals of (a) making a more precise measurement of the ^{8}He mass and (b) using this reaction for reaching further into the proton rich nuclear region. The detection system is essentially the same as is currently used in the (^{3}He,^{6}He) research[1] with the exception that a two-wire position sensitive proportional detector is used instead of a single wire detector. This has resulted in a background rate of less than 1nb/MeV-sr. Results so far indicate a cross section for the ^{26}Mg(^{3}He,^{8}He)^{21}Mg of less than 2nb/sr. Present plans include the search for the ^{13}C(^{3}He,^{8}He)^{8}C reaction which is expected to have a larger cross section and to also yield information on the yet unobserved ^{8}C nucleus.

1. E. Kashy, W. Benenson, I. Proctor, P. Hauge, G. Bertsch, Phys. Rev. C6, 2251(1973).

Search for New Isotopes in the N=Z=50 Region*

M. Edmiston, K. Kosanke, F. M. Bernthal, and Wm. C. McHarris

A search has been undertaken to find ^{90}Tc by use of the ^{92}Mo (p,3n)^{90}Tc reaction. The Q-value for this reaction is -35 MeV and that for the (p,4n) reaction is -44 MeV. Thus we are required to use the MSU cyclotron near its high energy limit for protons: the γ-ray spectra are obtained by using the Helium-Jet-Transport System to carry activity from an in-beam target to a Ge(Li) detector. A novel target is being employed which is made by adhering ^{92}Mo powder to a 2-mil aluminum backing with "Zip-grip" brand adhesive. "Zip-grip" has a relatively featureless γ-ray spectrum and apparently forms a thin enough coating over the powder to allow the recoils to escape through the back of the target.

So far, data for an excitation function have been collected and are being analyzed. A half-life determination for lines tentatively attributed to ^{90}Tc decay is in progress.

Further experiments are planned to utilize both the ^{3}He and proton beams available to search for additional new isotopes far from β-stability in the Z=N=50 region.

*Supported by the U. S. Atomic Energy Commission and by the National Science Foundation.

Fermi Beta Decay and the Masses of ^{22}Mg, ^{26}Si, ^{30}S and ^{34}Ar

J. C. Hardy,* H. Schmeing,* W. Benenson, G. M. Crawley, E. Kashy and H. Nann

The object of this experiment was to measure the masses of several T_z=-1 nuclei in the sd shell which are crucial to beta decay theory. The energy of the decay and hence the mass of the initial state enter directly into ft value determination. The mass of ^{34}Ar was particularly important since in the A=34 nuclei a large mirror asymmetry between ft values has been observed.[1]

The experiment was performed in the spectrograph with a ^{36}Ar gas target. The rigidity of tritons from the $^{36}Ar(p,t)^{34}Ar$ reaction at 22.50 was compared to that of tritons from the (p,t) reaction on other gasses mixed with the ^{36}Ar. The particles were detected on plates and also in a current division wire counter backed by a plastic scintillator. The results for ^{34}Ar are given in the table below. Although the results are in agreement with all preceeding measurements, they differ from the 1971 mass table value by 16 keV. The mirror asymmetry is thus reduced from -4.6± 1.7% to 0.0±0.6%. The masses of ^{22}Mg, ^{26}Si, ^{30}S, ^{31}S and ^{35}Ar were measured as well. In every case the agreement with the most recent and accurate experiments is excellent as can be seen in the second table below.

*Visitors from Chalk River National Laboratory.

1. J. C. Hardy, H. Schmeing, J. S. Geiger, R. L. Graham and I. S. Towner, Phys. Rev. Lett. 29, 1027(1972).

TABLE I.--The mass excess of ^{34}Ar.

Experiment	Measured mass excess (keV)	Reference
$^{32}S(^{3}He,n)^{34}Ar$	-18394 ± 30[a]	W. R. McMurray, et al., Nucl. Phys. A92, 401(1967).
	-18395 ± 15[a]	R. G. Miller and R. W. Kavanagh, Nucl. Phys. A94, 261(1967).
	-18394 ± 30[a]	M. Hagen, et al., Phys. Lett. 26B, 432(1968).
$^{36}Ar(p,t)^{34}Ar$	-18370 ± 11	R. A. Paddock, Phys. Rev. C5, 485(1972).
	-18379 ± 3	this experiment

[a] Values used in obtaining the mass excess quoted in the 1971 mass tables: viz. -18395 ± 12 keV.

TABLE II.--Measured Mass Excesses.

Nucleus	This Experiment		Previous most accurate value
^{22}Mg	- 399±3	- 394±2	J. Nolen, et al., Nuc. Inst. and Meth. (in press)
^{26}Si	- 7143±3	- 7147±8	1971 Mass Table
^{30}S	-14062±3	-14065±10	"
^{31}S	-12818±3	-12817.8±3	A. Moalem and H. B. Wildenthal (to be published)
^{35}Ar	-13028±3		1971 Mass Table

Anomalous ε/β^+ Branching Ratios in Allowed Transitions*

R. B. Firestone, Wm. C. McHarris, W. H. Kelly, and R. A. Warner

We have measured a number of anomalous ε/β^+ branching ratios for transitions that are known to be allowed. Most of these involve odd-mass nuclei in the region below N=82. A rule of thumb statement seems to be that in a hindered allowed transition, one that involves a nuclear rearrangement in addition to the "simple" conversion of a proton into a neutron plus leptons, the β^+ branch is much worse than the ε branch. At the very least, this implies that the nuclear matrix elements for β^+ and ε decay are not the same. Explanations range from interference effects from second-forbidden decay to hints that weak interaction theory itself may be incorrect. One of the most clear cut examples is the decay of ^{145}Gd, which we illustrate below.

Relative β^+ feedings to levels in ^{145}Eu were measured in the $\gamma^{\pm}$-γ coincidence experiments where coincidences between two 511-keV $\gamma^{\pm}$ pulses tagged a β^+ event and a third γ-ray labeled the β-fed level. Corresponding ε feedings were obtained from X-γ coincidence experiments. These two sets of intensities were normalized to each other by assuming the theoretical value of the $\varepsilon(\text{tot})/\beta^+$ branching ratio to the 1757.8-keV level in ^{145}Eu. Additional, straightforward, corrections for K/L, K/M, etc., capture ratios were also made. The $\varepsilon(\text{tot})/\beta^+$ branching ratios thus arrived at are presented in Table I.

The feedings to the 1757.8-, 1880.6-, 2494.8-, and 2642.2-keV levels appear quite well predicted by theory. The β-transitions to the 1757.8- and 1880.6-keV levels are well understood. Simplistically, they involve the transition of an $h_{11/2}$ proton from a proton pair to the $h_{9/2}$ neutron orbit, forming the three-quasiparticle states $(\pi h_{11/2})(\nu h_{9/2})(\nu s_{1/2})^{-1}$. Presumably the transitions to the 2494.8- and 2642.2-keV levels involve similar modes, but this is uncertain at this time. The branching ratio to the 1041.9-keV level shows signs of anomalous feedings, and that to the 808.5-keV level differs considerably from theory. These transitions are to simple single-particle levels but their modes are quite complicated. [The single-particle nature of the final state is demonstrated quite well from stripping experiments, E. Newman, et al., Phys. Rev. C 1, 1118 (1970).] They presumably involve the breaking of a $d_{5/2}$ proton pair, formation of an $s_{1/2}$ neutron pair, and promotion of the odd proton to an $s_{1/2}$ or $d_{3/2}$ level. The slowness of such transitions is evident from the log ft values.

Current β-decay theory assumes a constant force in all forms of decay but this work suggests that certain hindered transitions involve different matrix elements for ε vs. β^+ decay. The possibility of such a complex beta force leads to conclusions such as interference effects from second-order decay or even implications for weak interaction theory and such aspects are currently under investigation.

TABLE I.--Measured $\varepsilon(\text{tot})/\beta^+$ Branching Ratios for Decay of ^{145}Gd to States in ^{145}Eu.

Energy (keV)	% β (Total)[a]	$[\varepsilon(\text{tot})/\beta^+]$ Theoretical[b]	$[\varepsilon(\text{tot})/\beta^+]$ Experimental	log ft[a]
808.5	5.1	0.45	8.02	6.9
1041.9	8.7	0.60	0.71	6.5
1757.8	35.7	1.17	1.17	5.6
1880.6	36.3	1.37	1.33	5.6
2494.8	1.3	3.39	3.02	6.7
2642.2	2.0	4.41	4.68	6.4

[a]Values from R. E. Eppley, Wm. C. McHarris, and W. H. Kelly, Phys. Rev. C3, 282 (1971).

[b]Values calculated in Nuclear Data A10, 205(1971).

*Work supported by the U.S. Atomic Energy Commission and the U.S. National Science Foundation.

Search for ^{141}Eu

M. Slaughter, K. Kosanke, M. Edmiston, R. A. Warner

R. Firestone, Wm. C. McHarris and W. H. Kelly

A search for ^{141}Eu has been conducted with the 45 MeV proton beam of the MSU cyclotron and the helium jet recoil transport system. γ-ray singles spectra were taken with a Ge(Li) detector having a photopeak efficiency of 10.4% of 1333 keV (relative to a 3x3 NaI(Tl) detector). The optimum resolution of the system is 2.1 keV FWHM at the same energy. Targets were originally made by fixing ^{144}Sm oxide to an aluminum foil backing with an adhesive, but later we dispensed with the adhesive and relied on a pressure of approximately 20 tons per square inch to press the ^{144}Sm onto the backing.

Initially a very crude half-life determination was attempted by varying the speed of the paper tape upon which the activity was collected. The tape speed was varied between experiments so that the activity was counted for periods of 5 min, 1 min, 20 sec, and 10 sec following collection. A few γ-ray peaks of unknown origin were observed and their half-life was estimated as ~15 sec. A second, more extensive half-life determination was made using the data-taking program TOOTSIE to accumulate 10 successive spectra with each counted for 9.4 sec. A cadmium-beryllium absorber was placed between the tape and the detector to reduce the bremsstrahlung background. Only two transitions were observed with half-lives comparable to that expected of ^{141}Eu based on our previous study of the growth of ^{144}Sm activity following the retrieval with a pneumatic rabbit of activity prepared by the ^{144}Sm(p,4n)^{141}Eu reaction, and on the work of L. Westgaard, et al.[1] who report a half-life of 37±3 sec. These peaks are at 584.5 and 1611.4 keV and have a half-life of 45±10 sec. In addition to half-life experiments, γ-ray singles spectra were collected for bombardment energies of 45 MeV, 41 MeV, and 39 MeV. The 584.5- and 1611.4-keV peaks were most intense at 45 MeV as would be expected if our assignment is correct.

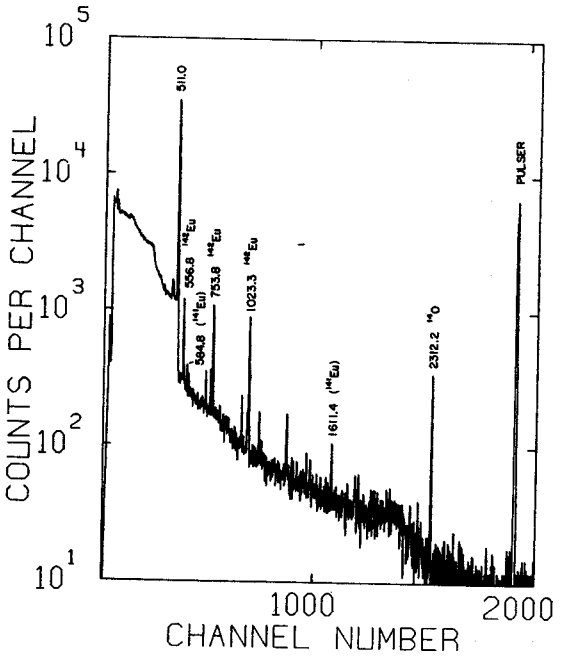

Fig. 1.--Spectrum of γ-rays from activity deposited by the HeJRT system on moving paper tape. Recoils were obtained from an oxide target enriched in ^{144}Sm, bombarded with 45-MeV protons.

1. L. Westgaard, P. G. Hansen, B. Johnson, H. L. Raun, and S. Sundell, The ISOLDE Collaboration, International Conf. on Nuclear Physics, Munich, 1973.

Excited States of ^{48}V

L. E. Samuelson, W. H. Kelly, R. A. Warner, and Wm. C. McHarris

As a continuation of our study of the excited states of ^{48}V (see Ref. 1 and summary in Table I) two additional experiments have been performed. In the first, the $^{48}Ti(p,n\gamma)^{48}V$ reaction with E_p=7.20 MeV was used to determine half-lives in the nanosecond region. The ^{48}V γ rays were counted with a high-resolution planar Ge(Li) spectrometer. A beam sweeping system which removed every other cyclotron beam burst allowed counting in several 5.177-nsec time bands between the on-target beam pulses. The time bands were defined using the MSU cyclotron on-line Σ-7 computer data-acquisition program TOOTSIE.[2] A TAC measured the time intervals between start signals from events in the Ge(Li) detector (determined by constant-fraction timing discrimination) and stop signals derived from the cyclotron r.f. The cyclotron r.f. provided the time calibration.

The γ-ray spectra obtained from this experiment are shown in Fig. 1. As can be seen ^{48}V γ rays of 98.0-, 112.5-, 210.4-, and 308.3-keV are delayed. Since the half-life lower limit for this experiment is approximately 1 nsec, no other ^{48}V states below 1.7 MeV of excitation have half-lives greater than 1 nsec. The decay curves of the four delayed γ rays are plotted in Fig. 2. The decay curve of the 112.5-keV γ follows closely those of the 98.0- and 210.4-keV γ's, thus this delay must be caused by γ-feeding and the half-life of the 420.8-keV state itself must be much shorter than 1 nsec. Weighted least-squares fits (the straight lines of Fig. 2) to the data yield half-lives of 7.12±0.04 and 2.72±0.06 nsec for the 308.3- and 518.8-keV states, respectively. The measured half-life of the 308.3-keV state is compared with previous measurements using the ε-decay of ^{48}Cr in Table II. The excellent agreement lends confidence to our experimental techniques and data analyses.

The 7.12-nsec half-life of the 308.3-keV state is expected because of the energy and E2 multipolarity of its only possible γ decay. However, the 2.72-nsec half-life of the J=1 518.8-keV state is unusually large. If this low-lying state were to have positive parity, one would expect it to have particle configurations similar to the ground and first three excited states, thus facilitating rapid M1 decay. On the other hand a negative parity with particle configurations of $(\pi d_{3/2})^{-1}(\pi f_{7/2})^{4}(\nu f_{7/2})^{5}$ or $(\pi s_{1/2})^{-1}(\pi f_{7/2})^{4}(\nu f_{7/2})^{5}$ would yield j-forbidden E1 decays. Assuming E1 transitions, we obtain B(E1)'s of 6.39×10^{-5} and 1.05×10^{-5} e^2fm^2 for the 98.0-and 210.4-keV γ's, respectively. These are retardations of 1.3×10^{4} and 9.1×10^{4} over the single-particle estimates. Retardations by factors of 10^4-10^5 over single-particle estimates are commonly observed for E1 transitions of this sort.

In the second experiment we used the $^{46}Ti(\alpha,pn\gamma)^{48}V$ reaction with E_α =24 and 30 MeV

Table I: Energies and Spins of ^{48}V States and Energies, Branching Ratios, and Multipole Mixing Ratios of ^{48}V γ-rays from the $^{48}Ti(p,n\gamma)$ Reaction

Initial State (keV)	$J_i\pi_i$ →	$J_f\pi_f$	γ-Out (keV)	γ-Branching (%)	Mixing Ratio $\leq\delta\leq$
308.3±0.1	2 +	4 +	308.3±0.1	100	E2
420.8±0.1	1 +	2 +	112.5±0.1	100	-0.14 -0.02
427.9±0.1	5(+)	4 +	427.9±0.1	100	-0.15 -0.12
518.8±0.1	1(-)	1 +	98.0±0.1	38±2	-0.08 +0.37
		2 +	210.4±0.1	62±2	+0.01 +0.07
613.4±0.1	4(+)	5(+)	185.5±0.1	11±2	-0.02 +0.07
		4 +	613.4±0.1	89±2	-0.21 -0.17
627.3±0.2	6(+)	5(+)	199.3±0.2	37±5	-0.23 +0.03
		4 +	627.3±0.2	63±5	(E2)
745.1±0.1	2(-)	1(-)	226.3±0.1	92±1	-0.08 -0.06
		1 +	324.2±0.1	3.1±0.3	-0.21 +0.16
		2 +	436.8±0.1	4.9±0.4	-0.21 +0.14
765.0±0.1	3(+)	4(+)	151.7±0.2	2.2±0.3	----
		2 +	456.7±0.1	55±2	-0.03 -0.01
		4 +	764.9±0.1	43±2	-0.05 +0.00
1055.9±0.2	3(-)	2(-)	310.8±0.1	92±3	----
		1(-)	537.2±0.2	8±3	(E2)
1099.3±0.2	4	4 +	1099.3±0.2	100	-0.21 +0.22
1264.6±0.2	5(+)	6(+)	637.3±0.2	25±4	----
		4(+)	651.2±0.2	75±4	-0.26 -0.03
1521.5±0.2	2(+)	3(+)	756.4±0.1	20±2	-0.02 +0.13
		1 +	1101.0±0.2	35±4	-0.05 +0.03
		2 +	1212.9±0.2	45±4	+0.14 +0.28
1557.6±0.2	4(-)	3(-)	501.8±0.1	78±4	-0.11 -0.06
		2(-)	812.2±0.3	22±4	(E2)
1685.6±0.3	(5)	4	586.3±0.2	100	----
1781.0±0.2	3(+)	4(+)	1167.8±0.2	42±5	-0.20 +0.07
		2 +	1472.5±0.2	43±5	-0.12 +0.07
		4 +	1780.9±0.3	15±3	----
1998.6±0.2	(3)-	4	899.4±0.2	----	----
		2(-)	1253.3±0.2	----	----

to measure γ-γ coincidences with a Ge(Li)-Ge(Li) coincidence spectrometer. The primary objective of this investigation is to look for high spin states which were weakly excited at best, in the (p,nγ) work. Preliminary results show that a very strong 627.3-keV line is a narrow multiplet (in coincidence with itself) with the number of components uncertain. The 199.3- and 427.9-keV γ's and a new 395.2-keV γ appear to be in coincidence with the entire multiplet, making the placement of the multiplet components and the 395.2-keV γ uncertain. A 504.7-keV γ is found in coincidence with the 226.3-, 310.8-, and 501.8-keV γ cascade suggesting a new state at 2062.3 keV.

1. L. E. Samuelson, et al., MSU Cyclotron Annual Report, p. 16(1971-72).
2. TOOTSIE, a computer code written by D. Bayer, MSU Cyclotron Laboratory (unpublished).
3. P. D. Bond, J. D. McGervey, and S. Jha, Nucl. Phys. A163, 571(1971).
4. B. K. Patnaik, Carnegie Mellon University, Thesis (1968).
5. K. Auerbach, J. Braunsfurth, and H. W. Flender, Nucl. Phys. A94, 427(1967).
6. R. W. Bauer, J. D. Anderson, and L. J. Christensen, Phys. Rev. 130, 312(1963).

Fig. 1.--γ-ray spectra from ^{48}V half-life determination experiment.

Fig. 2.--Decay curves of four ^{48}V γ rays. Where not shown error bars are smaller than the data point symbol.

TABLE II.--Half-life measurements of the 308.3-keV state of ^{48}V.

$t_{1/2}$ (nsec)	Reference
7.12 ± 0.04	Present Work
7.21 ± 0.21	3
7.07 ± 0.14	4
7.09 ± 0.07	5
7.55 ± 0.28	6

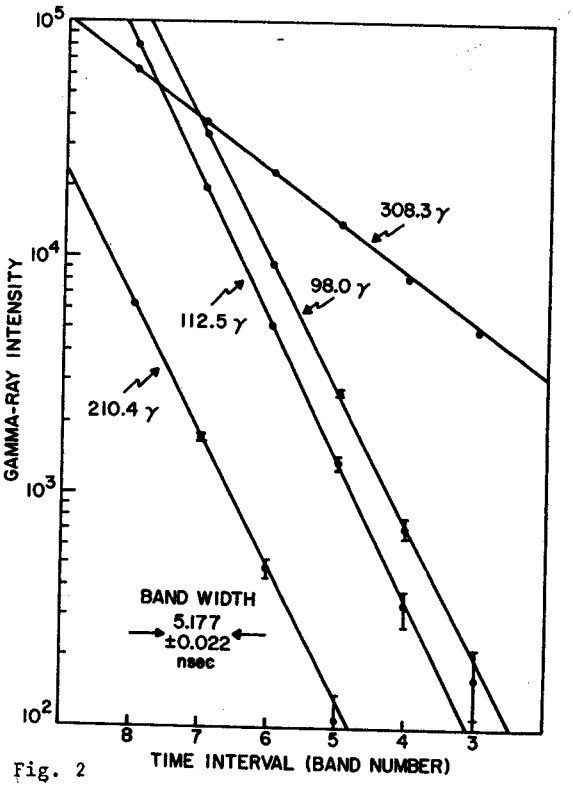

Fig. 2

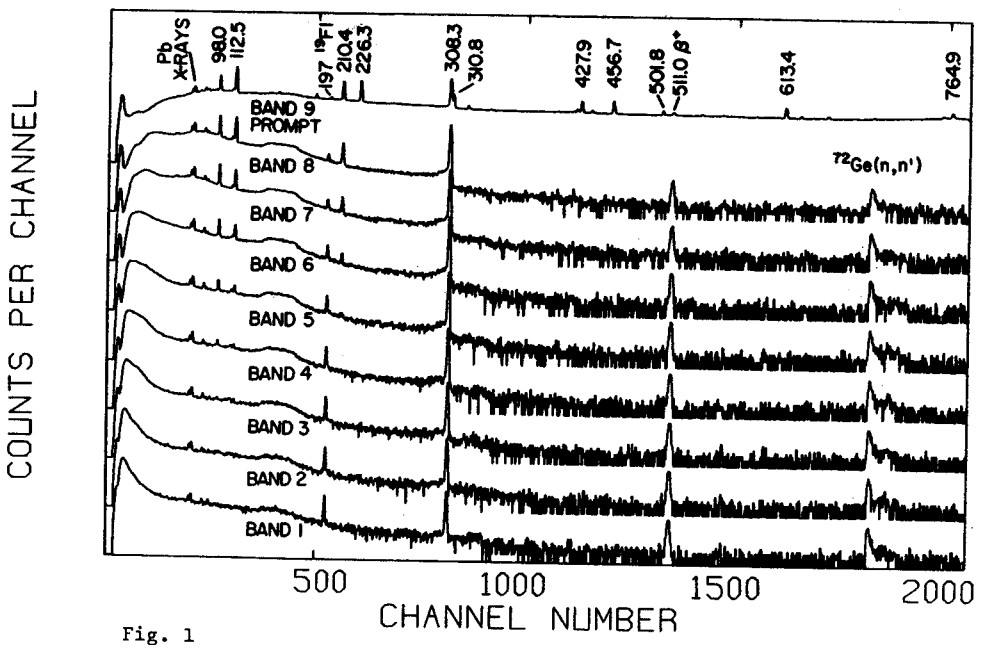

Fig. 1

γ-γ Coincidences from the Decay of ^{56}Co

L. E. Samuelson, C. B. Morgan, W. H. Kelly and Wm. C. McHarris

The radioactive decay of 77.3-d ^{56}Co has been studied quite extensively.[1] However, no γ-γ coincidences obtained with a Ge(Li)-Ge(Li) spectrometer have been reported.[2] In the present work, a 4.5%-efficient Ge(Li) detector and a 7%-efficient Ge(Li) detector were arranged in 150° geometry with a graded (Pb-Sn-Cu) absorber placed between them to suppress coincident Compton scattering from one detector into the other. A typical two-parameter fast-slow coincidence arrangement with constant fraction timing discrimination in the fast timing network was used. A resolving time $2\tau \tilde{} 40$ nsec. was obtained. Addresses corresponding to the energies of coincident γ rays were listed in pairs on magnetic tape. This listing yielded a 4096x 4096-channel array of prompt coincidence events which were later sorted off-line in gated slices. Each gated slice included careful subtraction of background coincidences which were determined from the adjacent continuum. The commercially obtained ^{56}Co source[3] was positioned such that counting rates of approximately 15000 cps were obtained in each detector. A total of 15.8 million coincidence events were recorded in approximately 22h (coincidence rate 200 cps). The estimated chance coincidence rate ($2\tau N_1 N_2 \tilde{} 9$ cps) was approximately 4.5% of the total coincidence rate. Both integral spectra and representative gated spectra are shown in Fig. 1. The size of the 846.78-keV peak appearing in its own gate is indicative of the importance of the chance coincidence rate. The coincidence results are summarized in Table I.

The γ-γ coincidence results (excluding those γ's too weak to be seen) are consistent with the decay scheme of Ref. 1. The only exception (possibly because of poor peak statistics) is the 733.70 keV γ which is not observed to be in coincidence with the 1037.83 keV γ. In the 733.70 keV gated spectrum the 1037.83 keV peak should be as strong as the 846.78 and 1238.28 keV peaks which stand out nicely above the background. An alternative placement of the 733.70 keV γ cannot be made without the introduction of a new energy level, possibly at 2818.76 keV. More detailed analyses of the data are underway.

---

1. D. C. Camp and G. L. Meredith, Nucl. Phys. A166, 349(1971), and references therein.

2. M. N. Rao, Nuclear Data B3 (Nos. 3,4), 85 (1970).

3. The radioactive ^{56}Co source material was obtained from New England Nuclear, Boston, Massachusetts.

4. J. F. Wild and R. A. Meyer, Bull. Am. Phys. Soc. 15, 195(1970).

TABLE I.--Results of two parameter γ-γ coincidence experiment from ^{56}Co decay. All coincidences indicated by an X are definite. The γ-ray energies are from Ref. 4. γ-ray photo-peaks not listed were too weak to be observed.

E Gate (keV) \ E_γ (keV)	511.00	733.70	846.78	977.46	1037.83	1175.13	1238.28	1360.22	1771.49	1963.94	2015.36	2034.92	2113.80	2213.10	2598.58	3010.20	3202.30	3253.60	3273.25	3451.55	3548.05
511.00	X		X		X		X								X						
733.70			X				X														
846.78	X			X	X	X	X	X	X	X	X	X	X		X	X	X	X	X	X	X
977.46		X			X		X														
1037.83	X		X	X		X	X														
1175.13			X		X		X														
1238.28	X		X	X	X	X		X	X	X	X	X		X							
1360.22			X				X														
1771.49			X				X														
2015.36			X				X														
2034.92			X				X														
2598.58	X		X																		
3202.30			X																		
3253.60			X																		
3273.25			X																		
3451.55			X																		

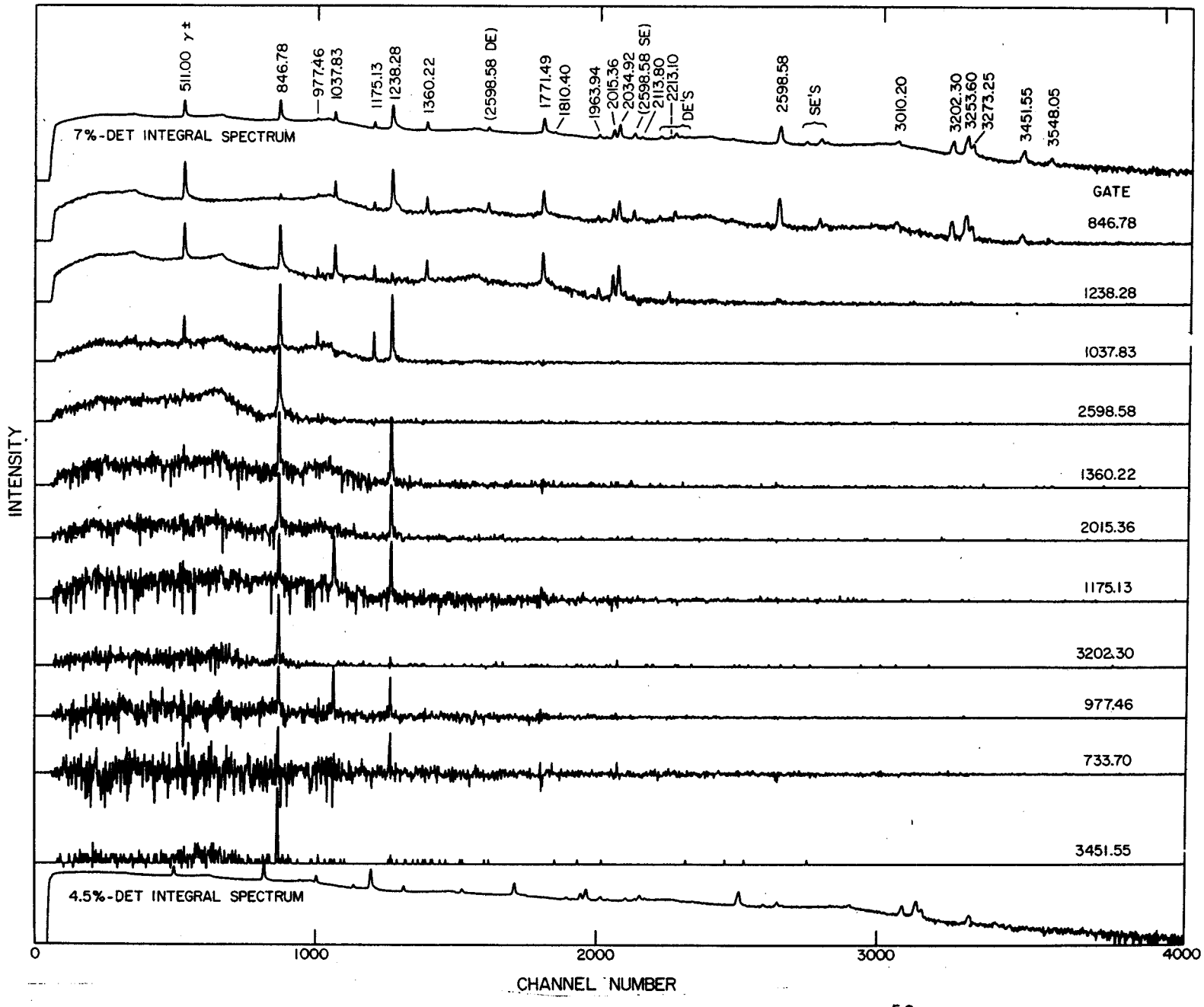

Fig. 1.--Integral and representative gated γ-γ coincidence spectra from ^{56}Co decay. Coincidence displays of the 7% detector were gated on the 4.5% detector. γ-ray energies are those of Ref. 4. The notations SE and DE stand for single and double escape, respectively. Note that the energy scales of the two integral spectra are slightly different.

Studies of Odd-Odd Nuclei Near the Z=50 and N=82 Closed Shells

W. B. Chaffee, C. B. Morgan, Jean Guile, R. A. Warner, L. E. Samuelson,
W. H. Kelly, Wm. C. McHarris, E. M. Bernstein*, and R. Shamu*

Introduction

The residual n-p interaction is still one of the most important problems facing the nuclear spectroscopist. Some fundamental understanding of its manifestations can be obtained from the study of odd-odd spherical nuclei. Unfortunately, these nuclei are very rich in states, making such investigations difficult. Some simplifications are possible near closed shells. A series of investigations of odd-odd nuclei, along with the on-going studies of the adjacent odd mass nuclei, have been initiated near the Z=50 and N=82 closed shells. Here one has a comparatively large number of stable isotopes that can be conveniently used as targets to investigate, for example, the systematic effects as one adds pairs of neutrons for the similar cases of Z=51 or pairs of protons for the N=81.

Because of the complexity of the excited nuclear states, it is necessary to use as many different experimental techniques as possible to study them. We are using those of in-beam gamma ray spectroscopy via the (p,xnγ) and (α,xnγ) reactions [where x=1,2,3], beta decay, and the high resolution scattering reactions, such as the (p,d), (^{3}He,t), (α,d).

The next sections briefly describe the work in progress on ^{116}Sb and ^{118}Sb and a following section describes that on ^{140}Pr.

The Odd-Odd Nucleus $^{116}_{51}Sb_{65}$

We have performed a series of in-beam gamma-ray experiments using the (p,nγ) reaction. These consist of excitation function data, gamma-gamma coincidence, and lifetime measurements. In addition, some preliminary work has been done using the (α,3nγ) and (p,3nγ) reactions which transfer larger amounts of angular momentum.

The (p,nγ) excitation data were taken with thick targets (≈5 mg/cm^2) in 100 keV steps from 5.68 to 7.48 MeV. Approximately 90 gamma-rays have been identified in this 1.8 MeV interval. Analysis of these data gives growth curves for the transitions and branching ratios for level depopulation.

Coincidence data have been taken at 6.54, 7.28, 7.99, 8.40, and 11.75 MeV. Only 44 of the transitions appear in the coincidence data. Most of the remaining gammas are too weak to appear.

The energy level diagram below 1.6 MeV that is consistent with the excitation data and the coincidence data is given in Fig. 1.

Lifetime measurements using the beam sweeping system indicate that only the 93.7 keV transition is delayed more than two nanoseconds. This lifetime is larger than 0.5μ sec, which is the maximum time duration between successive swept cyclotron beam bursts with our current system.

The electron capture decay of 2.5 h 0^+ ground state of ^{116}Te has also been investigated briefly. Only three gamma rays were definitely identified with this activity. The intensities of the 103.0 and 628.7 keV gamma transitions are approximately the same while that of the 93.7 keV transition is about 5 times stronger. This supports our placement of these three transitions using the (p,nγ) data, shown in Fig. 1. The electron capture feedings to the 757.1 and 93.7 keV levels have log ft. values of 4.8 and 5.3, respectively (assuming no unobserved feedings to other states).

Gamma ray angular distribution measurements are in process to determine the levels spins and parities. (^{3}He,t), (α,t) and (α,d) experiments are planned for the near future.

The First 1.2 MeV of $^{118}_{51}Sb_{67}$

The in beam gamma-ray experiments were performed using the ^{118}Sn(p,nγ)^{118}Sb reaction. The early, preliminary results of the excitation function data and the gamma-gamma coincidence data, the preliminary results of the comparatively low resolution ^{118}Sn(^{3}He,t)^{118}Sb, ^{117}Sn(^{3}He,d)^{118}Sb, and ^{117}Sn (^{4}He,t)^{118}Sb scattering experiments were reported on in our last annual report.[1] Since then high precision energy calibration experiments and lifetime measurement experiments have increased the refinement of the suggested energy level diagram.

At present 118 gammas have been identified as very probably belonging to the de-excitation of the levels of ^{118}Sb up to about 1.2 MeV. Of these 56 gammas are intense enough to have been identified as being in coincidence with one or more other transitions.

The energy level diagram for levels up to 1.2 MeV incorporating the best present experimental information is shown in Fig. 2.

The lifetime measurements show that three of the gamma rays (238.46 keV, 187.72 keV, and 103.67 keV) that decay from the 269.6 keV state decay with a half-life of 13.3 n sec. The 115.40 keV gamma shows both a prompt (≈2 n sec.) and a delayed component with a half-life of 13.2 n sec.

Gamma ray angular distribution measurements are planned for the near future to facilitate the assignment of spins to the states. The level density in this nucleus is so high that the charged particle scattering experiments have

been of limited value for this purpose.

*Department of Physics, Western Michigan University, Kalamazoo, Michigan.

1. W. B. Chaffee, et al., Michigan State University Cyclotron Laboratory Annual Report 1971-1972, p. 32.

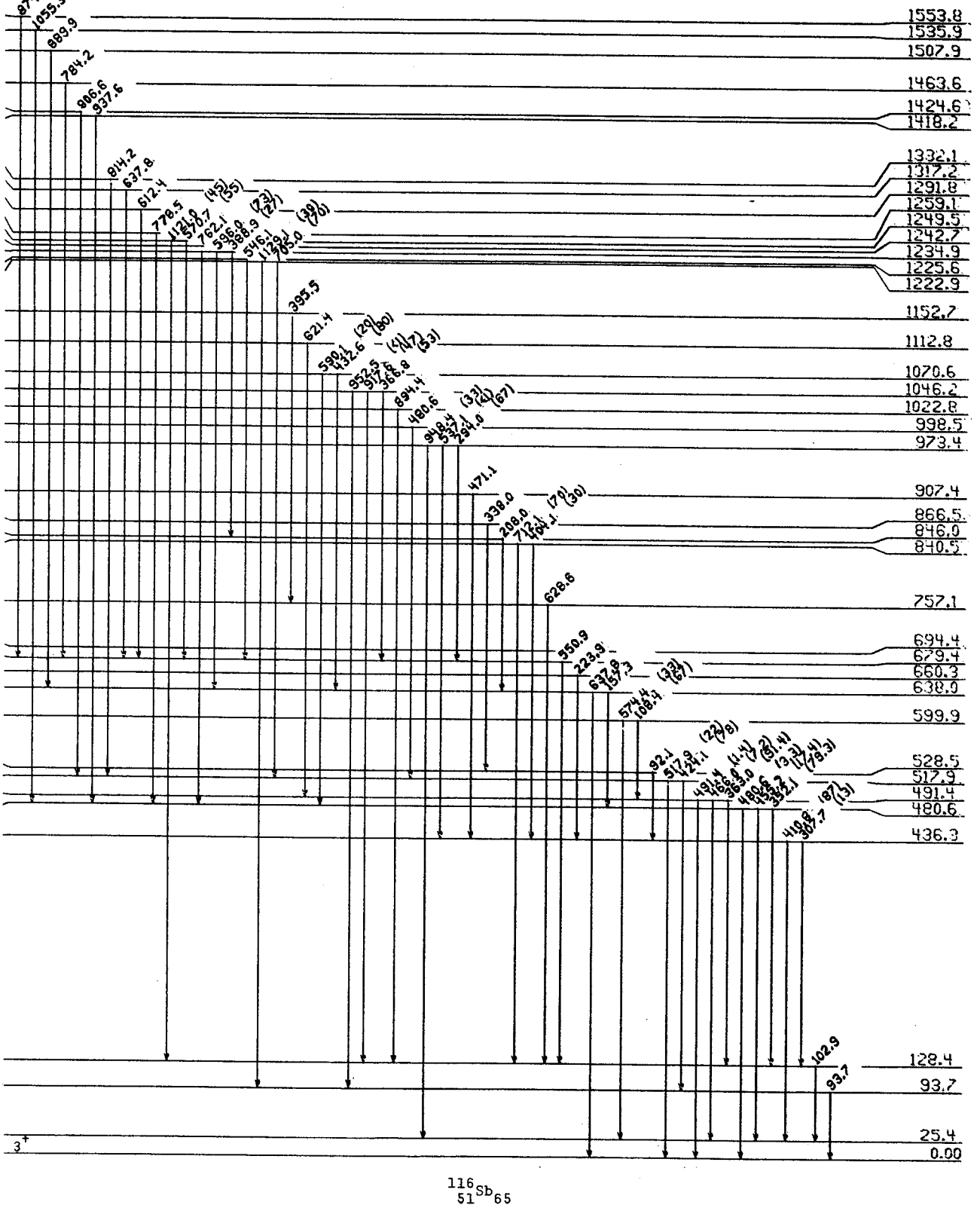

$^{116}_{51}Sb_{65}$

Fig. 1.--The preliminary energy level diagram of $^{116}_{51}Sb$ below 1.6 MeV obtained from (p,nγ) experiments. The states at 757.1 and 93.7 keV are fed by the 2.5 h electron capture decay of the 0^+ ground state of ^{116}Te. Assuming no feedings to other states, the log ft. value for decay to these two states are 4.8 and 5.3, respectively.

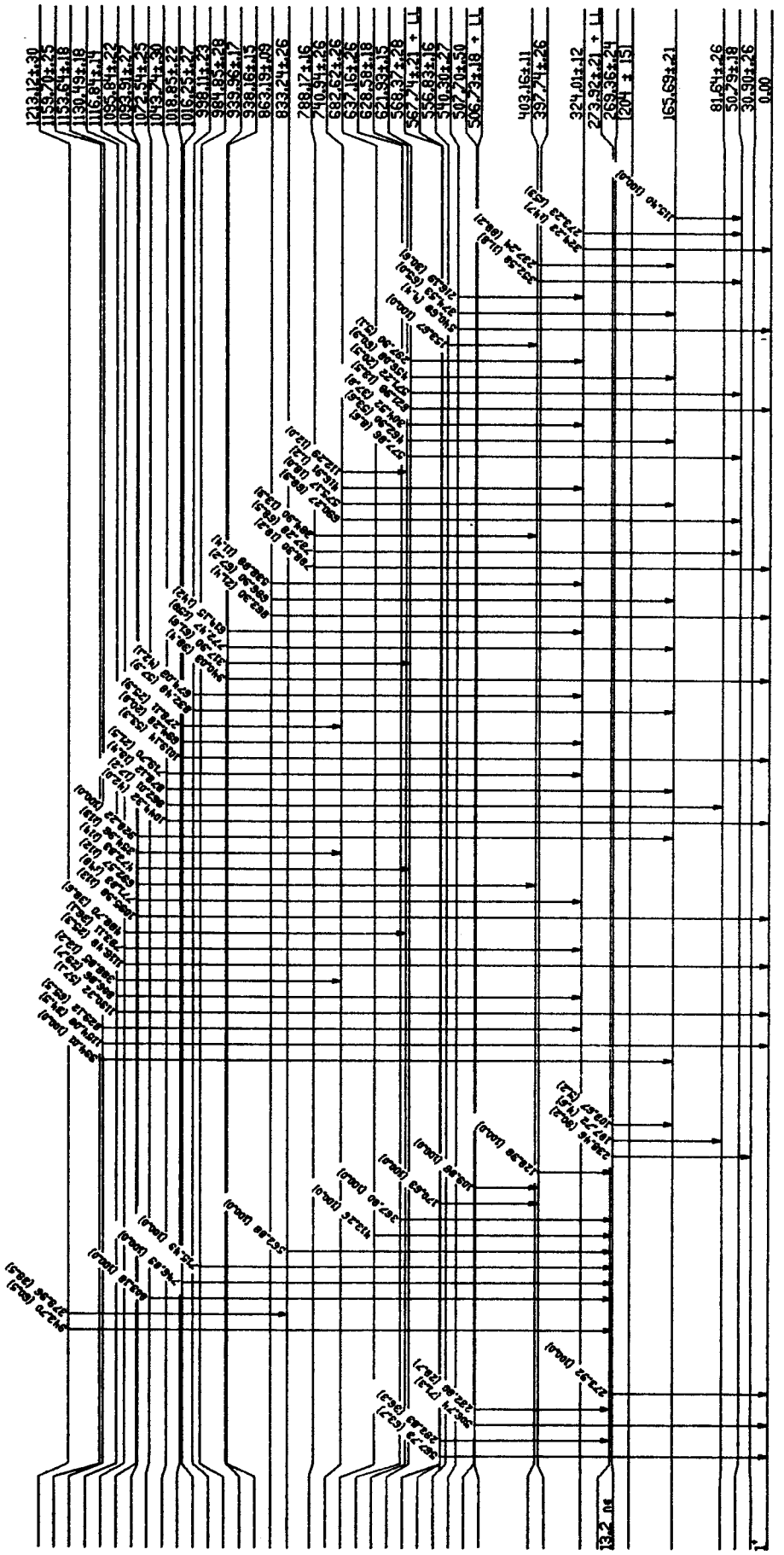

Fig. 2.--Tentative and partial energy level diagram of $^{118}_{51}Sb$.

Using the $^{140}Ce(p,n\gamma)$, $^{141}Pr(p,d)$, $^{139}La(\alpha,3n\gamma)$ and $^{142}Ce(p,3n\gamma)$ to Study the Odd-Odd Nucleus ^{140}Pr

Jean Guile, C. B. Morgan, R. A. Warner, R. W. Goles, Wm. C. McHarris
W. H. Kelly, E. M. Bernstein*, and R. Shamu*

A series of investigations of the N=81 odd-odd nuclei are underway to study the residual p-n interaction near the N=82 closed shell and to see if shape isomerism exists in these "spherical" nuclei. The high density of the states of odd-odd nuclei require the use of high resolution spectroscopies using a variety of nuclear reactions and experimental techniques in complementary ways. Last year we reported[1] the results of some initial work using the (p,nγ) and (p,d) reactions for the investigations of $^{140}_{59}Pr_{81}$. This is a continuation of that study.

Figure 1 is the energy level diagram obtained involving only those states below 1200 keV that are excited in the (p,nγ) reaction. This is based upon the (p,d) reaction data, excitation function measurements with the (p,nγ) reaction and extensive coincidence measurements with the (p,nγγ) reaction. This energy level diagram represents a refinement of that reported last year, with substantial additions.

In order to clarify certain discrepancies that appeared between the present (p,nγ) data, the earlier $^{141}Pr(\gamma,n\gamma)^{140}Pr$ work of Krehbiel[1] and the (p,d) data, we have also performed some additional gamma ray experiments using the $^{139}La(\alpha,3n\gamma)$ and $^{142}Ce(p,3n\gamma)$ reactions both in beam and pulsed beam. These discrepancies have been removed with the placement of a delayed state ($t_{\frac{1}{2}}$=3.0μsec) at 763.2 keV (not shown in Fig. 1). This is depopulated by a 635.7-keV gamma transition to the 0.5 μsec 127.5 keV state. The 763.2 keV state is populated via a ℓ=5 transition in the (p,d) reaction and is not populated significantly in the (p,nγ) reaction. Apparently this inhibition is due to the low angular momentum transfer of the low energy (p,nγ) reaction.

The gamma ray spectra from the $^{142}Ce(p,3n\gamma)$ and the $^{139}La(\alpha,3n\gamma)$ reactions are considerably more complex than those of the (p,nγ) reaction for approximately the same energy of excitation in the residual nucleus. This indicates that the energy level diagram is considerably more complex than that indicated in Fig. 1 or by the (p,d) data. Presumably, the additional states are higher spin states which would be excited more strongly with the higher average angular momentum transfer of the (α,3nγ) and (p,3nγ) reactions.

Considerable coincidence data have been obtained with the (p,3nγ) reaction and these are presently undergoing analysis. We are planning some gamma ray angular distribution measurements in the near future. Those, coupled with the results of our (p,d) studies, should aid in the assignment of the spins and parities of the states and the determination of the multipolarities of the gamma transitions. Comparisons of these results with limited shell model calculations should aid in the understandings of the natures of the states.

---

*Department of Physics, Western Michigan University, Kalamazoo, Michigan.

1. Jean Guile, R. W. Goles, C. B. Morgan, Wm. C. McHarris, W. H. Kelly, E. M. Bernstein and R. Shamu. Annual Report of the Michigan State University Cyclotron Laboratory (1971-1972), p. 37.

2. H. Krehbiel, Phys. Letters 13, 65 (1964).

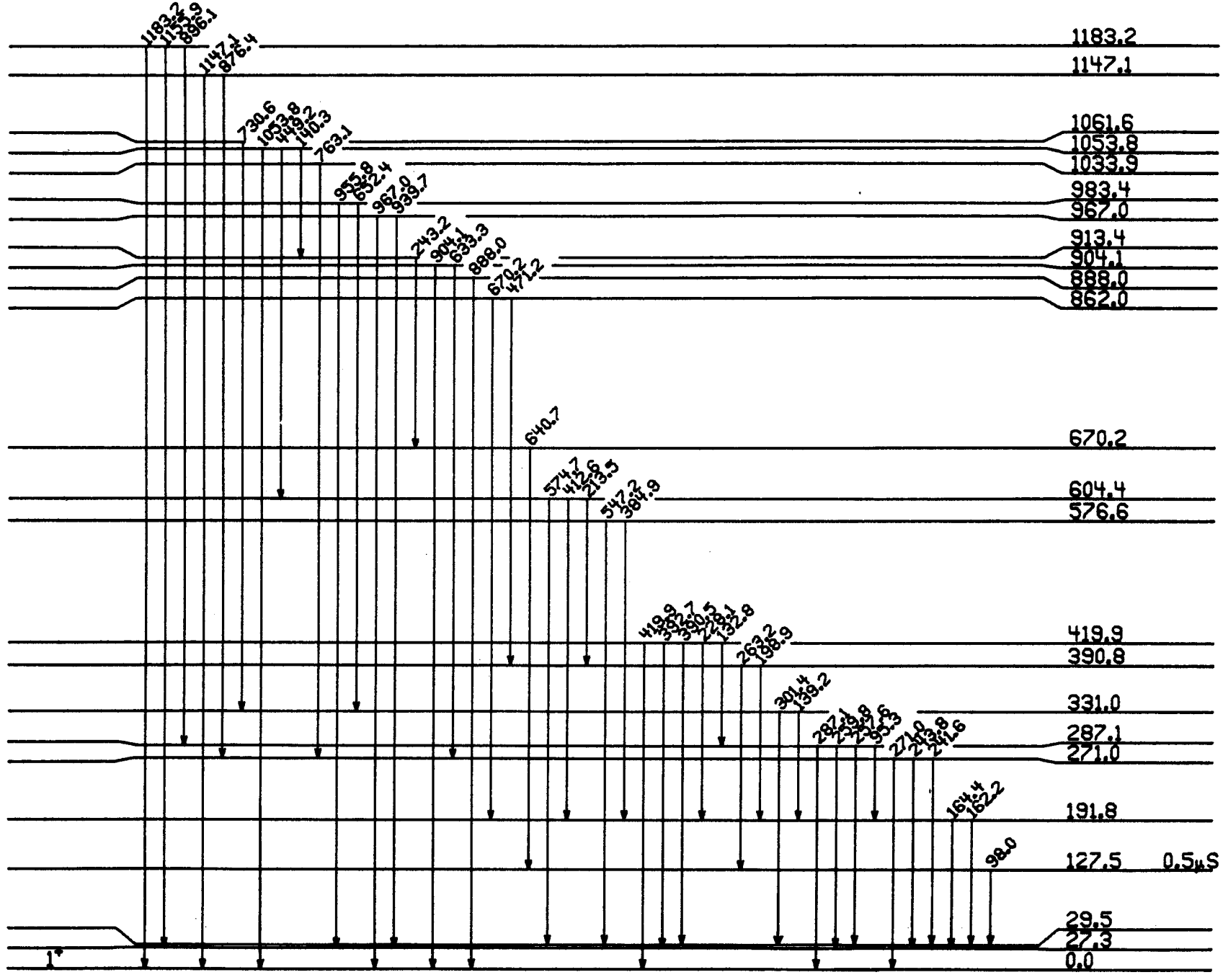

Fig. 1.--The energy level diagram of $^{140}_{59}Pr_{81}$ below 1200 keV obtained from the (p,nγ) data.

The Decay Chain $^{143}_{63}Eu_{80} \rightarrow ^{143}_{62}Sm_{81} \rightarrow ^{143}_{61}Pm_{82}$ *

R. B. Firestone, Wm. C. McHarris, and W. H. Kelly

Our work is essentially completed on the ε/β^+ decays of 2.61-min ^{143}Eu and 8.9-min ^{143}Sm.[1] These isotopes were prepared by the reaction, ^{144}Sm(p,2n)^{143}Eu, using 28-MeV protons. Extensive γ-γ coincidence measurements have been made, including two-parameter "megachannel" coincidence experiments in which the events were listed on magnetic tape to be recovered later. Also, the ε/β^+ ratios were measured, using an 8"x8" NaI(Tl) split annulus as a pair spectrometer and using x-ray vs γ-ray coincidence experiments to confirm the results. Some of these ratios are listed in Table I along with theoretical predictions.[2] It can be seen that there are some major discrepancies, although not quite so blatant as for ^{145}Gd decay.[3]

These nuclei are important both for their own sakes and also for the way they fit into our overall studies of odd-mass nuclei below N=82, where we have been able to trace proton-pair occupation numbers via β decay and have found ε/β^+ decay to three-quasiparticle multiplets.[4] The two decay schemes are presented in Fig. 1. Although it is not too obvious from the ^{143}Sm decay scheme alone, comparing its decay with that of ^{145}Gd and ^{141}Nd indicates that here again we have decay into a three-quasiparticle multiplet including the $3/2^+$ states at 1402.5 and 1514.5 keV (possibly even some of the 1056.2- and 1173.0-keV states, although these are primarily $d_{3/2}$ and $s_{1/2}$ states). We interpret this as the $h_{11/2}$ proton orbitals' receiving some occupation by pairs (not so much as in ^{145}Gd) and the $h_{11/2}$ neutron orbitals' having some small amount of vacancy, so the decay can be stylized as $\pi h_{11/2} \rightarrow \nu h_{11/2}$. Only the high-multiplicity of this decay causes it to be even as fast as it is.

Similarly, the decay of ^{143}Eu to states like those at 1536.69 and 1912.60 keV present some problems of interpretation and they may involve some sort of three-quasiparticle configuration. It is more difficult to pin this down at this point, however, and we plan to explore it further in a forthcoming paper.

*Supported by the U.S. Atomic Energy Commission and U.S. National Science Foundation.

1. For more introductory information, see our articles in last years' annual report: R. B. Firestone, Wm. C. McHarris, and W. H. Kelly, MSU Cyclotron Laboratory Annual Report for 1971-72, pp. 46 and 48.

2. P. F. Zweifel, Phys. Rev. 96, 1572(1954); 107, 329(1957).

3. R. E. Eppley, Wm. C. McHarris, and W. H. Kelly, Phys. Rev. C 2, 1929(1970); R. E. Eppley, Wm. C. McHarris, and W. H. Kelly, Phys. Rev. C 3, 282(1971).

4. D. B. Beery, W. H. Kelly, and Wm. C. McHarris, Phys. Rev. 188, 1851(1969); R. E. Eppley, R. R. Todd, R. A. Warner, Wm. C. McHarris, and W. H. Kelly, Phys. Rev. C 5, 1084(1972).

TABLE I.--Experimental and theoretical $\varepsilon(tot)/\beta^+$ branching ratios for ^{143}Eu and ^{143}Sm decays.

	State Energy in Daughter (keV)	$\varepsilon(tot)/\beta^+$ Exp.	$\varepsilon(tot)/\beta^+$ Theor.
^{143}Sm	1056.58	≡9.7	9.7
	1173.18	52±13	13
	1403.06	35±9	29
	1514.98	48±12	49
^{143}Eu	1107.15	≡0.72	0.72
	1536.69	1.3±0.2	1.17
	1565.85	0	1.21
	1715.14	1.7±0.3	1.48
	1912.60	1.5±0.4	1.95

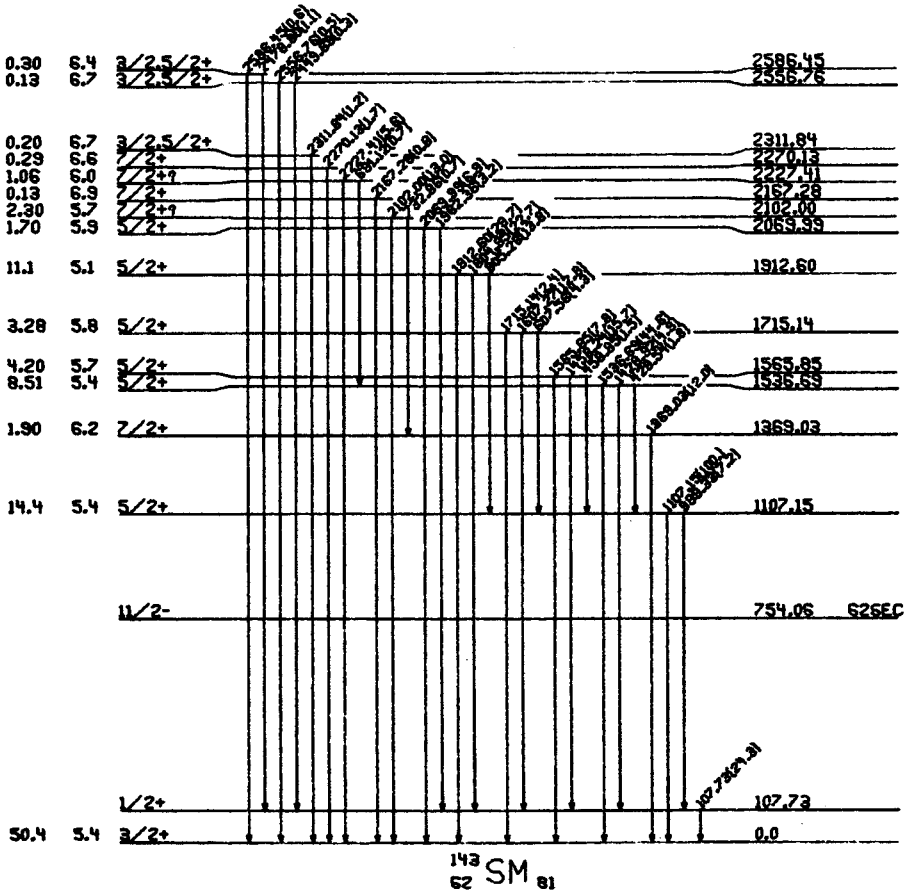

Figure 1.--Decay scheme of ^{143}Eu. Q=5 MeV, $t_{1/2}$=2.3 min.

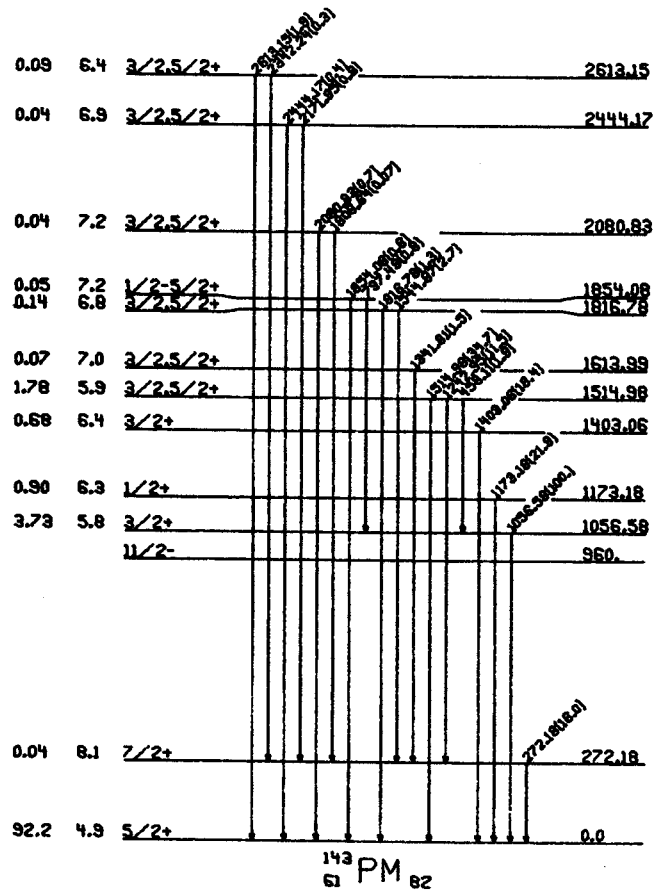

Figure 2.--Decay scheme of ^{143}Sm. Q=3.32 MeV, $t_{1/2}$=8.9 min.

Decay of ^{177}Ta to Levels of ^{177}Hf*

B. D. Jeltema and F. M. Bernthal

The EC-β^+ decay of ^{177}Ta has been under study in hopes that low lying positive parity states associated with the $i_{13/2}$ family of Nilsson single particle orbits might be seen in levels of ^{177}Hf.[1] Study of this decay has been based on γ-ray singles and γ-γ coincidence spectroscopy as described in Ref. 1, and energies and intensities of γ-rays produced by the decay are given in Table 1.

The decay scheme for ^{177}Ta is shown in Fig. 1, and represents some modification of the decay scheme proposed by West, et al.[2] Figure 2 consists of representative coincidence spectra which brought about these modifications. Figure 2a is a spectrum of γ-rays in coincidence with the 420.8-keV transitions. It can be seen that γ-rays of 313.8, 177.0, and 105.3 keV are present, corresponding to a level at 426.7 keV which is well known from ^{177m}Lu decay. This indicates that the 420.8-keV γ-ray is a transition out of the level at 847.4 keV, and represents a substantial change in the decay scheme, as West had thought this γ-ray to be a transition to the ground state from a $3/2^+$ level at 421 keV.

Figure 2b is a spectrum resulting from a gate set on the 805.7-keV γ-ray. This transition is in coincidence with γ-rays of 197.1 and 142.4 keV, and is evidence for the newly assigned levels at 805.7, 948.0, and 1002.8 keV. The level at 873.0 keV is based primarily on energy sums and differences. However, this level and the level at 805.7 keV are in agreement with the (d,p)-(d,t) reaction work of Rickey and Sheline,[3] in which $3/2^-$ and $5/2^-$ states are observed at 804 and 878 keV, respectively.

The conversion coefficients of γ-rays produced in ^{177}Ta decay are included in Table 1, and were calculated using the conversion electron data of West, et al. These data were normalized to the 249.7-keV γ-ray, known from ^{177m}Lu decay to be E2. Multipolarities listed in Table 1 were determined from the conversion coefficients using the theoretical values of Hager and Seltzer.[4]

In calculating β-decay feeding, the 78% branching to the ground state of ^{177}Hf, and the value Q_{ec}=1.166 MeV proposed by West, et al. were assumed correct. Branching ratios for the decay were then determined using the measured relative γ-ray intensities, and log (ft) values were calculated using the tables of Love and Martin.[5]

The main point of interest in this level scheme is the even parity state at 1002.8 keV. The choice of even parity for this state is based on the K conversion coefficient of the 256.9-keV γ-ray, and is considered tentative due to the large error in this measurement. If the assignment is correct, the level could be the $5/2^+[642]$ state, associated with the $i_{13/2}$ family of Nilsson orbits. Additional evidence for this assignment is the similarity of log (ft)'s of the state at 1002.8 keV, and the $9/2^+[624]$ and $7/2^+[633]$ band heads. The log (ft)'s are quite high for "allowed" β-decay, consistent with the nucleon transition over two major oscillator shells required by the $7/2^+[404] \rightarrow 5/2^+[642]$, $7/2^+[633]$, and $9/2^+[624]$ β-decay transformations. It is expected that new conversion electron data will become available shortly, hopefully allowing a more definite assignment for the parity of the 1002.8-keV level.

---

*Supported by the USAEC and the NSF.

1. B. D. Jeltema and F. M. Bernthal, MSU Cyclotron Laboratory Annual Report, 1971-72, p. 60.

2. H. I. West, Jr., L. G. Mann, and R. J. Nagle, Phys. Rev. 124, 527(1961).

3. R. A. Rickey, Jr., and R. K. Sheline, Phys. Rev. 170, 1157(1968).

4. R. S. Hager and E. C. Seltzer, Nucl. Data A4, Nos. 1 and 2 (1968).

5. N. B. Gove and M. J. Martin, Nucl. Data 10, No. 3(1971).

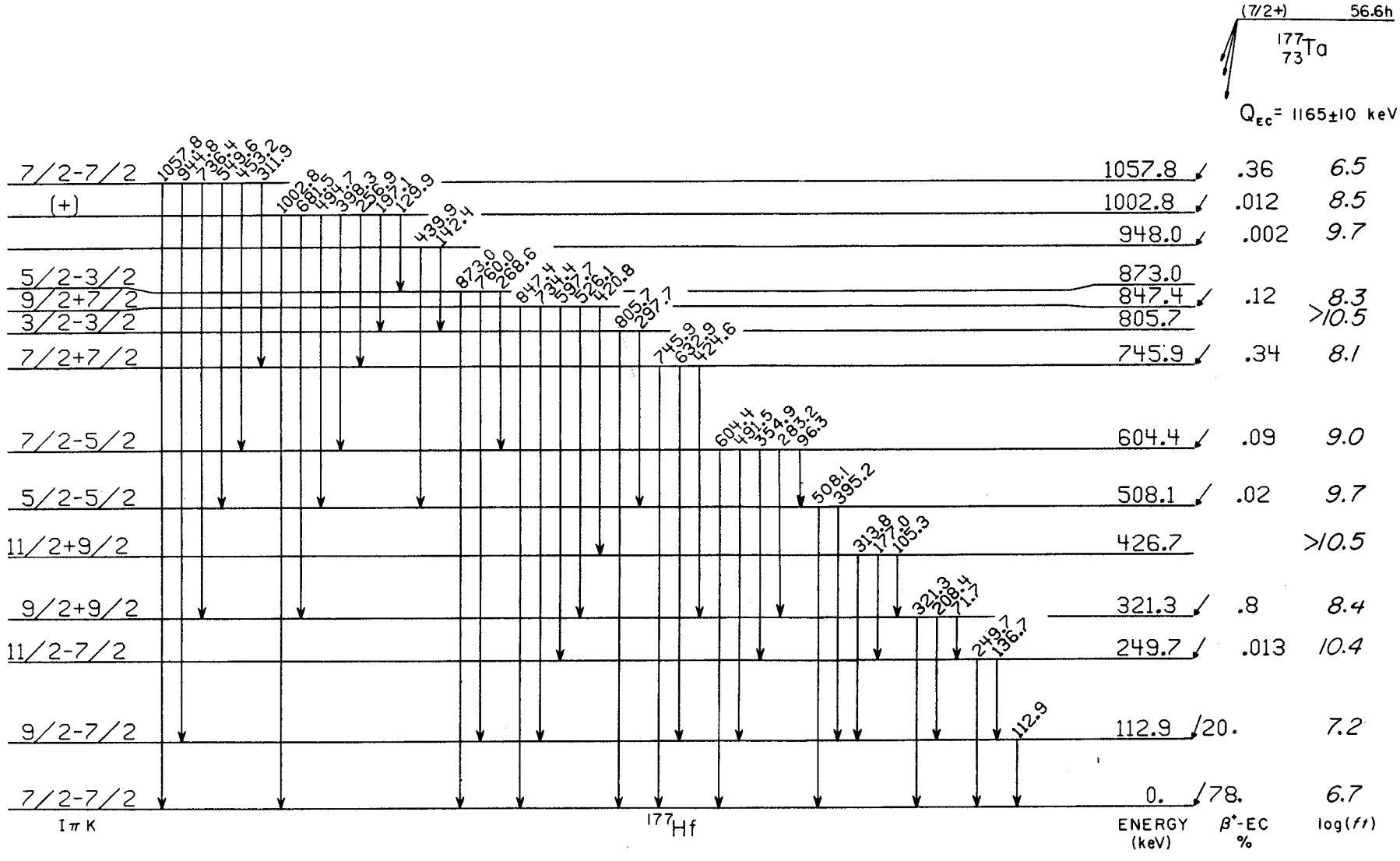

FIGURE 1.--Decay of ^{177}Ta to levels of ^{177}Hf.

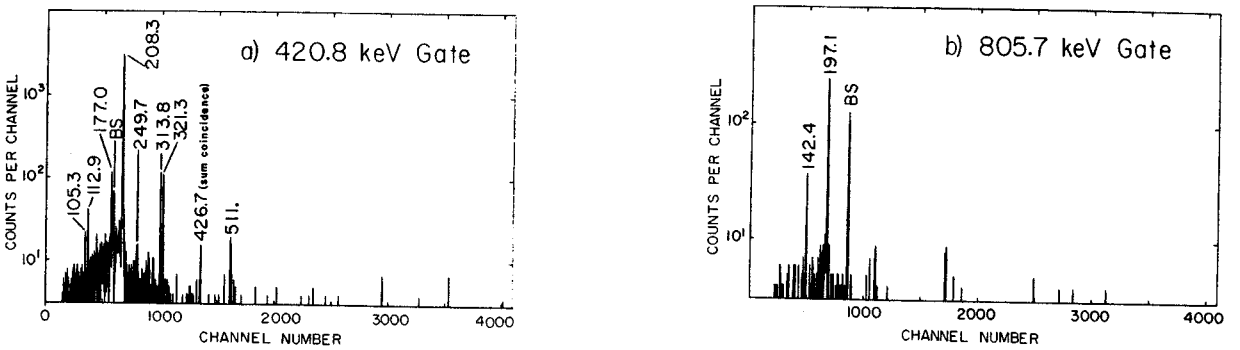

(a) (b)

FIGURE 2.--Gated coincidence spectra for ^{177}Ta decay.

γ-Ray Transitions Seen In Decay of ^{177}Ta

γ-Ray Energy (keV) [a]	γ-Ray Relative Intensity [b]	α_K [c]	α_L [c]	Multipolarity
96.3	13. ± 2.		1.2 ± .3	
105.3	8.9 ± .9			M1 + E2 [e]
112.9	10000. ± 1000.	0.63 ± .1	1.1 ± .2	E2 + M1 [e]
129.9	1.5 ± .2			
136.7	11. ± 1.	0.42 ± .04	0.39 ± .03	E2
142.4 ± .2	0.75 ± .12			
177.0	2.8 ± .3			
197.1	4.0 ± .3			
208.4 [c]	1300. ± 100.	0.043 ± .004	0.0070 ± .0006	E1
249.7	43. ± 3.	[0.090]	0.035 ± .003	E2
256.9	1.2 ± .1	0.6 ± .4		(M1)
268.6	0.18 ± .05			
283.2	0.76 ± .08			
297.7	1.8 ± .2	0.10 ± .02		E2 + ≈40% M1
311.9 ± .2	0.67 ± .07			
313.8 ± .2	0.98 ± .11	<0.3	<0.1	
321.3	30. ± 3.	0.078 ± .007	0.017 ± .002	E1
354.9	2.5 ± .2	0.06 ± .02	0.03 ± .02	(M1 + E2)
365.1	0.22 ± .05			
395.2	7.3 ± .58	0.036 ± .005		E2 + ≈20% M1
398.3 ± .2	0.78 ± .11			
420.8	43. ± 3.	0.051 ± .009	0.011 ± .003	M1 + (E2)
424.6	150. ± 12.	0.058 ± .006	0.010 ± .002	M1
439.9 ± .2	0.48 ± .10			
453.2	3.1 ± .3	0.047 ± .007		(M1)
491.5	43. ± 3.	0.042 ± .004	0.0064 ± .0007	M1
494.7	5.9 ± .6			
508.1	97. ± 8.	0.031 ± .003	0.0050 ± .0005	M1 + ≈35% E2
526.1	23. ± 2.	0.027 ± .002	0.0046 ± .0008	M1 + ≈40% E2
549.6	8.3 ± .7	0.030 ± .003		M1
597.7	13. ± 1.	0.005 ± .003		
604.4	30. ± 2.	0.0092 ± .0010	<0.002	E2 + (M1)
632.9	40. ± 3.	0.0033 ± .0004	<0.0008	E1
681.5	1.1 ± .2			
734.4	54. ± 4.	<0.0037 [d]		E1
736.4	22. ± 2.	<0.0093 [d]		E1
745.9	290. ± 20.	0.0023 ± .0003		E1
760.0	0.91 ± .09			
805.7	3.8 ± .3			
847.4	37. ± 3.	0.0015 ± .0002	0.0009 ± .0007	E1
873.0	1.2 ± .1			
944.8	76. ± 6.	0.0079 ± .0008	0.0016 ± .0002	M1
1002.8	1.4 ± .1			
1057.8	400. ± 30.	0.0057 ± .0005	0.0010 ± .0001	M1 + (≈20% E2)

a) Unless otherwise indicated, errors may be taken as ± 0.1 keV.
b) Normalized to 112.9 keV γ-ray.
c) Conversion electron data taken from West et al. (Ref 2) normalized to 249.7 keV line. Doublet not resolved in conversion electron spectra. The values of α_K represent in both cases the total electron intensity produced by the doublet.
d) Known from ^{177m}Lu decay.
e)

Decay of ^{199}Tl to Levels in ^{199}Hg*

G. Matthews and F. M. Bernthal

The region just below the ^{208}Pb doubly closed shell has been the subject of considerable interest and some speculation in recent months for several reasons, among them: (1) the apparent rotational-like structure of odd-A Hg isotopes at very high spins; (2) the discovery by the CERN group of sharp isotope-shift anomalies near ^{186}Hg; (3) the prediction of a possible "bubble" structure in ^{200}Hg. For these reasons, among others, we have begun a study of the decays of Tl isotopes into their Hg daughters. Such studies are often of great significance to the correct interpretation of the in-beam γ-ray data.

The lower-spin level scheme of ^{199}Hg is of interest in its own right, ^{199}Hg being traditionally assigned the role of a "typical" deShalit[1] core excitation nucleus. Later and more precise data have indicated that this simple picture may require modification to explain experiment. The work on ^{199}Tl decay now in its final stages in our laboratory indicates that indeed the ^{199}Hg level is not well-described by the simple core-excitation picture. The difficulties present with even the more refined treatment of Kalish and Gal[2] persist. Our decay data are consistent with the recent (d,p) and (d,t) transfer data of Moyer[3] and support the idea that the shell-model single-particle strength is in many cases fragmented among the various low-lying states in ^{199}Hg. This is especially true of the $3p_{3/2}$ shell model state; at least 4 low-lying $I^{\pi} = 3/2^-$ states are identified below 750 keV in ^{199}Hg, and none of them appears to be predominantly single-particle $p_{3/2}$, or particle-phonon ($p_{1/2}$-2^+') or ($p_{1/2}$-2^+") in character.

The ^{199}Tl decay scheme is largely unchanged from that proposed earlier,[4] and so is not reproduced here again; one problem remains to be resolved, i.e. the possible doublet character of the 455.5-keV ($1/2^- \rightarrow 1/2^-$) γ-ray, the most intense line in the ^{199}Tl γ-ray spectrum.

Details of the ^{199}Tl decay investigation will be described in a forthcoming publication.

---

*Supported by the U.S. Atomic Energy Commission and the National Science Foundation.

1. A. deShalit, Phys. Rev. 122, 1530(1961).

2. R. Kalish and A. Gal, Nucl. Phys. A175, 652 (1971).

3. R. A. Moyer, Phys. Rev. C5, 1678(1972).

4. MSUCL Annual Report 1971-72, p. 72.

New Levels in ^{199}Tl from ^{199m}Pb Decay*

M. W. Johnson, R. A. Warner, Wm. C. McHarris, and W. H. Kelly

Previous work at this facility[1] reported many new levels in ^{199}Tl populated by the decay of the 90-minute ground-state ^{199}Pb. A total of 89 transitions among 29 levels were identified with this decay. In addition, the neutron-deficient lead isotopes have relatively long-lived metastable states based on the low-lying $i_{13/2}$ neutron level. For ^{199m}Pb, a $t_{1/2}$ of 12.7 minutes has been reported[2]; the only known γ-ray emission is the 425-keV isomeric transition. Here we report several new levels and transitions from this activity.

The ^{199}Pb isotope can be produced through a variety of reactions on thallium and mercury. Most satisfactory for our purposes was the (^{3}He,4n) reaction on ^{200}Hg. This was accomplished by bombardment of a target of separated (88%) isotope ^{200}HgO with 70-MeV ^{3}He ions from the MSU cyclotron, degraded to 35 MeV with aluminum. Although this energy is slightly above the threshold for formation of ^{198}Pb, we observed the latter only in negligible amounts. The targets were then counted with Ge(Li) detectors in both singles and coincidence modes. A typical singles spectrum (Figure 1) contained approximately 125 peaks ranging in energy from x-rays through a 2751-keV transition.

Most of the peaks observed are known from the earlier work as belonging to the decay of ^{199g}Pb, but there are several new peaks as well. The most prominent addition is the 382-keV transition from the metastable state (9/2-) in the daughter nucleus ^{199}Tl to the known 366.9-keV first excited state (3/2+). Although this peak has little independent significance as it is known from other work, it is indicative of formation of high-spin ^{199m}Pb, as the ground-state decay does not populate such a high-spin state to any appreciable extent. As the $t_{1/2}$ of ^{199m}Tl is short (28 msec) compared to that of ^{199m}Pb, it is possible to use the relative intensity of this and the 425-keV isomeric transition as a function of time to determine those peaks to which the metastable decay contributes heavily. A list of such peaks appears in Table 1.

As coincidence data for this decay are currently lacking, it is not possible to say with certainty what, if any, new levels are observed from the metastable decay. However, there seems to be fairly good evidence for a new level at 2612 keV, as well as several levels proposed by Doebler but not included in his final scheme for ^{199g}Pb. The evidence is strongest for a level at 2019 keV and another at 1647 keV; however, other levels at 1602 keV, 2399.2 keV, and possible 2751.9 keV are also suggested. The latter energy must be viewed with suspicion as it is very close to that found in the decay of 15.0-h ^{24}Na, which is known to exist as a contaminant based on neutron capture. However, the peak demonstrates a time dependence consistent with a half-life on the order of 50 min, so one may suspect a component from the decay being studied. In addition, it appears that the known 1695-keV level is much more strongly populated by metastable decay than ground-state decay.

Our future plans include gamma-gamma coincidence studies and more exacting examinations of variation of intensities with time. In addition, we plan to continue examination of light lead nuclei by looking at the next odd-mass nucleus, ^{197}Pb.

*Supported by the U.S. Atomic Energy Commission and the U.S. National Science Foundation.

1. R. E. Doebler, Ph.D. Thesis, Michigan State University, COO-1779-42 (1970).

2. R. Stockendal, T. Novahov, B. Johannson, and I. Bergström, Ark. Fys. 11, 165(1956).

TABLE 1.--New transitions (energies in keV).

145.1 ± 0.15	1223.2 ± 0.15
323.4 ± 0.4	1602.2 ± 0.2
387.1 ± 0.1	1891.0 ± 0.5
416.5 ± 0.4	2399.2 ± 0.4
896.1 ± 0.4	2612.9 ± 0.4
947.3 ± 0.17	2751.9 ± 0.4

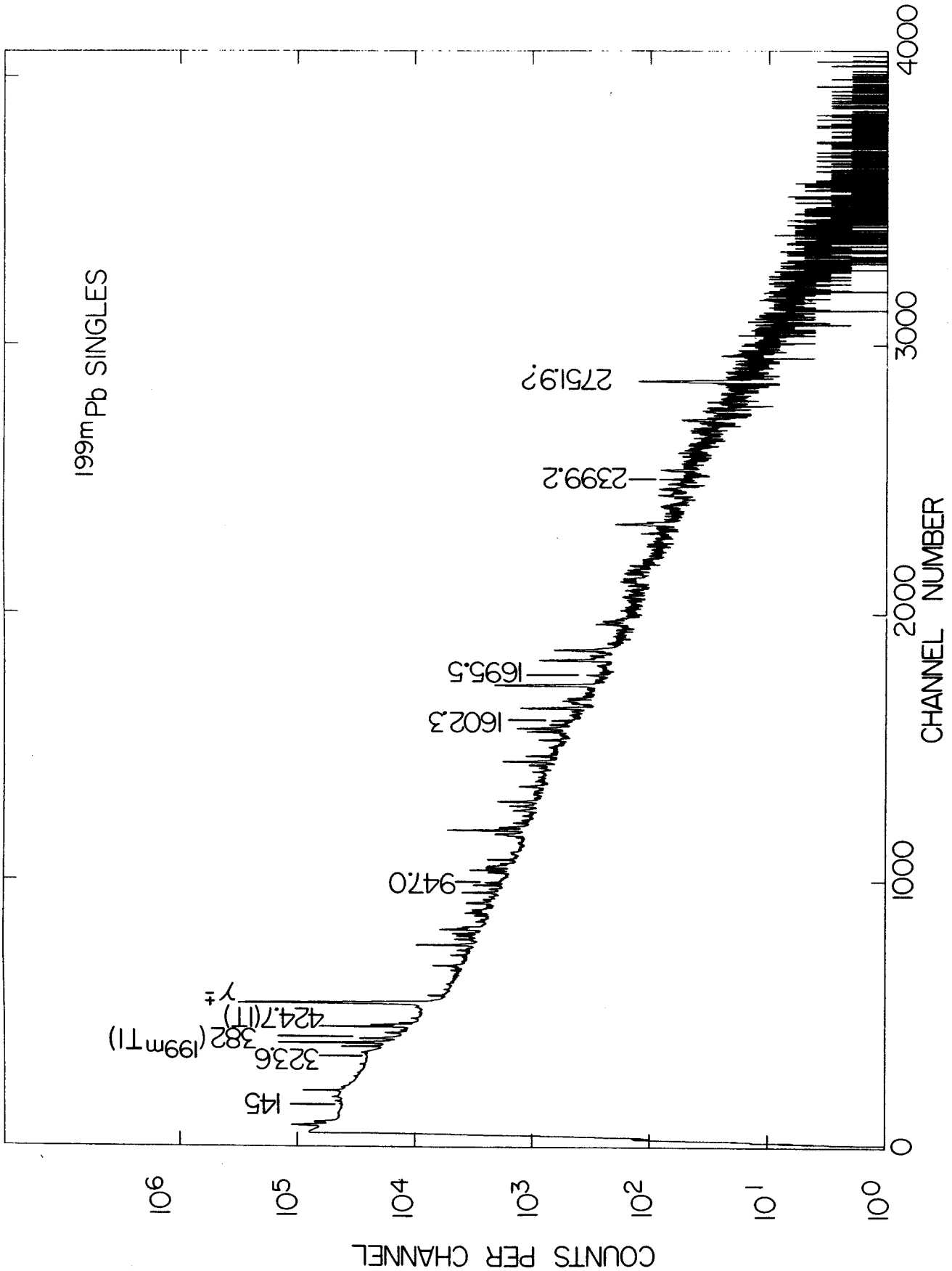

Figure 1.--Single γ-ray spectrum for ^{199m}Pb decay taken with a 10.4% Ge(Li) detector.

An Experimental Demonstration of Backbending from a Band-Crossing in ^{154}Gd

T. L. Khoo, F. M. Bernthal, J. S. Boyno and R. A. Warner

At high spins the rotational bands of a number of nuclei exhibit a phenomenon commonly referred to as back-bending--a name derived from the characteristic S-shaped plots of the moment of inertia, $2\mathcal{J}/\hbar^2$, vs the square of the nuclear rotational frequency, $(\hbar\omega)^2$.[1-3] This anomalous behavior has been attributed to the Mottelson-Valatin[4] effect, which is a phase transition from the normal superfluid state to one in which the nucleon pairs have been coherently broken by the Coriolis force. It is also possible to explain the back-bending effect in terms of a band which intersects the ground band to become the yrast band.[5,6] The question then reduces to one of the intrinsic character of the band. This intersecting band might be the Mottelson-Valatin[4] type unpaired band, the decoupled band of Stephens and Simon,[5] or perhaps even a quasiparticle or vibrational band. However, until now there has been no experimental evidence that explicitly demonstrates the band-crossing feature. We shall show here a case in which back-bending in the yrast band can be directly attributed to band-crossing.

The levels of ^{154}Gd have been studied by means of the ^{154}Sm(α,4n)^{154}Gd reaction using α-beams from the Michigan State University sector-focused cyclotron. Both γ-singles and γ-γ coincidence measurements were performed with Ge(Li) detectors of 4.5 and 8% efficiency (at 1.3 MeV). Measurements of the angular distributions of the γ-rays as well as the γ-γ coincidence experiments were performed with 48 MeV α-beams, while excitation function measurements were made with beams of 41, 45, 48 and 50 MeV. Supplementary singles data from the ^{152}Sm(α,2n)^{154}Gd reaction with 24 MeV α's were also accumulated.

Members of two rotational bands--ostensibly the ground and β-bands--have been identified and these are shown in Fig. 1. There is an ambiguity regarding the spin 18 members, and for Fig. 1, the yrast and yrare levels have been grouped together--an yrare level is defined here as the first excited state above the lowest (yrast) state of the same spin. Other levels not included in Fig. 1 have also been observed and these are presently being investigated.

The interband to intraband ratios, given in brackets in Fig. 1, show a dramatic increase from $<10^{-3}$ to 1.4 as I' increases from 12 to 18. It can be shown that unless there is a crossing of the ground- and β-bands, the B(E2) values of the transition from each of the spin-18 members cannot have the comparable magnitudes observed. The observed B(E2) branching ratios thus provides evidence that there has been a crossing between I=16 and 18. It is in fact possible to account for all the observed B(E2) branching ratios for I=12'-18' and I=18 by assuming an admixture between the ground- and β-bands. Calculations involving 2-band mixing with a number of suitable interactions have been carried out which predict the B(E2) ratios satisfactorily. These calculations show that the I=18 (yrast) level actually contains more of the β-band than the ground-band, while in the I=18' (yrare) level the admixtures are reversed.

A plot (Fig. 2a) of the moment of inertia, $2\mathcal{J}/\hbar^2$, vs the square of the nuclear rotational frequency, ω^2, yields backbending curves in both the yrast and yrare sequences (filled symbols). The open symbols in Fig. 2a represent the alternative band assignment for the spin-18 levels, i.e., according to the predominant ground- or β-band structure. Clearly no backbending occurs in the predominately ground band: this is a feature of the yrast states. Furthermore, the above discussion leads one to conclude that the backbending arises from a crossing of the ground and β-bands. This is believed to be the first explicit demonstration of backbending from a band-crossing. In this regard, it should be noted that in previously reported cases, the anomalous behavior of backbending was a characteristic of the yrast states, no distinction having been made between the yrast and ground bands. The band-crossing is illustrated in Fig. 2b where the lines connect points with the same predominant (ground- or β-band) structure. Notice that points for I=12', 14', 16' and 18 fall along a straight line, indicating that the β-band behaves like a perfect motor and with a moment of inertia equal to the rigid rotor value.

For I>12, the "perfect rotor" behavior of the β-band, the rigid moment of inertia, and the small matrix elements (25 keV for I=18) between its members and those of the ground band at these high spin values, all lead one to question whether it still is the β-band as such. In fact, the data may be satisfactorily interpreted in terms of a new band which intersects the β-band to become the yrare sequence for $I \geq 12$, and further intersects the ground band to form the yrast levels for $I \geq 18$. The evidence for the intersection with the ground band has already been presented; however, we have not yet found any direct evidence for the crossing of the β-band by the postulated "intersecting band", nor is the intrinsic character of this band known. It would however, be difficult to identify it with a band formed by

decoupling two $i_{13/2}$ particles, which Stephens and Simon[5] suggest is responsible for back-bending in yrast states. Such a band would not be expected to fit the straight line of Fig. 2b since, in the decoupled limit, the band begins to form only after I=12, with the spin given by I=R+12 and the energy spacing given by $\Delta E(I \to I-2) \sim \Delta E_{gsb}(R \to R-2)$ (R, the rotational angular momentum, takes on values of 2,4..., and ΔE_{gsb} is the energy spacing in the ground state band with the appropriate I=R values.) The rigid moment of inertia of this band tempts one to speculate that it arises from a coherently unpaired Mottelson-Valatin[4] type state.

Before any definite statements can be made about the postulated "intersecting band", it is clear that further experiments are necessary. In particular it is important to determine the intrinsic nature of the yrare levels with $I \geq 12$. A detailed study of the levels in the vicinity of the I=12' state is being planned to search for explicit evidence for a band-crossing in this region. We propose to perform γ-γ coincidence measurements with the $^{152}Sm(\alpha,2n)^{154}Gd$ reaction, since this reaction tends to populate a broader range of states and might thus be more favorable for such a study than the (α,4n) or (heavy ion, xn) reactions.

A study of ^{152}Gd, using the $^{152}Sm(\alpha,4n)^{152}Gd$ reaction has also been under taken, in order to determine if the situation here is similar to that in ^{154}Gd. However, the data from this case has yet to be analyzed.

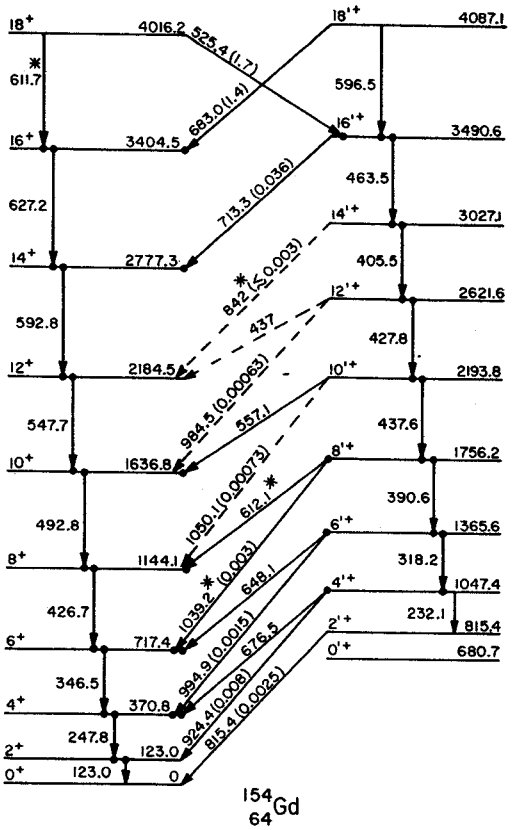

Fig. 1.--Partial level scheme for ^{154}Gd, showing the yrast and yrare bands. The numbers in brackets give the interband to intraband B(E2) ratios, B(E2 I'→(I-2)/B(E2 I'→(I-2)') or B(E2 I→(I-2)')/B(E2 I→(I-2)). The transitions indicated by asterisks are members of unresolved multiplets. The 612 keV line was separated into the $18^+ \to 16^+$ and $8^{+\prime} \to 8^+$ components based on the branching ratio, $I(8^{+\prime} \to 8^+)/I(8^{+\prime} \to 6^{+\prime})$, determined from the ($\alpha$,2n) reaction in which the $18^+ \to 16^+$ component was practically absent.

1. A. Johnson, H. Ryde, and S. A. Hjorth, Nucl. Phys. A179, 753(1972).
2. A. Johnson and Z. Szymanski, Phys. Reports 7C, 183(1973).
3. R. A. Sorenson, Rev. Mod. Phys. 45, 353(1973).
4. B. R. Mottelson and J. G. Valatin, Phys. Rev. Lett. 5, 511(1960).
5. F. S. Stephens and R. S. Simon, Nucl. Phys. A183, 257(1972).
6. A. Molinari and T. Regge, Phys. Lett. 41B, 93(1972).
7. E. Der Mateosian, Nucl. Inst. and Meth. 105, 595(1972).

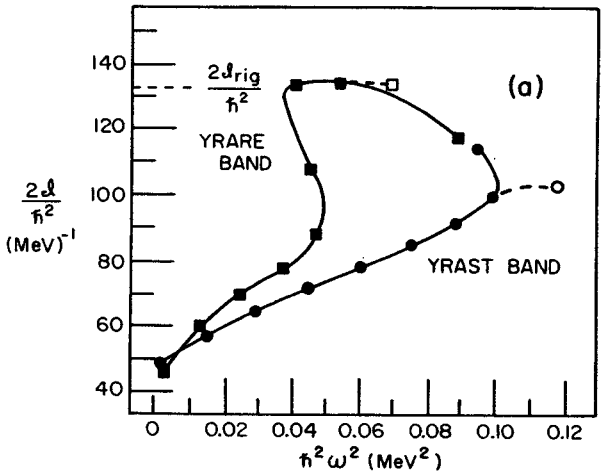

Fig. 2a.--Plots of the moment of inertia against the nuclear rotational frequency for both the yrast and yrare levels (filled symbols). The open symbols represent the alternative band assignments for the spin 18 levels. The points were obtained in the manner described in Ref. 7.

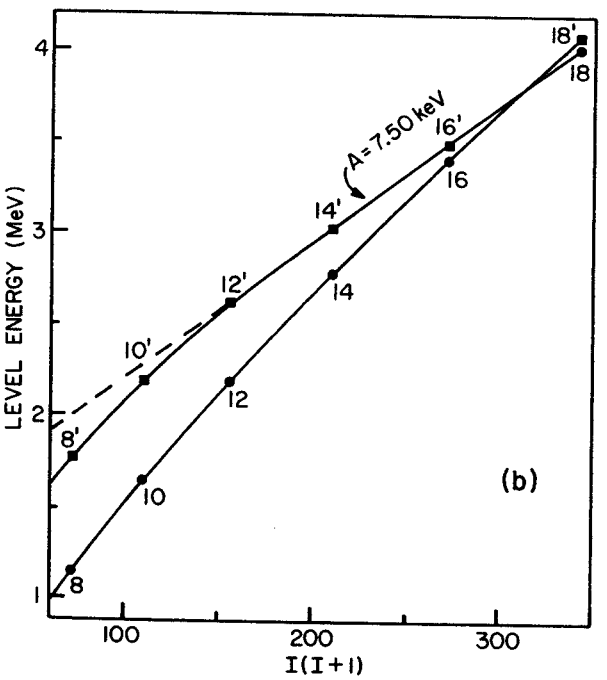

Fig. 2b.--Plot of the level energy against I(I+1). The circles and squares denote the yrast and yrare levels, respectively; the lines connect states which are either predominantly ground- or β-band. The dashed portion, which is an extrapolation of the straight line through the points for I=12', 14', 16' and 18 and which extends to E=1.45 MeV at I=0, illustrates the possible existence of the postulated "intersecting band."

Backbending in Os Isotopes*

R. A. Warner, F. M. Bernthal, J. S. Boyno, T. L. Khoo, G. Sletten,** and B. D. Jeltema

The discovery of phase transitions or backbending in ^{181}W and ^{182}Os, described in the 1971-72 Annual Report could not be understood in terms of the Stephens-Simon model.[1] For this reason we continued the search in other Os isotopes.

Self-supporting foils of separated tungsten isotopes ($^{182,184,186}W$) were prepared with the heavy-ion sputtering apparatus at the Niels Bohr Institute, and bombarded with beams of alpha particles from the MSU cyclotron. Gamma-ray spectra accompanying the (α,xn) reactions on these targets have been analyzed to establish the yrast cascades in $^{182,184,186,188}Os$. Table I contains a partial list of the transitions observed. Selected γ-ray spectra, γ-γ coincidence gates, γ-ray anisotropies, and excitation functions for ^{186}Os are displayed in Figs. 1 through 4 respectively, as representative of the data collected. In the ^{186}Os experiment more than 13 million coincidence events were accumulated, while in each of the other cases, more than 5 million events were recorded.

TABLE I.--Transition energies in keV for yrast and near-yrast cascades in four osmium isotopes.

	^{182}Os	^{184}Os	^{186}Os	^{188}Os
2→ 0	127.0	119.8	137.2	155.0
4→ 2	273.4	263.8	296.8	322.9
6→ 4	393.3	390.3	434.8	462.3
8→ 6	483.0	500.7	552.1	574.5
10→ 8	533	596.2	647.4	655.1
12→10	533	675.6	713.1	685.9[b]
14→12	493.5	712.7	658.8 776.8[a]	
16→14	479.4	528[b]	494.8	
18→16			559.5[b]	

[a]This transition feeds the 12^+ level in the yrast cascade, and displays an angular distribution and an excitation function consistent with assignment as a stretched quadrupole transition.

[b]The initial spins assigned to these transitions are less certain than are the others in the Table.

The levels shown in Fig. 2 correspond to the transitions listed in Table I. The curves in Fig. 6 result from plotting $2\mathcal{J}/\hbar^2=\Delta[I(I+1)]/\Delta E$ vs. $\hbar^2\omega^2=[\Delta E/\Delta\sqrt{I(I+1)}]^2$ for each transition. The values of $\Delta[I(I+1)]$, ΔE and $\Delta\sqrt{I(I+1)}$ are determined from Table I. The $^{178,180}Os$ curves, included for completeness, are computed from published results.[2] Attention should first be directed to the point in Fig. 6 connected by a dashed line to the other ^{186}Os points. This point is computed from the 776.8-keV transition feeding the 12^+ g.r.b. state from a non-yrast 14^+ state. The experimental level spacing and excitation function for this transition are precisely those expected for the g.r.b., while the same measurements for the yrast $14^+\rightarrow12^+$ transition yield quantities anomalous for the g.r.b. Thus the yrast states above spin 12 in ^{186}Os appear to be members of some other band. Furthermore, this band must be relatively unmixed with the g.r.b., as a search for the E2 transition from the yrast 16^+ state to the g.r.b. 14^+ state was negative. The B(E2) strength of this unseen line is less than 30% of that for the branch to the yrast 14^+ state. The intrinsic structure of the band composed of yrast states above spin 12 remains undetermined.

A perfect rotor would be represented in Fig. 6 by a horizontal line. At low spin the heavier Os isotopes appear to be the best rotors, but $^{184,186}Os$ also display two of the most pronounced examples of backbending behavior known. At first glance, this behavior seems at odds with the explanation offered by Stephens and Simon[1] for backbending in other nuclei. However, the location of the Fermi surface among the $i_{13/2}$ neutron states is not the only factor of importance to a discussion of backbending. Coriolis matrix elements also depend on the rotational parameter $\hbar^2/2\mathcal{J}$. This parameter is significantly larger for the Os isotopes than for the more deformed rare-earth nuclei for which backbending has been reported. In addition, the large hexadecapole moments found in the Os region[3] lead to a compression of the low-Ω states, thereby enhancing the mixing between the various $i_{13/2}$ Nilsson orbitals. Thus, $i_{13/2}$ neutrons may still be effectively decoupled in the even-mass Os isotopes, despite the location of the Fermi surface far from the low-Ω levels. Alternatively, Stephens, et al. have recently suggested[4] that decoupling of $h_{9/2}$ protons, apparent in odd-mass Re data,[5] may contribute to the Os backbending.

* Work supported by the USAEC and NSF.

** The Niels Bohr Institute, University of Copenhagen, Denmark.

1. F. S. Stephens and R. S. Simon, Nucl. Phys. A183, 257(1972).

2. J. Burde, R. M. Diamond and F. S. Stephens, Nucl. Phys. A92, 306(1967).

3. D. L. Hendrie, B. G. Harvey, J. C. Faivre, and J. Mahoney, Lawrence Radiation Laboratory Nuclear Chemistry Annual Report, UCRL-20426, p. 87 (1970); S. G. Nilsson, C. F. Tsang, A. Sobiczewski, Z. Szymanski, S. Wycech, C. Gustafson, I. L. Lamm, P. Moller, and B. Nilsson, Nucl. Phys. A131, 1(1969).

4. F. S. Stephens, P. Kleinheinz, R. K. Sheline, and R. S. Simon, private communication.

5. J. R. Leigh, J. O. Newton, L. A. Ellis, M. C. Evans, and M. J. Emmott, Nucl. Phys. A183, 177(1972).

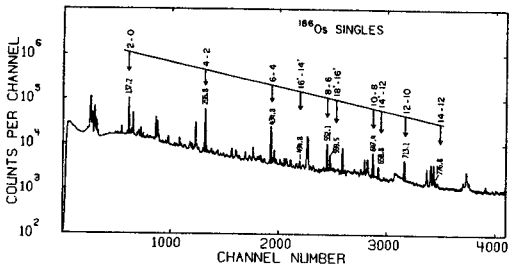

Fig. 1.

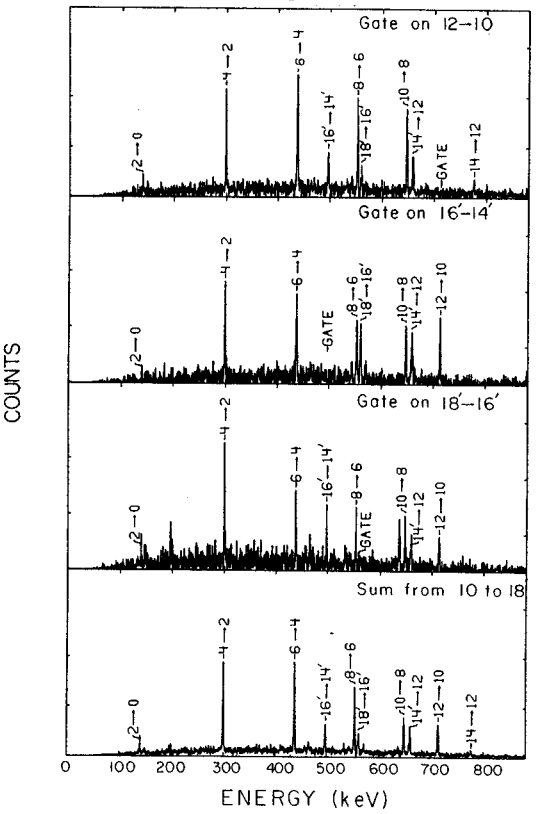

Fig. 2.

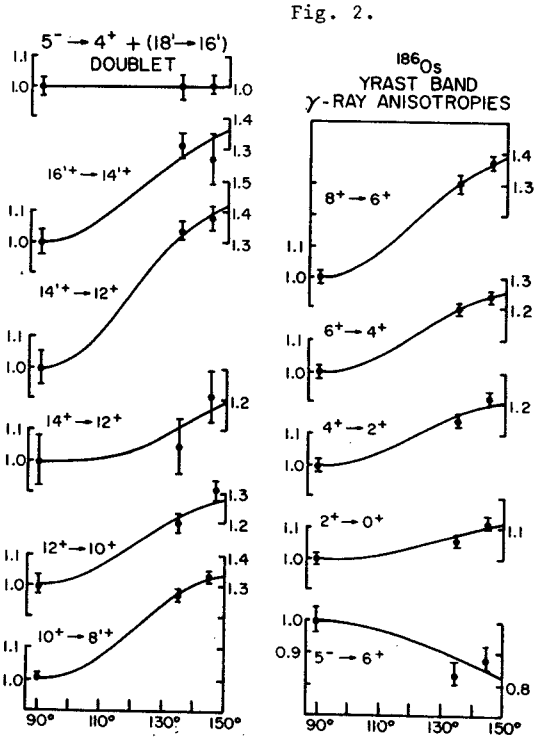

Fig. 3.

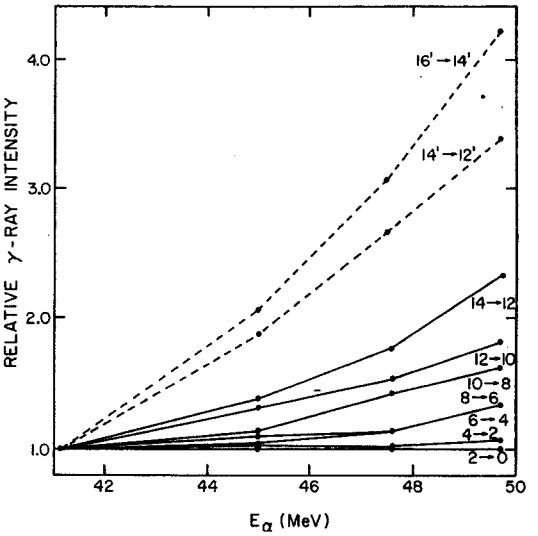

Fig. 4.

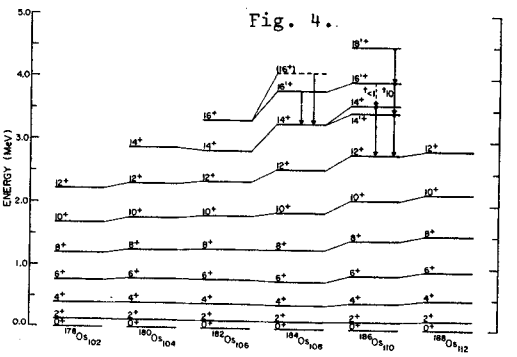

Fig. 5.

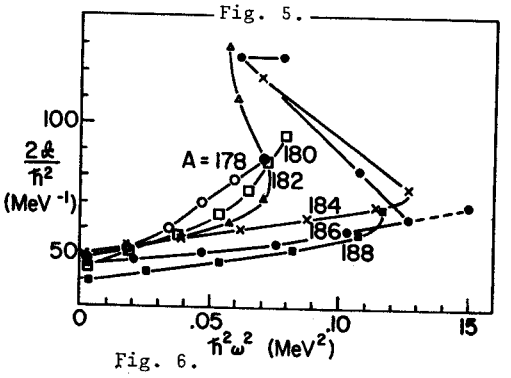

Fig. 6.

Fig. 1.--Spectrum of γ-rays resulting from 48-MeV α-particles on ^{186}W.

Fig. 2.--Coincidence spectra selected to show yrast transitions in ^{186}Os. Note the absence of the 14→12 peak in the spectra gated on the 16'→14' and 18'→16' transitions.

Fig. 3.--Anisotropies of some ^{186}Os transitions.

Fig. 4.--Excitation functions relative to the 2→0, for transitions in ^{186}Os.

Fig. 5.--Yrast and ground-state rotational band levels in even Os isotopes. The ^{178,180}Os data are from Ref. 2.

Fig. 6.--Moment of inertia plotted against the square of rotational frequency for each yrast transition in even-mass osmium isotopes. The curve joining the data for each isotope is labeled with the mass number. The ^{178,180}Os data are from Ref. 2. The quantities plotted are defined in the text.

Backbending and Forking in ^{182}W*

B. D. Jeltema and F. M. Bernthal

In the past year, the MSU γ-ray spectroscopy group has been very active in the study of backbending in rotational nuclei. This study has employed primarily in-beams γ-ray spectroscopy, using (α,xn) reactions on self-supporting targets to populate levels in various even-mass Os,W, and Gd nuclei[1,2]. In continuation of the survey of the Z=74 nuclei, we decided to deduce the levels of ^{182}W, and to look for backbending in this nucleus.

Levels in ^{182}W were populated via the $^{180}Hf(\alpha,2n)^{182}W$ reaction using a beam of 26 MeV α particles produced by the MSU cyclotron. Figure 1 shows the singles spectrum of γ-rays associated with levels of ^{182}W. It can be seen that the γ-ray energies follow the I(I+1) spacing predicted by the rotational model up to spin 12. At this spin there is a change in the pattern, in that two $12^+ \rightarrow 10^+$ transitions occur.

Three parameter γ-γ coincidence data were taken in-beam, and Fig. 2 shows the spectra resulting from gates set on ground band transitions. It can be seen that the two $12^+ \rightarrow 10^+$ transitions are in coincidence with the rest of the ground band, but not with each other. Thus there can be no doubt that both γ-rays result from transitions to the 10^+ level, and the conclusion that two distinct 12^+ levels exist must be considered. Preliminary analysis of the γ-ray angular distributions and excitation function data for these transitions allow the indicated spin assignments to be made unambiguously.

Figure 3 is a plot of the moment of inertia, $2\mathcal{I}/\hbar^2$, vs. the square of the rotational frequency, $\hbar^2\omega^2$. The plot clearly displays the backbending nature of the yrast band. In addition, the higher energy 12^+ level fits nicely on the straight line formed by the ground band, which is further evidence for the spin assignment. If these tentative spin assignments are correct, ^{182}W represents a very clear case of backbending and forking in the ground band.

*Supported by the USAEC and the NSF.

1. R. A. Warner, Backbending in W and Os Isotopes, this report, p. 68 .
2. T. L. Khoo, Backbending in Gd Isotopes, this report, p. 65 .

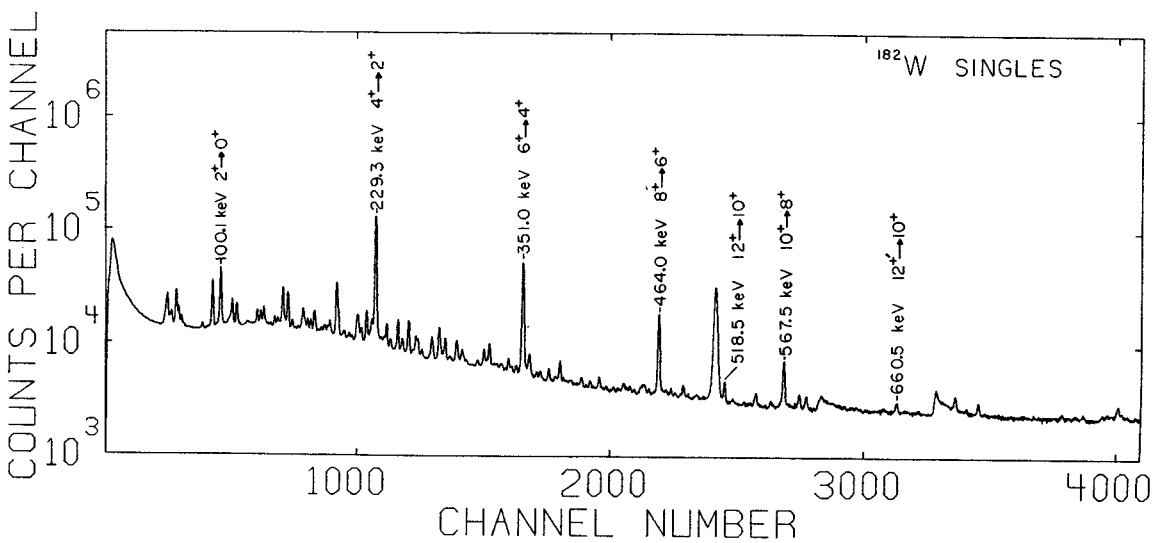

Figure 1.--^{182}W γ-ray singles spectrum.

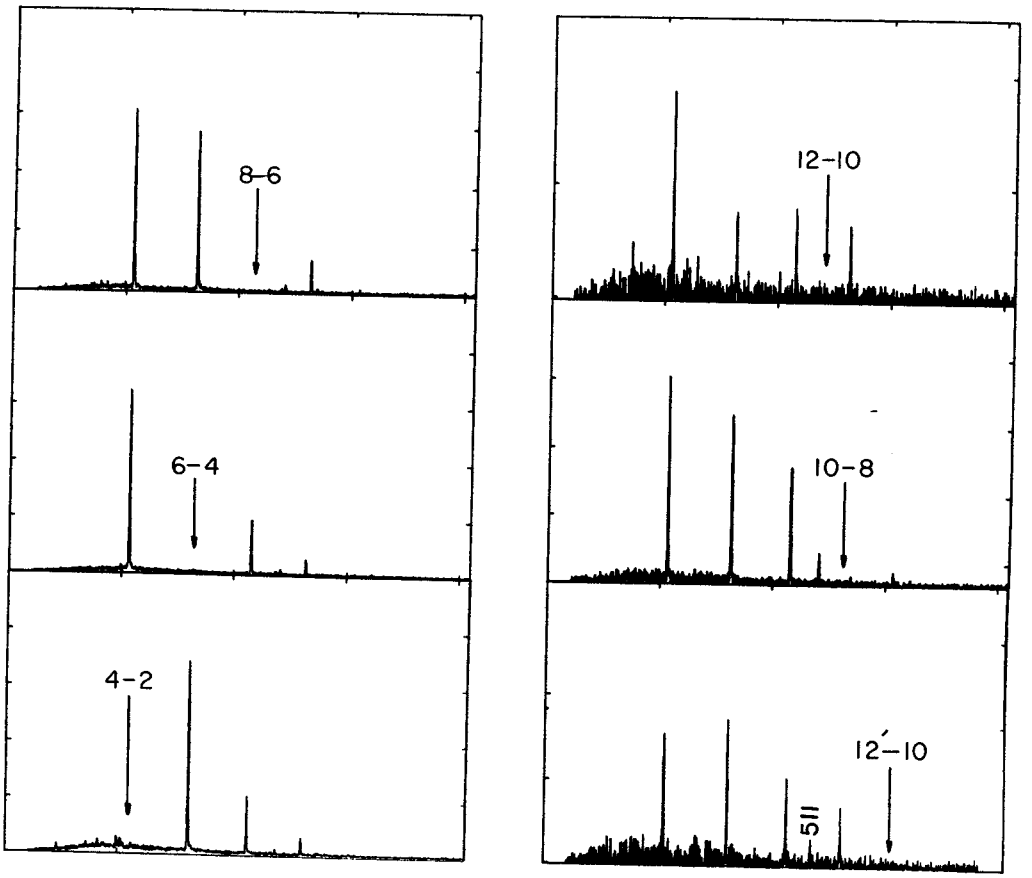

FIGURE 2.--Gated coincidence spectra of ^{182}W ground band. Arrows indicate gates.

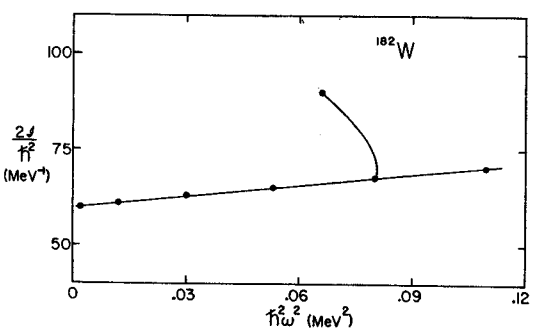

FIGURE 3.--Moment of inertia plotted vs. rotational frequency for ^{182}W.

Rotational Band Structure in the Odd-N Isotonic Series N=105-111*

F. M. Bernthal, J. S. Boyno, C. L. Dors, T. L. Khoo and R. A. Warner

Closely related to the in-beam gamma-ray investigations of rotational behavior at very high spins is the rotational band structure in the neighboring odd-A species. Our systematic study of the N=105, 107, 109, an 111 isotones is continuing; data have now been gathered for ^{179}W, ^{181}W, ^{183}Os, and ^{187}Os. Results for these four nuclei are now largely finalized[1] and preliminary data have been gathered on ^{181}Os. The experimental procedure is similar in every case: the $(\alpha,xn\gamma)$ reaction is used to populate rotational band structure in the residual nucleus, and (γ,θ) angular distribution, excitation function, and γ-γ coincidence data are gathered to support the assignments.

The initial impetus for this project was the desire to investigate the highly-perturbed unique-parity $i_{13/2}$ neutron orbitals in this region where the Ω= 9/2 and Ω= 11/2 orbitals lie near the Fermi surface. One of the most puzzling aspects of the unique-parity band structure in both odd-N and odd-Z nuclei is the apparent attenuation of the Coriolis matrix elements near the Fermi surface. Such an empirical attenuation is generally found to be requisite to an explanation of the perturbed band structure in these nuclei. Though the difficulty has been and remains oft-noted in the literature, the explanation is still an open question, though recently some promising attempts to explain the experimental data have appeared.[2]

At the same time, however, a largely unanticipated relevance of the odd-mass rotational band structure to the surprising phenomenon of "backbending" in even-even nuclei has become evident. The interpretation of the now frequently reported effect is still in doubt;[3] it is apparent however that the Stephens-Simon[4] interpretation of the "backbending" effect relies on the very same attenuation of Coriolis matrix elements as has been empirically deduced in the odd-N nuclei. Moreover, extension of the SS model to explain the very sharp effects first observed in this laboratory in the neutron-rich even-even Os and W isotopes requires evidence for decoupling of even higher-Ω_i $i_{13/2}$ neutrons from the rotation of the core of the nucleus. This evidence is provided in a qualitative way in Fig. 1, where the data from other laboratories[5] on the indicated lower-$\Omega i_{13/2}$ bands in ^{161}Er and ^{169}Hf are compared with ^{179}W, ^{183}Os, and ^{187}Os data taken in our laboratory. The former bands are understood to be largely decoupled from the core at high spins, but as the persistence of the Ω= 1/2 perturbation in ^{187}Os indicates, it is possible that even here the $i_{13/2}$ neutrons may decouple from the rotating core to produce at high spins the observed effects in the neighboring even-even species. Finally, we note that the answer to the question of what is occurring in even-even nuclei at very high spins may lie in an investigation of the odd-A species at comparable core rotational frequencies. An attempt several months ago in our laboratory to observe such very high spins in ^{165}Tm was unsuccessful. Further experiments to explore this latter possibility are planned.

---

*Supported by the U.S. Atomic Energy Commission and the National Science Foundation.

1. Cf. MSUCL Annual Report, 1971-72, pp. 63 & 65; this report, pp. and

2. I. Rezanka, J. O. Rasmussen, F. M. Bernthal, C. T. Alonso, J. R. Alonso, S. Hultberg, and M. Ryde, Nucl. Phys. A197, 430(1972); N. I. Pyatov, M. I. Chernej, and M. I. Baznat, Dubna preprint E4-5468 (1971).

3. cf. pp. and , this report.

4. F. S. Stephens and R. Simon, Nucl. Phys. A183, 257(1972).

5. S. A. Hjorth, H. Ryde, K. Hagemann, G. Lovhoiden, and J. C. Waddington, Nucl. Phys. A144, 513(1970); I. Rezanka, private communication (1973).

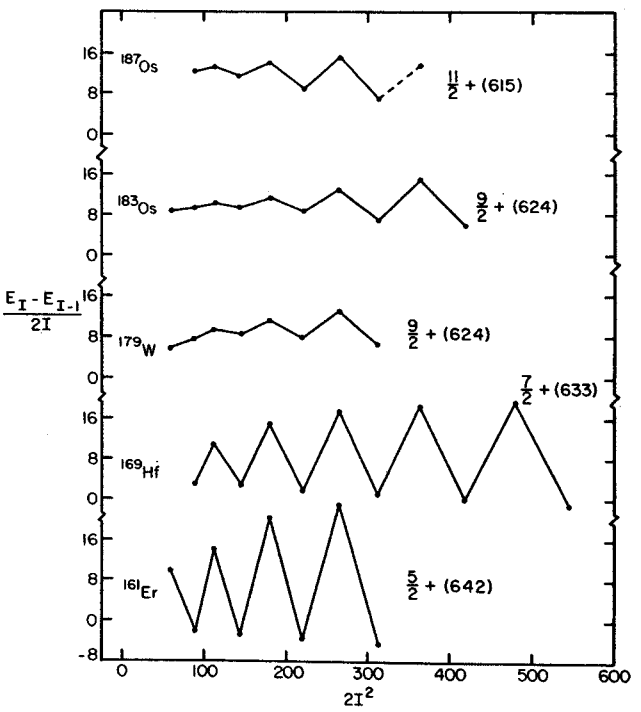

Fig. 1.--Perturbed rotational band structure for Nilsson orbitals arising from $i_{13/2}$ shell-model state. The data for ^{161}Er and ^{169}Hf are from Refs. 5.

Rotational Bands in ^{182}Re

M. Slaughter, R. A. Warner, W. H. Kelly and Wm. C. McHarris

The rotational band structure of ^{182}Re is being studied by the (α,3nγ) reaction on a 0.1 mil ^{181}Ta target. γ-γ coincidence and γ-ray lifetime measurements have been completed. Coincidence data were taken with 4.5% and 7% Ge(Li) detectors (efficiency is given at 1333 keV relative to a 3x3 NaI(Tl) detector) at a geometry of 180°. Also, Cu-Cd absorbers were placed between each detector and the target to reduce coincidences due to Compton backscattering. A tentative decay scheme consisting of the first two rotational bands that have been identified is shown in Figure 1. The rotational band structure is quite evident in the spectrum of all coincidence events shown in Fig. 2. The order of the bandheads is opposite to that reported by Hjorth, et al.[1] and is supported by the fact that the 289.2-keV transition is not observed in coincidence with any transitions of the first band (except the 154.1 keV transition which it feeds) but is seen in coincidence with the entire second band. This has also been suggested by Medsker, et al.[2] New transitions observed are 391.1, 493.8, 539.9, 584.0, 303.1, 321.4, 624.6, 281.8, 585.9, (662.7) and (647.4) keV with new levels at 1331.6 and 1634.7 keV in the first band and 1912.5 and 2233.9 keV in the second band.

Of particular interest are the similarities of the energies of the transitions between the upper members of two bands. This suggests a strong decoupling between the odd proton-odd neutron and the even-even core.

The γ-lifetime measurements were made with the cyclotron beam sweeper and a Low Energy Photon Ge(Li) detector. Ten successive spectra were taken with each counted for 54 nsec. and the results analyzed. The upper band is found to be delayed with a half-life of 91±3 nsec. while the 443.3-keV level is fed by an unidentified prompt transition. Future work planned includes completing the analysis of the coincidence data, obtaining more accurate lifetime measurements and performing angular distributions experiments.

---

1. S. A. Hjorth, H. Ryde, and B. Skånberg, Arkiv för Fysik 38, 29(1968).

2. L. R. Medsker, G. T. Emery, P. P. Singh, L. A. Beach, and C. R. Gossett, Bull. Am. Phys. Soc. 16, 515(1971).

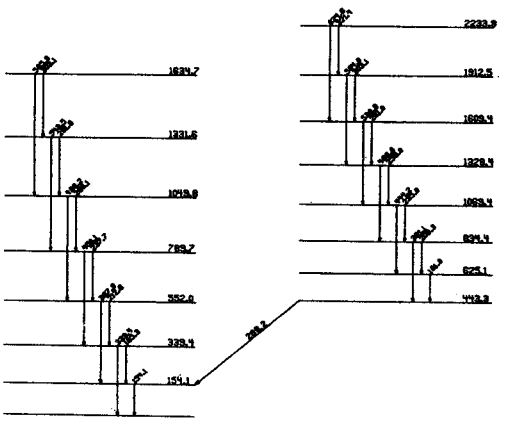

Fig. 1.--Tentative scheme of levels populated strongly in the ^{181}Ta(α,3n)^{182}Re reaction.

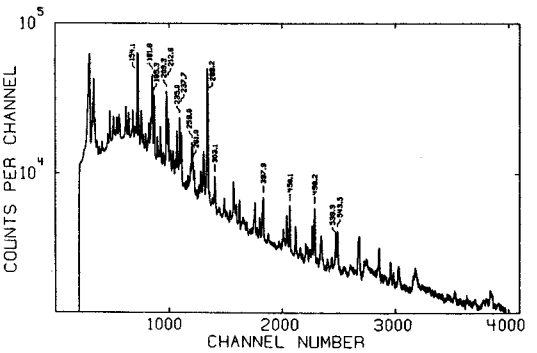

Fig. 2.--Integral coincidence spectrum for γ-rays from ^{182}Re.

Rotational Bands in ^{183}Os

C. Dors, F. M. Bernthal and R. A. Warner

Investigation of the rotational band structure of ^{183}Os is continuing via in-beam γ-ray spectroscopy. The levels in ^{183}Os are populated in the (α,3nγ) reaction on ^{182}W and in (p,3nγ) on ^{185}Re. The $9/2^+$ [624] ground band in ^{183}Os has been identified up to spin 33/2, the $7/2^-$ [514] band has been tentatively identified up to spin 15/2, and there is also evidence for the population of at least one other band, probably the 5/2 - [512].

For the (α,3nγ) studies, a self-supporting foil[1] of ^{182}W was bombarded with 38-MeV α-particles from the MSU cyclotron. Prompt γ-ray singles as well as delayed spectra were obtained. Angular distribution and excitation function data were obtained for the γ-ray singles spectrum in the region 50-700 keV with use of a low-energy photon spectrometer (LEPS) (resolution 650 eV at 122 keV). Gamma-Gamma coincidence measurements were also taken using 4.5% and 7% Ge(Li) detectors. In the delayed γ-ray experiment, the cyclotron beam sweeper was used to select one of every nine beam bursts to scan the time region ~500 nsec following the beam burst; with the sweeper off, a 500 nsec scan was made between beam bursts to search for very short-lived decays.

Preliminary results show little change from our previously reported data for the 9/2 + [624] band[2] and good agreement with the data recently reported by the Stockholm group.[3] In addition, we now tentatively place the 7/2 - [514] band head at 392.5 keV, with other members at 558.4, 749.1, 958,5, and 1180.0 keV. Further analysis should yield additional data on this band. Progress is also being made on describing the levels associated with the 5/2 - [512] and 1/2 - [521] bands, expected to lie near the ^{183}Os ground state. The ^{185}Re(p,3nγ) experiments now beginning should aid in the identification of these non-yrast bands which are populated so weakly in the (α,3nγ) experiments.

---

1. We are indebted to Dr. G. Sletten and the Niels Bohr Institute for preparing the ^{182}W foil.

2. MSU Cyclotron Laboratory Annual Report, 1971-72, p. 70.

3. R. Bethoux, P. Kleinheinz, Th. Lindblad, R. H. Price, and B. Schmidt-Nielsenn, Research Institute for Physics, Stockholm, Annual Report, 1972, p. 21.

High Spin 4 Quasiparticle States in ^{176}Hf

T. L. Khoo and F. M. Bernthal

Five high-K 2 quasiparticle bands have recently been identified[1] in the even-even nucleus ^{176}Hf, based on the following high-Ω orbitals: $5/2^-(512)n$, $7/2^-(514)n$, $9/2^+(624)n$, $7/2^+(404)p$, $9/2^-(514)p$, $5/2^+(402)p$. Four quasiparticle states with low-K couplings based on these orbitals have also been observed[2] in the decay of ^{176}Ta. It is therefore of interest to identify the corresponding high-K couplings of these 4 quasiparticle states. To this end, we have studied the delayed (by up to 0.5 μsec.) gamma rays from the ^{176}Yb(α,4n)^{176}Hf reaction at an alpha beam energy of 48 MeV. Delayed transitions from members of two known[1] $K=8^-$ bands have been observed. A preliminary analysis indicates the existence of an isomer ($T_{1/2}>0.5$ sec.) at 2827 keV, which decays to the 11^- and 12^- members of the two $K=8^-$ bands. Further analysis is necessary for a definite isomer spin assignment, but the decay pattern is consistent with the isomer having a spin of 12. Indeed, from the known 2 quasiparticle energies,[1] the lowest 4 quasiparticle state is expected to be the $K=12^+$ [7/2+(404)p, 5/2+(402)p,7/2-514)n,5/2-(512)n] configuration at approximately 3 MeV.

At a somewhat higher (100-400 keV) energy two $K=14^-$ states are expected and efforts will focus on identifying them. The energies of the 4 quasiparticle states will then be compared with those predicted from the known 2 quasiparticle energies, taking into account the various residual interactions.

---

1. T. L. Khoo, et al., Phys. Rev. Lett. 28, 1717 (1972); T. L. Khoo, J. C. Waddington and M. W. Johns, to be published in Can. J. Phys.

2. F. M. Bernthal, J. O. Rasmussen and J. M. Hollander, Phys. Rev. C3, 1294(1971).

High K States in ^{174}Hf

T. L. Khoo, F. M. Bernthal, J. S. Boyno and R. A. Warner

In the nuclei around ^{176}Hf there is a proliferation of high Ω orbitals in the vicinity of the Fermi level. This leads to the consequence that many of the low-lying two quasi-particle states in this region have large K-values. The rotational bands built on five high-K states have been observed[1] in ^{176}Hf. Similar states are also expected in ^{174}Hf.

One of the most interesting observations from Ref. 1, was that there was an unusally large interaction (210 keV) between a $K^{\pi}=6^{+}$ $(7/2^{+}[404]_{p}, 5/2^{+}[402]_{p})$ state and a $K^{\pi}=6^{+}$ $(7/2^{-}[514]_{n}, 5/2^{-}[512]_{n})$ state. Although this phenomenon was initially unexpected it can be accounted for through the residual neutron-proton interaction.[2,3]

In order to extend our understanding of this problem in the rare earth deformed region, there is a need for more experimental information on other high-K states. We have therefore begun an investigation of ^{174}Hf, using the ^{174}Yb(α,4n)^{174}Hf and ^{172}Yb(α,2n)^{174}Hf reactions. Singles γ-spectra have been recorded from both reactions, and γ-γ coincidence measurements have been performed using the (α,4n) reaction. γ-spectra, delayed up to 0.5 μsec, have also been studied. In addition to the usual analysis of the 3 parameter (E_1-E_2-T_{12}) γ-γ coincidence data for prompt coincidences, delayed coincidence relationships have also been obtained by setting appropriate TAC gates during the sorting.

Two rotational bands have been observed; one built on a known $K=6^{+}$ isomeric state[4] at 1549.4 keV has been identified to spin 12. Four members of the other band, also built on a new isomer at 1609.9 keV have been tentatively identified. This new isomer with $t_{1/2}>0.5$ μsec., decays to the known isomer through a 60.5 keV transition. Another newly discovered isomer at 3269.1 keV with a half-life >1 μsec., decays to the $IK^{\pi}=12,6^{+}$ and $11,6^{+}$ members and must therefore have a very high spin ($I\geq 12$) and a correspondingly high K. With the available Nilsson orbitals, a state of such high K is most likely a 4 quasiparticle state.

The data from the experiments are still being analysed and we expect soon to extract the intrinsic g-factors, g_K, of the observed rotational bands. As described in Ref. 1, this should lead to a knowledge of the intrinsic structure of the states.

Although attention has been focussed mainly on the high-K states, members of the ground state band have also been identified to spin 18. The levels spacings do not indicate any anomalous variation in the moment of inertia, which has been observed in a number of other nuclei (e.g., see p. and in this report).

---

1. T. L. Khoo, J. C. Waddington, R. A. O'Neil, Z. Preibisz, D. G. Burke, and M. W. Johns, Phys. Rev. Lett. 28, 1717(1972); T. L. Khoo, J. C. Waddington and M. W. Johns (Can. J. Phys. in press).
2. J. O. Rasmussen, et al. (private communication; to be published).
3. T. L. Khoo and G. F. Bertsch, this report p. .
4. H. Ejiri, S. M. Ferguson, R. H. Heffner and H. Wieman, Radioactivity in Nuclear Spectroscopy, ed. J. H. Hamilton and J. C. Manthuruthil.

Levels of ^{187}Os*

J. S. Boyno, F. M. Bernthal, T. L. Khoo and R. A. Warner

A study of the complex γ-spectra obtained in the $^{186}W(\alpha,3n)$ reaction is in progress. The level spectrum of ^{187}Os has been previously investigated with γ-ray spectra obtained from the decay of ^{187}Ir[1,2,3] and with particle spectra obtained from the (d,p), (d,t) and (d,d) reactions.[3,4] Low spin members of numerous Nilsson configurations have been identified, and this previous work is complementary to the present study. The (α,3n) reaction excites both high and low spin states of yrast and near-yrast configurations.

Coincidence measurements were performed with 35 MeV α-particles bombarding a self supporting target of ^{186}W. Two 7% Ge(li) detectors were used for γ-γ coincidence measurements. In addition, γ-singles were recorded at four angles using a low energy photon spectrometer. This afforded us the high resolution necessary to separate closely spaced peaks and allowed us to determine, from the angular distributions, the multipolarities of the γ-rays. Other measurements were made using the MSU cyclotron beam sweeping system, which allowed us to directly measure the half lives of isomeric transitions in the 0.5-500 nsec. region.

There are approximately 120 γ-rays of between 100-700 keV in the ^{187}Os spectrum. The singles data have been fitted using the peak fitting program SAMPO, which, in one case, was used to satisfactorily ascertain the energies and intensities of a quintuplet, where there are five peaks separated in total by five keV. Preliminary analysis of the coincidence data has been performed by setting gates on approximately sixty of the stronger peaks in the spectrum, using the program IIEVENT RECOVERY. A quick analysis of the data obtained very recently in a beam sweeping experiments has shown that, in addition to the well known 156.6 keV isomer ($\tau_{1/2}$=231μsec), there are approximately ten delayed transitions, with half-lives in the 2-20 nsec range.

A preliminary level scheme is shown in Fig. 1. As expected, we excite the yrast, $11/2^+[615]$ band to high spin. The compression evident in the ΔE(I,I-1) values for the 17/2→15/2, 21/2→19/2 and 25/2→23/2 transitions is similar to that observed for the lower spin members of the i 13/2 neutron band in lighter rare earth nuclei.[5] This is indicative of the strength of the Coriolis interaction which mixes the i 13/2 levels, the alternate compression being due to the effect of the $1/2^+[660]$ level.

Somewhat surprisingly the $3/2^-[512]$ band is rather strongly excited up to the spin $15/2^-$ member. The (α,3n) reaction is expected to populate yrast and near yrast levels, and both the $9/2^+[624]$ and $7/2^-[503]$ band heads are known to be in the low energy region of this spectrum (cf. Fig. 1). Further analysis will undoubtedly reveal the rotational levels of these latter bands, but the fact remains that the $3/2^-[512]$ configuration is strongly excited.

Further analysis will include recovery of further coincidence gates and the planned running of excitation function experiments which are useful in determining the spin of transitions in (α,xn) reactions.

---

*Supported by USAEC and NSF.

1. K. Ahlgren and P. J. Daly, Nucl. Phys. A189, 368(1972).

2. S. G. Malmskog, V. Berg, B. Fogelberg and A. Backlin, Nucl. Phys. A166,573(1971).

3. P. Morgen, et al., Nucl. Phys. A204, 81(1973).

4. R. Thompson and R. K. Sheline, Phys. Rev. C7, 1247(1973).

5. F. M. Bernthal and R. A. Warner, Michigan State University Cyclotron Laboratory Annual Report (1972), 65.

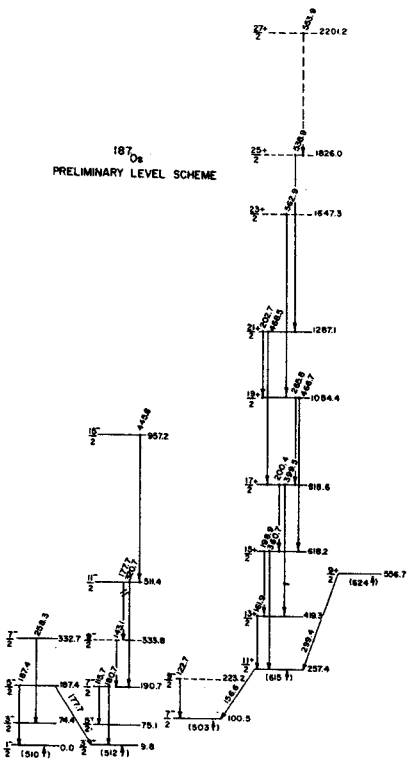

Figure 1

Nitrogen Fixation

C. P. Wolk,* Sam M. Austin, and Aaron Galonsky

As part of the long-range goal of understanding the process of cell differentiation, we have been studying nitrogen fixation in long filaments of blue-green algae. A filament contains ~50-100 or more cells, much like a string of beads, a cell being a cylinder of 3-1/2-micron diameter and 4-micron length. The cells are mostly of one type--vegetative cells; about every fifteenth cell in the variety of algae we use is of a different type. This less numerous type, the so-called heterocyst, is somewhat larger than the vegetative cell; it has a different boundary structure; and it appears obviously different when the algae are viewed under a microscope. As a filament grows, the spacing between heterocysts increases until the number of vegetative cells encompassed in ~30. Then a new heterocyst develops from a vegetative cell about halfway between the two older heterocysts--cell differentiation has occurred.

In attempts to understand the value to the organism of this transformation, it has been suggested that nitrogen for algal growth of the filament is fixed solely by the heterocysts. Although numerous, biochemical experiments have not been consistent in supplying evidence either for or against this hypothesis. As described in previous annual reports, we have determined the site of nitrogen fixation by autoradiography of ^{13}N. Under the microscope, the cell of origination was clearly identified for more than 1,000 positron tracks. More than 42,000 cells were examined. About 25% of the tracks came from heterocysts; the rest were uniformly distributed amongst the vegetative cells. The distribution function is shown by the open circles (○) in the figure; n is the number of cells to the nearest heterocyst. For comparison, the solid circles (●) represent the perfectly uniform distribution. The fluctuations of the observed distribution from uniformity are small except at n=11 and 12 where the points represent only 3 tracks and 2 tracks, respectively. With a typical spacing of 15 cells between the heterocysts, there are not many cases to be found having n=11 or 12.

One may still hold to the 100% heterocyst theory, arguing that all nitrogen enters at heterocysts and then diffuses down the filament. In our experiments the algae lived about 4 minutes between fixation and autoradiography. This time was available for diffusion. The curves through the triangles and squares in the figure are track distributions predicted on the basis of heterocyst fixation followed by diffusion. For the solid squares (■) the diffusion time constant, τ, the time for the square of the displacement from the originating heterocyst to increase by unity, =60 sec; for the open squares (□) τ=10 sec; for the solid triangles (▲) τ=5 sec. For the open triangles (△) τ=6 sec and a reasonable rate for incorporation of nitrogen into non-diffusible macromolecules is included in the calculation. None of these distributions fits the data. A fit would require $\tau \lesssim 2$ sec, a value considered by some botanists to be far below the true value.

We may conclude with reasonable certainty that heterocysts, comprising only ~6% of the cells and fixing ~25% of the nitrogen, are ~4 times as effective as are vegetative cells, but vegetative cells also fix nitrogen.

*MSU-AEC Plant Research Laboratory.

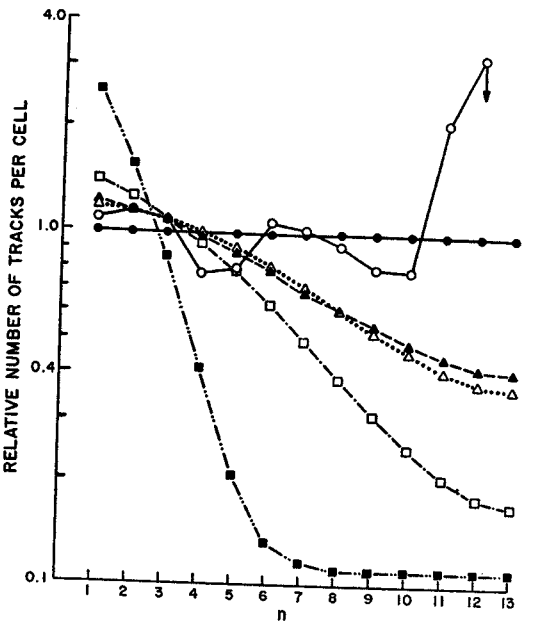

Target Fabrication

J. Nolen, H. Raut and D. Tody

The MSU target making laboratory has been in operation for several years, but considerable improvements and new developments have occured during the past year. Approximately 200 targets were made during this period of time for use at the cyclotron. A list of these targets along with some information about technique is given in the table.

Many of the isotopic targets were prepared from compounds which were reduced by Ta, Zr or C and evaporated simultaneously, as indicated in the table. Some of the self-supporting targets were made by evaporation onto a previously evaporated water soluble substrate and subsequent floating on distilled water. NaCl, $BaCl_2$, and CsI have been used as released agents, with CsI being the best in general. Other self supporting targets were made by scraping the evaporated layer from a glass slide with a razor blade or dissolving a metallic substrate in NaOH or acid. Carbon backed targets have used 10-100 $\mu g/cm^2$ commercially prepared C foils, with 20 $\mu g/cm^2$ foils being used most often. The carbon backings are often picked up on one or two layers of formvar for extra strength. Most of the targets listed in the table are on frames with 5/8" diameter holes.

New equipment in the target lab includes a homemade vacuum evaporator system with a 4" TM diffusion pump, a commercial electron gun which is used in the new evaporator, and a Cahn vacuum microbalance which is currently being modified to weigh targets during evaporation. There is currently storage space for 120 semi-reactive targets at a vacuum of ~10 microns, as well as a high vacuum ($<10^{-6}$torr) storage chamber and transfer system for 20 reactive targets. Currently under construction is a new fail-safe high vacuum storage and transfer system with a capacity of 90 targets.

TABLE.

Target Element	Chemical form of Target	Starting Material	Method of Fabrication	Backing[1]	Thickness ($\mu g/cm^2$)	Amount of Isotope required for 100 $\mu g/cm^2$ (mg)	Remarks
Be	Be	Be	Vac. Evap. Ta. tube source	S.S.	<50		scraping from glass substrate
N	Melamine	Melamine	Vac. Evap. W dimple boat	C	≤1,000		
O	MoO_3	MoO_3	Vac. Evap. BN crucible	C	<100		
	WO_3	WO_3	Vac. Evap. W dimple boat	C	<100		
F	CaF_2	CaF_2	Vac. Evap. W dimple boat	C	<200		
Na	Na	Na	Vac. Evap. Ta. tube source	C Mylar	<200 <5,000		
Mg	Mg	Mg	Vac. Evap.[3] Ta. point source	S.S. C formvar	>200 <200 <150		S.S. foil by scraping from glass substrate
$^{24,25,26}Mg$	Mg	Mg O	Vac. Evap. Zr point source[3] w/Zr powder & W, Chimney	S.S. C Au	>200 <200 <100	5.0	Ta tube source[4] used after reduction S.S. foil by scraping from glass substrate
Al	Al	Al	Vac. Evap. Al_2O_3 coated dimple boat	S.S. formvar C	>100 <25 <250		S.S. foil by CSI flotation
Si	Si O	Si O	Vac. Evap. Ta. point source	C	<500		
P	P	P	Vac. Evap. Ta. point source	C	<150		W-dimple boat also used
S	S	S	Vac. Evap. Ta. tube source	C, Au	<300		Sandwich between 2 layers of Au, also made.

TABLE.--Continued.

Target Element	Chemical form of Target	Starting Material	Method of Fabrication	Backing[1]	Thickness ($\mu g/cm^2$)	Amount of Isotope required for 100 $\mu g/cm^2$ (mg)	Remarks
	Cds	Cds	Pressing Vac. Evap. W-dimple boat	S.S. C	>20,000 <200		
	Zn S	Zn S	Vac Evap BN crucible	Au	<200		Sandwich between 2 layers of Au, also made. Sol in CS_2 used.
	Sulfonated Polystyrene	S & Poly St.	Dipping	S.S.	>1,000	-	
$^{35,37}Cl$	Nacl	Nacl	Vac Evap Ta point source	C	<200	5.0	Ta tube source also used.
K	K	K	Vac Evap Ta tube source	C	<200		
Ca	Ca	Ca	Vac Evap Ta tube source	C	<200		W-dimple boat also used.
$^{40,42,44,48}Ca$	Ca	$CaCO_3$	Vac Evap Zr point Source w/Zr powder	C Au	<200 <100	5.0	Simultaneous reduction & evaporation
Sc	Sc	Sc	Vac Evap Ta tube source*	C	<100		W-dimple boat also used.
Ti	Ti	Ti	Vac Evap Ta point source*	S.S.	<250		Scraping from glass substrate
	Ti	TiO_2	Vac Evap Ta point source*	S.S.	<250		
Cr	Cr	Cr_2O_3	Vac Evap C, crucible	C	<200		
Mn	Mn	Mn	Vac Evap Ta tube source*	S.S.	<100		Scraping from glass substrate
$^{54,56}Fe$	Fe	Fe_2O_3	Vac Evap C-crucible	C	<200	3.0	Simultaneous reduction & evaporation
			C-crucible Reduction	Havor	<1500	5.0	W-dimple boat also used*
			E Bomb C-crucible	C	<200		
Co	Co	Co	Vac Evap C-crucible W-dimple boat*	C C,S.S.	< 200		S.S. by scraping from glass substrate.
$^{58,60}Ni$	Ni	Ni	Vac Evap C-crucible Elec. Bomb C-crucible	C C	< 250	3.0	W-dimple boat also used*
$^{63,65}Cu$	Cu	Cu O	Vac Evap Ta point source Ta tube source	C	< 300	2.0	Simultaneous reduction & evaporation.
Zn	Zn	Zn	Vac Evap Ta tube source	S.S.	> 500		
		Zn O	Vac Evap Ta tube source	S.S.	>500 (1500)		Zr point source w/z powder also used.
^{64}Zr	Zn	Zn O	Vac Evap Zr point source w/z powder & W. chimney	C	<400	5.0	Ta tube source used after reduction.
Ge	Ge	GeO_2	Ta point source	C			

TABLE.--Continued.

Target Element	Chemical form of Target	Starting Material	Method of Fabrication	Backing[1]	Thickness ($\mu g/cm^2$)	Amount of isotope required for 100 $\mu g/cm^2$ (mg)	Remarks
Br	K Br	K Br	Vac Evap Ta tube source	C	<200		Ta. Point source also used.
Mo	$Mo O_3$	$Mo O_3$	Vac Evap BN crucible	C	<200		
Rh	Rh	Rh	Vac Evap W-dimple boat	C	<250		
Ag	Ag	Ag	Vac Evap Ta tube source	S.S.	>100		S.S. by scraping from glass substrate.
$^{107,109}Ag$	Ag	Ag	Vac Evap W-dimple boat	C C	<1000 <1000	1.5	
Cd	Cd	Cd	Vac Evap Ta tube source	S.S.			Scraping from glass substrate Disproportion also on heating.
	Cd	Cd O	Vac Evap Ta tube source	S.S.	>100		
^{115}In	In	In_2O_3	Vac Evap Ta point source	C.	<300	2.0	
$^{116,117,119,119,120}Sn$	Sn	Sn	Vac Evap Ta tube source W-dimple boat Al_2O_3 coated boat for melting & then rolling	S.S C	>200 <500	 2.0	Thicker targets made by rolling.
	Sn	SnO_2	Vac Evap Ta point source	C	<250	2.0	Simultaneous reduction & evaporation
Ce	Ce	Ce	Vac Evap W-dimple boat	S.S.	>500		deposition Ta Ta dissolved in 1:1 HF, HNO_3
^{140}Ce	Ce	CeO_2	Vac Evap Ta point source w/Th powder	C	< 100	10.0	Simultaneous reduction & Evap.
Pr	Pr	Pr	Vac Evap W-dimple boat Ta point source Ta tube source	C	$\leq$ 1,000		
Nd	Nd	Nd	Vac Evap Ta tube source	S.S. C	> 10,000 < 200		Similar to cerium.
^{142}Nd	Nd	Nd_2O_3	Vac Evap Ta point source w/Th powder	C	< 200	10.0	Similar to cerium.
^{144,147,148,149} $^{152,154}Sm$	Sm	Sm_2O_3	Vac Evap Zr point source with Zr powder & W. Chimney	S.S. C	> 500 < 400	4.0	S.S. by CSI floatation[4] Ta tube source used after reduction. S.S. by deposition Al, Al dissolved in Na OH.
Th	Th	Th	Vac Evap Ta tube source	C	<300		
$^{161,163}Dy$	Dy	Dy_2O_3	Vac Evap Ta point source w/Th powder	C	<200	5.0 mg	Simultaneous redn. & evap.
Ho	Ho	Ho	Vac Evap W-dimple boat	S.S. C	>500 <250		S.S. by deposit on Al, Al dissolved in Na oH.
Tm	Tm	Tm	Vac Evap Ta tube source	S.S. C	>500 <2500		S.S. by Na Cl floatation.

TABLE.--Continued.

Target Element	Chemical form of Target	Starting Material	Method of Fabrication	Backing[1]	Thickness ($\mu g/cm^2$)	Amount of isotope required for 100 $\mu g/cm^2$ (mg)	Remarks
$^{172,174,176}Yb$	Yb	Yb_2O_3	Vac Evap Zr point source w/zr powder & W. chimney	S.S. C	>500 <200	3.0 mg	Same as[4] in Sm. S.S. foil also made by scraping from glass substrate.
Lu	Lu	Lu	Vac Evap Ta tube source	C	≤50	4.00	
W	WO_3	WO_3	Vac evap W-dimple boat	C	<100		
Au	Au	Au	Vac Evap W-dimple boat Ta tube source	S.S. C Mylar Kapton Formvac	>100 <300 <500 <1,000 ≤25		S.S. made by CSI floatation
$^{203,205}Tl$	Tl	Tl_2O_3	Vac Evap Ta tube source	C	<1,000	1.5	
^{204,206,207,208}Pb	Pb	Pb	Vac Evap Ta tube source Elec-Bomb C-crucible	Form vac S.S. C S.S. C	<300 <5,000	2.0	S.S. made by scraping from glass substrate
	Pb	Pb O	Vac Evap Ta point Source Ta tube source	C	<5,000	2.0	$Pb(No_3)$[4] distoroportionates to Pbo, reduced by Ta.
	Pb	$Pb(NO_3)$					
Bi	Bi	Bi	Vac Evap Ta tube source Elec. Bomb C-crucible	S.S. C C	<5,000 <2,000 <2,000		S.S. made by separating from Ta.
	U	U	Elec. Bomb	C	<50		
U	UF_4	UF_4	C-Crucible Vac Evap W-dimple boat	C	<200		

[1]S.S., means self supporting targets, and C usually means 20 $\mu g/cm^2$ carbon plus formvar.

[2]Amount for evaporation at approximately 3 cms. distance in most cases.

[3]Ta or Zr point source means tube or ends smashed and small hole drilled in its side.

[4]Reduction is carried out and the isotope is condensed inside Ta tube boat, turned upside down. Also simultaneous reduction & evaporation has been done.

*Impurity from filament likely.

Preparation of Isotope Targets by Heavy Ion Sputtering*

M. Edmiston, F. Bernthal and J. Nolen

Isotope targets of refractory metals can be made by heavy ion sputtering.[1] Due to the small amounts of isotope usually available, cathodic sputtering (in which the material to be sputtered forms the cathode) cannot be used. Current techniques involve bombardment of the isotope with a highly focused 10kV argon beam. The ion gun, focusing assembly, and power supplies involved are complex and costly. Edwards High Vacuum manufactures an Ion Beam Etching Accessory in which an argon beam is produced in a very simple 2-electrode gun.[2] This accessory is being investigated for its possible application to sputtering refractory targets.

The Edwards equipment can produce a 200 mA beam current at 8kV. This is a factor of five less current and a little less potential than that used by others.[1] The rate of sputtering, S, is related to the current and the potential by the equation:

$$S=Ki(V-V_c)$$

where V_c is a critical voltage below which no sputtering occurs, and K is a constant depending on the metal to be sputtered.[3] Thus, using the Edwards accessory at its limit should yield a rate about one-sixth that of the equipment used by Sletten & Knudsen. For making satisfactory targets this would require continuous sputtering for several days. This should not present any problems except replacement of the cathode would be required approximately every 50 hours. We have not yet achieved such long-term, stable operation, though developmental work is continuing. It appears that it may be necessary to add one electrode to the apparatus for a small focusing effect. At present, the gun to isotope distance is 2-3 cm and over this distance the beam spreads to about 5 mm in diameter. It would be best if this could be reduced to 1-2 mm.

In preliminary trials, opaque copper films have been sputtered in about 30 minutes. The sputtering constant, K, is larger for copper than for metals of interest, but should not be more than 10-15 times larger. This would tend to indicate that sputtering yields are about as expected. Thus if the technical difficulty of long term operation can be overcome, it appears that the etching accessory may find application in sputtering.

---

1. G. Sletten and P. Knudsen, Nucl. Instr. & Meth. 102, 459(1972).

2. Edwards High Vacuum Div., The British Oxygen Co., Ltd., Manor Royal, Crawley, Sussex, England.

3. M. Pirami and J. Yarwood, Principles of Vacuum Engineering, Reinhold Corp., New York, 1961.

*Supported by the U.S. Atomic Energy Commission and the National Science Foundation.

Phase Selection Mechanisms

J. C. Collins and M. M. Gordon

For some years now, the M.S.U. cyclotron has produced small energy width (~1 part in 10^4), small radial emmittance (<1 mm-mr) beams by using a process known as phase selection.[1] By taking advantage of the longitudinal(E-ϕ)-radial coupling in particle motion, the beam phase width is defined by regulating the beam radial width using properly positioned slits. Given the excellent performance of these phase selective slits, it was deemed worthwhile to undertake a computer study of this coupling phenomenon to obtain a thorough understanding of it and determine how it is affected by various machine parameters.

The calculational procedure began with obtaining a magnetic field from "Fielder".[2] We then calculated accelerated equilibrium orbits (AEO's),[3] using which we found a central ray (CR) and a virtual ion source. We could then compare the orbits of rays with initial conditions deviating from those of the CR.

We found it convenient to define a quality factor Q using the radial separation between the CR and a ray initially displaced from it in phase by $\Delta\phi$ as:

$$Q = \Delta R/\Delta\phi = Q_{EO} + Q_x.$$

Q_{EO} is related to the radial separation between static equilibrium orbits,[4] a quantity depending mainly on $\phi_F(\tau)$ and the CR energy E, while Q_x pertains to the x component of the distance between representative phase points in the x-p_x phase plane.[3] Since Q_{EO} is easily calculated, it is the behavior of Q_x which we discuss below.

The most elegant way to view the growth of Q_x from zero at the source to its maximum (after about 10 turns), is as a resonance phenomenon existing while $|\nu_r - 1| \approx 0$ and driven by the asymmetries present in both the particle orbits and the rf times of gap crossings of the CR. The orbit asymmetries, arising from the field sector structure and the gap crossing resonance,[5] were identified by studying AEO properties. The rf asymmetries arise because the first derivatives of the rf waveform will, in general, be different from gap to gap so that time displaced particles will experience different relative energy gains at each gap. Varying the machine parameters listed below affects the longitudinal-radial coupling by changing one or the other of these driving asymmetries.

Our study concerned the effects of the number of field sectors, N, the Fielder phase curve, $\phi_F(\tau)$, the energy gain per turn, E_1, the dee angle, α (restricted to $180° \geq \alpha \geq 90°$), the relative orientation between the dees and the field sector structure, θ_{or}, and the acceleration harmonic, h.

We found that machines with N=3 have a definite advantage for phase selection over those with N=4. Magnetic fields of the latter type have highly symmetrical AEO's with almost no gap crossing resonance effect and small phase shifts between gaps. These characteristics make Q_x much smaller and insensitive to the other parameters listed above when compared with the results for N=3. In general, for N=4, $Q_x << Q_{EO}$, while for N=3, $Q_x > Q_{EO}$. These statements are valid after the first 10 or 15 turns.

This advantage for N=3 fields may be improved upon by raising $\phi_F(\tau)$ on early turns. This increases the rf driving asymmetry and can increase the final Q_x whether the rise in $\phi_F(\tau)$ is caused by a central cone or by proper manipulation of trim coil currents.

Also in fields with N=3, Q_x depends on θ_{or}, with a strong tendency for largest Q_x's to occur when the virtual ion source is located near the azimuthal center of a hill, at least for h=1, regardless of dee angle. At a fixed θ_{or}, the variation of Q_x with α is often as much as an order of magnitude, although there is no simple, general rule applicable to all θ_{or}'s and α's.

Changing acceleration harmonics obviously changes the rf times of gap crossings and, hence, the rf asymmetry effect. It also affects the gap crossing resonance so that for h=3, for instance, AEO's are very highly asymmetrical. The net result of these changes is that h=2 shows smaller Q_x's and h=3 much larger ones (for $180 \geq \alpha \geq 90°$) when compared with h=1 values.

Since all the codes used in our study assumed step-function energy gain at each gap, we investigated the effects of the electric fields present near the center of any machine by comparing the results from Devil with those from "Cyclone", a code utilizing measured M.S.U. electric field data. In general, one finds that the electric fields act to decrease Q_x by about a factor of two and modify the turn number at which the maximum value of Q occurs. The conclusion to be reached is that whenever final design orbit calculations for a phase selection system are to be made, the central region electric fields must be included.

---

1. H. G. Blosser, Fifth International Cyclotron Conference (Butterworths, London, 1971), 257.
2. M. M. Gordon and D. A. Johnson, AIP Conf. Proc. 9, 291(1972).
3. M. Gordon, IEEE Trans. Nucl. Sci. NS-13 (4), 52(1966).
4. H. S. Hagedoorn and N. F. Verster, Nucl. Instr. and Meth. 18-19, 201(1962).
5. M. Gordon, Nucl. Instr. and Meth. 18-19, 268 (1962).

Operation of the rf Beam Sweeper

T. L. Khoo, L. A. Finlayson and P. Sigg

The pulsed structure of the cyclotron beam makes it ideally suited for the lifetime measurements of short-lived isomers or for particle time of flight (TOF) studies. However, the short interval (46-70 ns) between beam pulses sometimes imposes a restriction on the lifetimes that may be measured or on the flight lengths in TOF studies. In order to extend the interval between pulses a high voltage rf beam sweeper has been constructed for use with the MSU cyclotron.

Briefly, the sweeper is an amplitude stabilized rf amplifier driven at a submultiple of the cyclotron frequency. The output of the sweeper, a sinusoidal voltage of 13-26 kV maximum (depending on the frequency, is applied to a pair of electrostatic deflecting plates, 1 m long and 25 mm apart, and located between quadrupoles 2 and 3. The phase of the applied voltage is then adjusted to deflect unwanted beam pulses onto a pair of downstream slits at Box 3. The displacement pattern of the beam bursts may be observed on a scintillator at Box 3.

The net effect is that the sweeper is used to accept 1 of n beam bursts from the cyclotron. The tuning range of the sweeper, 1.4-5 MHz, effectively imposes a restriction on the maximum valve of n that may be used. At the maximum cyclotron frequency n may, in principle, be as large as 14, but over the whole range of available cyclotron frequency n is restricted between 2 and 9. The system has so far been successfully used with n values of up to 9, with particles as energetic as 48 MeV α's. Beam intervals of up to ~0.5 μsec have thus been achieved.

The present system has been used for the observation of delayed γ-spectra from many nuclides under investigation in this laboratory. Details may be found in individual reports in this volume.

With the cyclotron rf modulation system, intervals of greater than ~1 msec have been achieved. There thus remains a gap of from 0.5 - 1000 μsec that we are unable to cover. We hope to bridge this gap with either a high voltage (>2 kV) pulser or a pulsed ion source.

Gamma Ray Coincidence Spectrum Recovery Program

C. B. Morgan, T. L. Khoo, R. A. Warner & R. Au

As a part of gamma-ray spectroscopic studies a large amount of γ-γ-time coincidence data has been taken, both two and three-dimensional. Because of the large coincidence counting rates which can be obtained in experiments in beam with nuclei containing rotational structure and the large number of transitions involved in odd-odd nuclei, we have, upon occasion, found the need to recover from 50 to 60 million events. With the present computing facilities, the limitation on recovery is the amount of spectra which can be contained within core. If the core requirements become too large, it becomes necessary to store pages temporarily on the disk. The swap time becomes prohibitively large with a small increase in program size and consequently the data recovery was very cumbersome and time consuming.

Our new technique involves the very simple procedure of sorting the data off the tape into a number of files on the diskpack. Each file is then sorted with its own set of gates, keeping within the limitations of the Sigma-7. The savings for a typical experiment can be as much as a factor of 5 or 6 in time and thousands of dollars of computed expenses because of the reduction of the need for expensive core.

New Computer Codes for the Indiana Cyclotron

M. M. Gordon and D. A. Johnson

Two new computer codes have been developed for calculating the orbits of ions moving in the symmetric magnetic field of the Indiana cyclotron, or of any similar cyclotron. The main input consists of the measured median plane field $B(r,\theta)$ which is stored in a polar grid. This grid extends from r_{min} to r_{max} in constant δr steps (equal to the magnet gap), and from $\theta=0$ (valley) to $\theta=45°$ (hill) in constant $\delta\theta=0.5°$ steps. This data is then used to calculate all the field components on or off the median plane as needed by the programs.

With θ as independent variable, the equations of motion are integrated using a very efficient predictor-corrector (Milne-Reynolds) routine with constant integration steps $\Delta\theta$. The value of $\Delta\theta$ must be a multiple of $\delta\theta$ and a submultiple of 45°. We use $\Delta\theta=0.5°$ (the minimum) when results having the greatest accuracy are required, but when some accuracy can be sacrificed for speed, we use $\Delta\theta=1°$. The minimum $\Delta\theta$, and hence $\delta\theta$, should be proportional to the ratio of magnet gap to magnet radius, which is about 1/40 for the Indiana cyclotron.

One new code "Symeon" calculates as a function of energy all of the important equilibrium orbit properties including: the hill and valley radii, the orbit rotation period, and the focusing oscillation frequencies, ν_r and ν_z. This basic cyclotron code differs from its predecessors by making specific use of the magnet symmetry. Its running speed is about 100 times faster than the previous Indiana code which it replaces. This code will become a subroutine in a least-square fitting program used to determine the trim coil currents required for isochronism.

The general orbit code "Indigo" is designed to study accelerated orbits and provide information on nonlinear effects in the radial and axial oscillations, as well as coupling effects between the radial, axial, and longitudinal motions. The equations of motion in this code utilize magnetic field components off the median plane which are correct to order z^2, that is, they contain all terms involving first and second derivatives of $B(r,\theta)$. Higher order terms are omitted because a large expenditure of time and space would be required for a relatively small gain in accuracy. The rf system is assumed to consist of two dees having constant angular width (40° in the Indiana case) which are symmetrically located in opposite valleys. It is further assumed that the rf field at each gap is so well localized that it can be represented by a delta function. Consequently, both the energy and the radial momentum change discontinuously at each gap, with the radial impulse being proportional to the rate of change of the dee voltage with radius.

Some preliminary studies have been carried out with the code Indigo using the 15-200 MeV proton field of the Indiana cyclotron. Although this field data is old and somewhat unrealistic, the results should still be meaningful in most respects. For axial oscillation amplitudes up to 0.2 in., the resultant final energy spread is less than 4 keV and proportional to z^2. This very encouraging result shows that the axial-longitudinal coupling effects are an order of magnitude smaller than previously reported. For radial oscillations with amplitudes up to 0.05 in., nonlinear effects (associated with the $\nu_r=4/3$ resonance) produce only a 4% increase in amplitude. Moreover, coupling effects between the radial and axial oscillations appear quite unimportant. The only new and significant effect observed results from the radial-longitudinal coupling. This coupling produces a compression in the phase width by a factor of 3.2 which is a direct consequence of the corresponding increase in the dee voltage with radius.

The Indigo code is not presently equipped to study the effects of field imperfections or of magnet displacements. Such effects are crucial, for example, for evaluating the results of accelerating through the $\nu_z=1$ resonance. The code is, however, equipped for a design study of the electrostatic channels required for beam extraction.

High Resolution Charged Particle Spectroscopy with the Dispersion Matching System

J. Nolen, R. Gleitsmann and G. C. Hamilton

The $^{40}Ca(p,p')$ reaction is currently being studied with the split-pole magnetic spectrograph. In this report we present some of the preliminary experimental results to indicate the capabilities of the high resolution dispersion matching system. The states of interest in this experiment are predominately $f_{7/2}$-particle $d_{3/2}$-hole states with spins 2^-, 3^-, 4^- and 5^- and isospin T=0 and T=1. These levels are found as high as 8.5 MeV in excitation energy and are relatively weakly populated in this reaction. They are important because they are relatively pure particle-hole states and their population in the (p,p') reaction is sensitive to the details of the nucleon-nucleon interaction. It is essential for this experiment to have high resolution and low background at high excitation energy.

An experimental resolution of 4-4.5 keV FWHM was attained in the spectra recorded to date. Data analysis is very preliminary but it appears that all of the particle-hole states of interest are identified and cleanly separated from nearby levels. The two figures show expanded views of the spectra near the 4^-(T=0) and 4^-(T=1) states at 5.614 MeV and 7.655 MeV excitation, respectively. The former is a member of a 16 keV doublet, while the latter was thought to be in a 4^-, 3^-. 2^+ triplet. It now appears that there may be two new energy levels in this vicinity.

In the 15° spectrum the ^{40}Ca elastic peak height to background ratio is ~10^6:1 which permits states as weak as ≲10μb/str to be seen above the background even at this low scattering angle. Since there are no slits in the beam transport system after the last 45° bending magnet, however, this background is very sensitive to the beam position and focussing conditions on target. In practice the background from the target frame is minimized by observing the count rate in a live focal plane detector with a blank target frame in position. The beam is then steered to minimize this rate prior to the plate exposures.

It is also significant that the resolution, which is empirically optimized for elastic scattering, does not deteriorate with excitation energy. Strictly speaking, the condition for simultaneous dispersion matching and kinematic compensation can apply to only one point in the focal plane at a time. The deviation is such a slow function of excitation energy, however, that it is not yet detectable at 10 MeV excitation.

The experimental resolution achievable in practice is a rapidly decreasing function of spectrograph solid angle. The present data was recorded with ~0.3 mstr aperture (1°x1°). Tests indicate that the resolution is ~50% worse with a ~1.2 mstr aperture (2°x2°). The resolution is not, however, sensitive to the slit settings of the beam transport system. These spectra were recorded with ~3μa of 35 MeV protons extracted from the cyclotron and up to 2μa of beam current on target. Even though the energy spread in this beam was probably ~15-25 keV it was not possible to improve the experimental resolution by selecting a narrower energy bite with the beam analysis system.

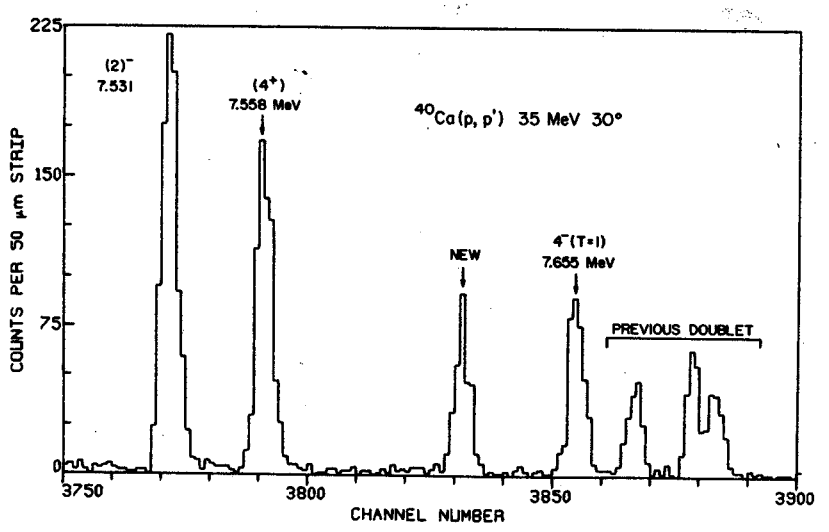

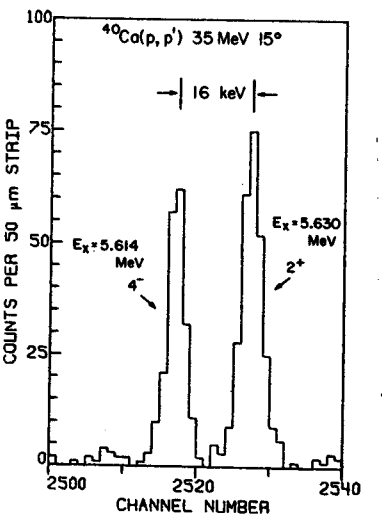

Helium-Jet Recoil Transport System*

K. L. Kosanke, Wm. C. McHarris and H. Robertson

Our initial motivation for the construction of the Helium-jet recoil-transport (HeJRT) system was its intended use as the first stage in an on-line mass identification system (see page 93). While this remains the case the HeJRT system has become a popular research tool in itself. It is being used with increasing frequency for the rapid transport of Cyclotron produced activities to a low background area for conventional nuclear counting experiments. We anticipate that the HeJRT system will remain an important research tool in itself even after we have developed an on-line mass identification system. Accordingly, a second research area is being constructed to allow the continuing use and development of the HeJRT system while the mass identification system is built in the area previously used by the HeJRT system.

A large portion of our time during the past three years has been devoted to collecting information on the operation of the HeJRT system both for the purpose of understanding its mechanism and to construct a effecient and reliable system. This collection of information is discussed in detail elsewhere[1] and only a portion of the graphical information is included here as figures 1-8. All descriptions of the experimental procedures and discussion of their results are referred to the above reference.

The target assembly of the HeJRT system has been completely reconstructed and now is of a modular design and is not encased in a larger container of helium. Each of its components is separate, beam window, collimator, target holder, recoil chamber, etc. Accordingly the assembly is quite flexible in design and changes are easily made during a run by simply loosening two wing nuts and sliding in or out new components. This now allows us to make radical changes in the assembly spending a minimum of machine shop time (by not duplicating the remaining components) and a minimum of experimental set-up time. The HeJRT system is now typically run in two configurations (steady flow[1,2] and pulsed flow[3]) and work is proceeding on a third configuration (compound gas flow, discussed below). This conversion is accomplished by simply switching recoil chambers. Figure 9 is an assembly drawing of the target assembly set up using the pulsed flow recoil chamber.

The compound gas flow configuration mentioned in the preceeding paragraph is the combination of a high purity helium-jet system and an ethylene cluster transport system.[4] The configuration has a conventional recoil chamber behind the target which is supplied with high purity helium. The jet of helium exiting the recoil chamber only travels 1 cm before entering a second chamber. Thus recoil activity is supplied to the second chamber which is free of the cluster to which it would normally be attached. A supply of ethylene is fed to the second chamber under conditions favoring the presence of ethylene clusters. Hopefully at this point the recoil activity will become bound to the ethylene cluters. A capillary is used to transport activity from this second chamber to our counting area in the same manner as in a conventional set up. The purpose of attempting to substitute non radiated ehtylene clusters for the radiated water or benezene clusters used typically, lies in the nature of the clusters and our intention of coupling the HeJRT system with an on-line mass identification system. It is hoped that the ethylene cluster will be easier to drive from the collecting surface, thereby simplifying the experimental set-up and at the same time increasing the β-recoil yield. To date we have not been very successful in our attempts, primarily because of the residual presence of bezene and pump oil, etc. in the system. The result has been to get a fair transport yield with even high purity helium flowing alone in the system.

---

* Supported by the U. S. Atomic Energy Commission and the National Science Foundation.

1. K. L. Kosanke, Ph.D. Thesis, Michigan State University, 1973.

2. R. D. Macfarlane, Wm. C. McHarris, Chapter II. C., "Techniques for the Study of Short-Lived Nuclei", to be published in Nuclear Reactions and Spectroscopy. ed. by J. Cerny, Academic Press, New York, 1973.

3. J. C. Hardy, J. E. Esterl, R. G. Sexto, J. Cerny, Phys. Rev. C3, 700(1971).

4. W. J. Wiesehahn, J. M. D'Auria, H. Dautet and B. D. Pate, Canadian J. Phys. to be published.

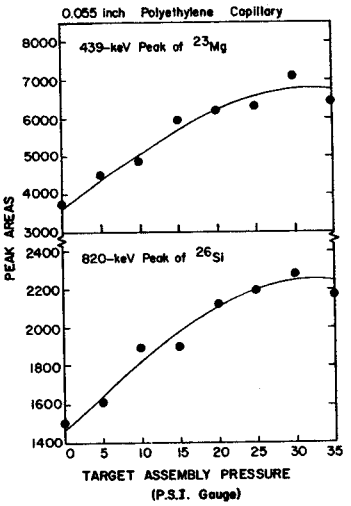

Fig. 1.--Dependence of HeJRT system efficiency on target assembly pressure using 20 ppm benzene vapor in helium.

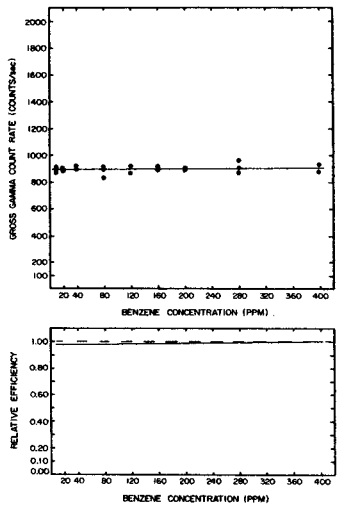

Fig. 2.--Relative HeJRT system efficiency as a function of benzene concentration.

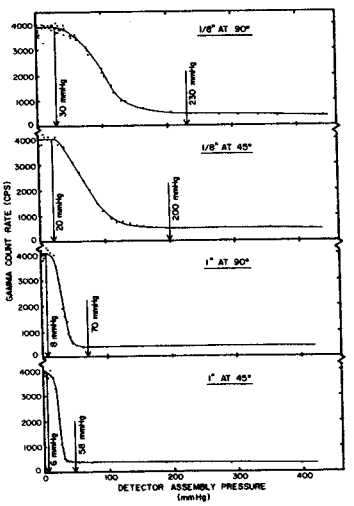

Fig. 3.--Collecting efficiency, expressed as the gross gamma count rate, as a function of collecting chamber pressure for different capillary to paper tape angles and distances.

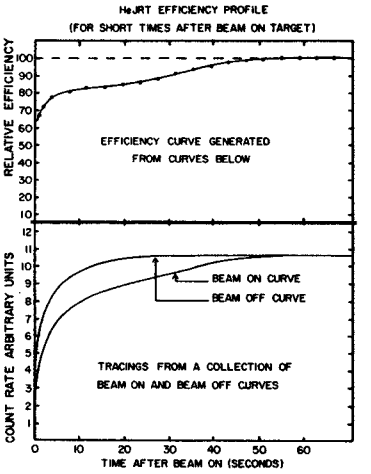

Fig. 4.--Short time efficiency profile for HeJRT system after initial cyclotron beam turn on.

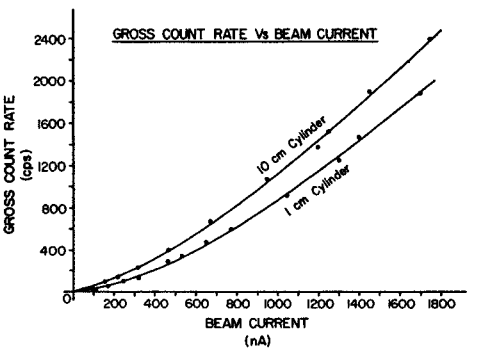

Fig. 5.--Non linear relationship between gross gamma count rate and cyclotron beam current for a long and short recoil cylinder.

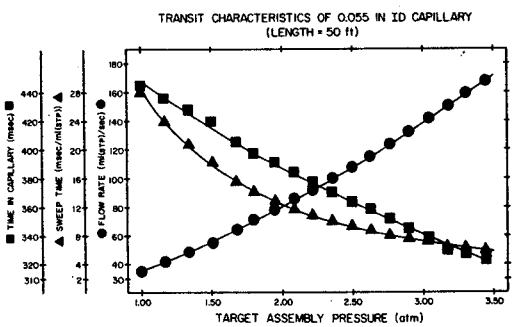

Fig. 6.--Transit characteristics of the HeJRT system using 50 feet of 0.055 inch capillary as a function of target assembly pressure.

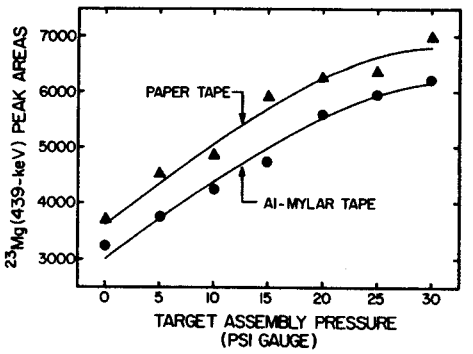

Fig. 7.--Comparison of the collecting efficiency using paper and the aluminized side of aluminized Mylar type using helium doped with 20 ppm benzene.

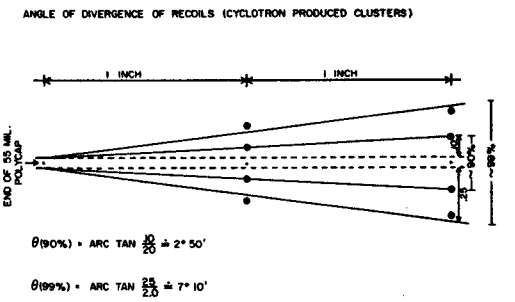

Fig. 8.--Angle of divergence of clusters generated from benzene leaving a 0.055 inch capillary under conditions of choked flow.

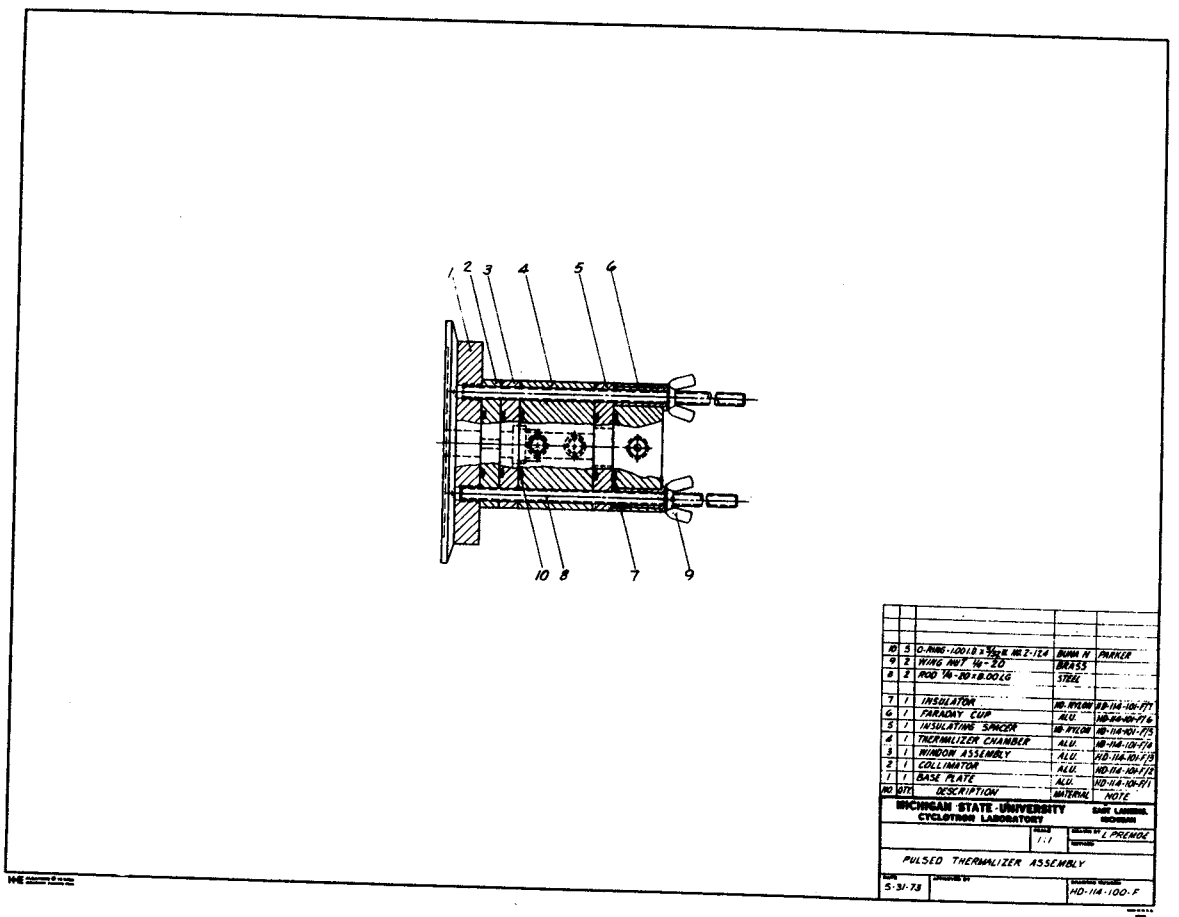

Fig. 9.--Assembly drawing of the new modular design for the HeJRT target assembly set-up in the "Pulsed Flow" mode.

Plasma Chemistry with the Helium-Jet Recoil Transport System*

K. L. Kosanke, M. Slaughter and Wm. C. McHarris

In the operation of the Helium-Jet Recoil-Transport (HeJRT) system we have observed some effects in the transport of activity that suggest the chemical nature of the nuclear recoil and the cluster molecule are important in determining the efficiency of the transport process. Further we have observed that it is possible to preferentially transport different components of a mixture of chemically differing recoils from the same target. In effect, in at least some cases, it is possible to achieve a partial chemical separation in the course of the transportation process. One possible explanation of this effect could be that the chemical nature of the recoil and cluster are effective in determining the cluster's ability to pickup and hold the recoil atoms. If this is the case, that component of a mixture of chemically different recoils which is preferentially picked up and held by clusters will, as a result, also be that component which is preferentially transported through the system. Those remaining components that are not readily picked up and held by the clusters will not have the benefit of the cluster's high transport efficiency through the system and will tend to become lost on the walls of the capillary leading to the counting area. It is, perhaps, worth pointing out that even if the above explanation is in gross error and the chemical nature of neither recoil nor cluster is the source of the effect, the effect is still real and can be used to achieve a preferential enhancement in the transport yield of chemically differing nuclear recoil in the HeJRT system.

The first observation was simply that the transport efficiency, as measured experimentally, differed substantially for physically similar recoils. For Zn, Cu and Co the total transport efficiencies are 50%, 75% and 90% respectively. These efficiencies were determined on the basis of a direct comparison of the HeJRT performance (collecting on paper tape --- 20 ppm benzene in helium) and the irradiation of thin foils. The only uncertainty in the determination lies in the range of the recoils in the target, taken from

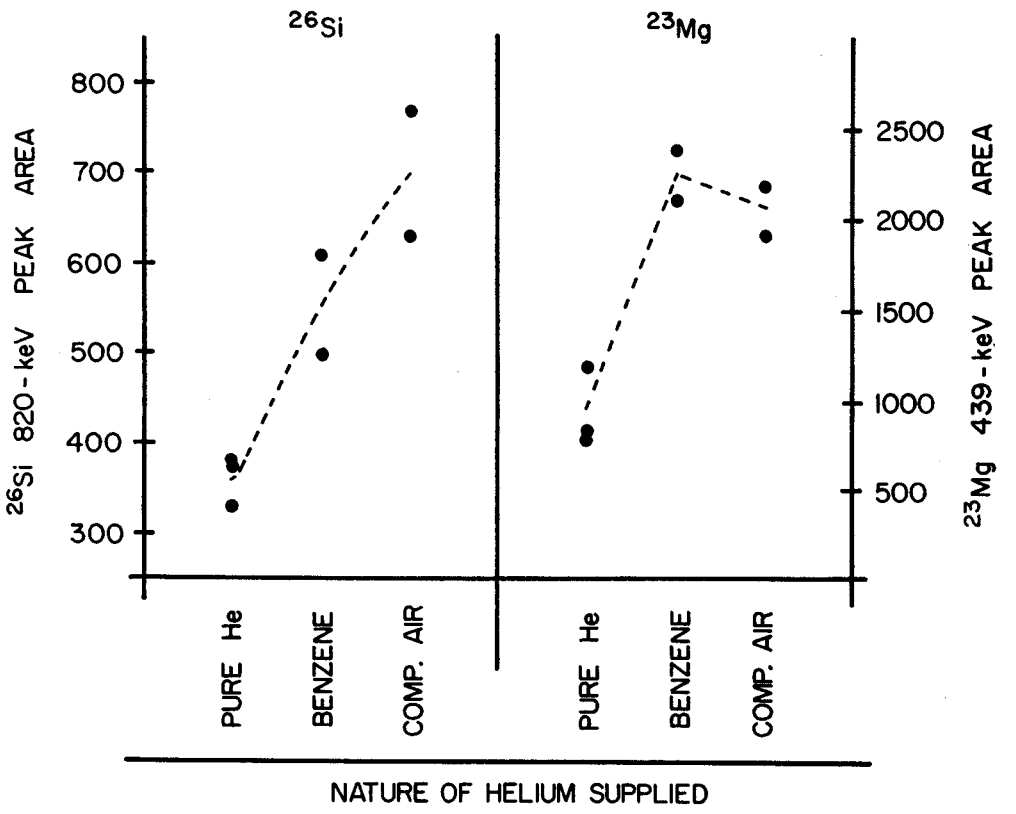

Fig. 1.--By changing the major cluster generating component in the helium supply the absolute system efficiency for a pair of activities can be made to change inversly.

Northcliffe and Schilling.[1] The second observation was that the absolute transport efficiencies for a pair of simultaneously generated activities could be shifted in opposite directions upon changing the major cluster generating component in the helium supply. The principle activities generated by a 30 MeV proton beam on aluminum are ^{23}Mg and ^{26}Si from (p,αn) and (p,2n) reactions respectively. Upon changing from compressed air to benzene as the major cluster generating component in the helium supply (there was also a small amount of water vapor present in both cases) first the ^{26}Si then the ^{23}Mg activity was preferentially transported through the HeJRT system, see Figure 1. Accordingly, it would seem the total transport efficiency of the HeJRT system is dependent on both the chemical nature of the nuclear recoil and of the molecular cluster. For a more complete discussion of these observations and their implications see K. L. Kosanke's Ph.D. Thesis.[2]

More recently when operating the HeJRT system using ethylene as the primary impurity in the helium we have observed a third effect. Again using 30 MeV protons on aluminum to produce ^{26}Si and ^{23}Mg activity it was found that the ratio of ^{26}Si to ^{23}Mg transported through the system was dependent on ethylene concentration. Preliminary results are shown in Figure 2. Both ^{26}Si and ^{23}Mg efficiencies increase with increasing ethylene concentration in the range from 50 to 200 ppm (strikingly different then when using benzene as the impurity) however the ^{23}Mg total transport efficiency increases much more rapidly in the low concentration range. The four points are the averages of a total of sixteen determinations. The error bars in the plot of ratios are just the average deviation of the points. Further runs are planned to fill in points at 25 ppm, 75 ppm and at concentrations above 200 ppm.

Thus the observations we have made are consistent with the hope that useful chemical separations can be achieved with in the HeJRT system and further that these separations will be compatible with the on-line mass analysis system described in page 93 of this report.

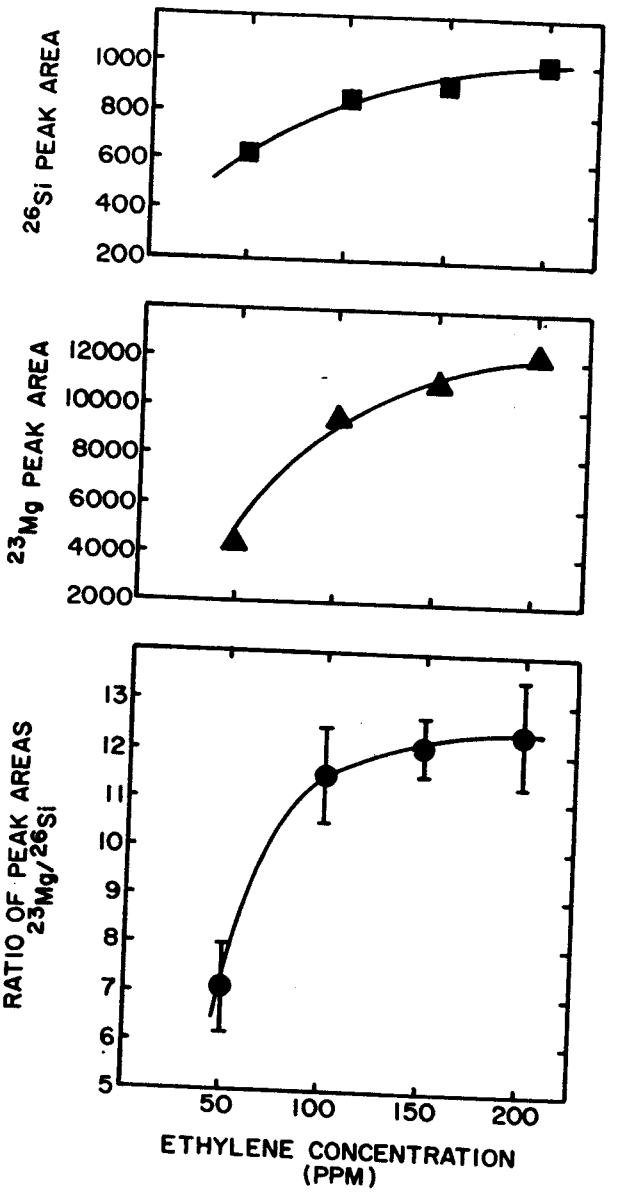

Fig. 2.--Effect of varying ethylene concentration in the helium supply on the total system efficiency for ^{23}Mg and ^{26}Si recoils.

*Work supported by the USAEC and the National Science Foundation.

1. L. C. Northcliffe and R. F. Schilling, Nuclear Data Tables, Vol-7, No. 3-4 Sec. A, Academic Press (1970).

2. K. L. Kosanke, Ph.D. Thesis, MSU, 1973.

Aqueous Chemistry On-Line with the Helium-Jet Recoil-Transport System*

K. Kosanke

After making the observation that it was possible to trap activities transported through the helium-jet recoil-transport (HeJRT) system in aqueous solution it seemed logical to pursue the possibility of performing "wet" chemistry with the trapped activities. This requires a freeing of the recoil activities from the cluster moleculars used to transport the activities through the HeJRT system.[1,2] Fortunately this seems to occur spontaneously on the introduction of the recoil cluster combination into the aqueous phase. Chemistry was further simplified by the observation that the low pressure end of the HeJRT system could be run at atmospheric pressure and above if necessary. This removes the necessity of performing the chemistry under conditions of a vacuum.

The potential usefulness of coupling aqueous chemistry on-line with the HeJRT system has been demonstrated in earlier reports.[3,4] These involved the separation of Ga activities from Cu and Zn activities using a set-up similar to the one sketched in Fig. 1. A flow of helium containing the recoil-cluster combination was combined with a flow, generated with a tubing pump, of 8N HCl containing Cu and Zn carrier in a mixing chamber. The mixing is quite turbulent due to the large volume of helium flowing from the HeJRT target assembly, about 40 STD CM^3/Sec. Also, the large volume of helium flowing rapidly transports the acid solution to the ion-exchange column, loaded with large mesh DOWEX-1 resin. The eluant solution was then drawn through the resin using a second tubing pump and run to a shielded storage container. A Ge(Li) detector had been set up to look at the Ga activities held up on the column.

The sketch of the present set-up, shown in Fig. 1, differs from that described previously[3,4] in that the second tubing pump for drawing the eluant through the ion-exchange column has been eliminated by using the helium flow to force the eluant solution through the column. The primary motivation for this change was the simplification of the apparatus. However, it also had the effect of slightly reducing the time consumed in performing the chemistry. We estimate the time to transport the activities to the chemical system to be ~1 sec and the time to conduct the chemistry to be .5 sec, such that the time elapsing between the generation and counting of the chemically separated activities is of the order of 1 second.

*Supported by the US Atomic Energy Commission and the National Science Foundation.

1. K. L. Kosanke, Ph.D. Thesis, Mich. State Univ., COO-1779-76, 1973.

2. R.D. MacFarlane and Wm. C. McHarris, Chapter II.C. "Techniques for the Study of Short Lived Nuclei," to be published in Nucl. Reactions and Spectroscopy, ed. by J. Cerny, Academic Press, New York, 1973.

3. K. L. Kosanke and Wm. C. McHarris, paper presented at the N.Y. A.P.S. Meeting Jan 29-Feb. 1, 1973.

4. K. L. Kosanke, Wm. C. McHarris, R. A. Warner and W. H. Kelly, Accepted for publication in Nucl. Instr. and Meth.

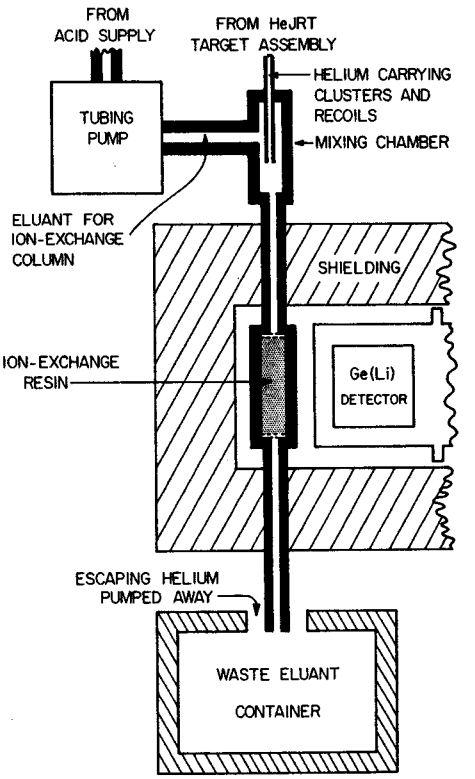

Fig. 1.--Simplified, yet faster, chemical set-up for use with the HeJRT System.

Progress on the MSU Time-of-Flight Spectrometer and Helium-Impurity Thermalizer-Transport System.*

K. L. Kosanke, M. Edmiston, and Wm. C. McHarris

The second half of the MSU time-of-flight spectrometer and helium-impurity thermalizer-transport system is presently under construction and is patterned directly after R. D. Macfarlane's MAGGIE system.[1] Figure 1 is a cross sectional assembly drawing of the system in which the target assembly of the helium-impurity thermalizer-transport (HeJRT system discussed in Section of this report) has not been included.

Activities generated in the target assembly recoil from the target and are thermalized within the helium atmosphere of the assembly. The thermal recoils then become bound to cluster molecules generated from impurities added to the helium supply within the plasma formed by the passage of the cyclotron beam. The recoil-cluster combination is then swept out of the target assembly and through a capillary tube and is transported to a low background area. This is accomplished by pumping on the remote end of the capillary. Because of the extremely large mass of the cluster molecules (up to 10^8 amu) the recoil-cluster combinations are extremely well collimated as they exit the capillary. At this point most of the helium will be removed by directing the flow at a conical skimming nozzle. Most of the recoil-cluster combinations will pass through the skimmer to a heated surface on which they collect. The heated collecting surface has the primary effect of driving off the cluster molecule material, leaving the nuclear recoil activity only weakly bound to the surface.

As the activities on the collecting surface β decay, a number of β-recoiling atoms are freed from the collecting surface. A β detector located behind the collecting surface provides a start signal used in timing the events to follow. A number of the β recoils experience electron shake-off and will be accelerated away from the collecting surface at +10-20 kV to a grid at ground potential. The accelerated recoils that pass through the grid travel down the time-of-flight path to a chevron detector. The chevron detector generates a time-of-flight stop signal, so that time of flight is proportional to m/e of the recoil and provides a "mass signature" for the β-decay event.

It should be pointed out that the system described to this point is in no way speculative but has proven itself as R. D. MacFarlane's MAGGIE system.[2] There have, however, been significant modifications to the MAGGIE system in the time since the writing of references 1 and 2. The modifications[3] were the result of the observation that significant thermalization of the β-recoils occurred before they became free of the collecting surface. As a result, the accelerating grid in front of the collecting surface was added to supply energy to the recoil. Further, the thermalization and subsequent acceleration was so effective in aligning the path of the recoil along the time-of-flight line that the necessity of having the particle guide was eliminated and it was removed.

It is our intention to mount one, and possibly a second, detector in the region of the collecting surface. In most instances these detectors will be Ge(Li) γ-detectors but may also be x-ray and/or β-detectors. In all cases, excepting those involving isomeric transitions, the γ deexcitation of the nuclei after β decay will be complete before the recoiling nucleus has traveled a significant distance from the collecting surface and the detector located there will be capable of recording the deexcitation process. Running in a coincidence mode, we will then take the mass (i.e. time) information from the time-of-flight and the γ energy information and list the coincidence events on magnetic tape. A play-back of the tape will generate a series of spectra which will be characterized according to the mass of the recoil resulting from the β decay. There is some hope that it will be possible to resolve isobars in the time-of-flight[2] spectrum using a long flight path. However, if that is not possible, an effective differentiation could also be achieved by imposing the additional requirement of an x-ray coincidence either on- or off-line with the collection of the mass information, depending on the count rate that is achieved. Also, it is possible to consider determining β energies by using a larger, full-energy β detector.

---

*Supported by the U. S. Atomic Energy Commission and the National Science Foundation.

1. H. Jungelas, R. D. Macfarlane, and Y. Fares, Radiochem. Acta. 16, 141(1971).

2. R. D. Macfarlane and Wm. C. McHarris, Chapter II. C., "Techniques for the Study of Short-lived Nuclei", to be published in Nucl. Reactions and Spectroscopy, ed. by J. Cerny, Academic Press, New York, 1973.

3. R. D. Macfarlane, private communication.

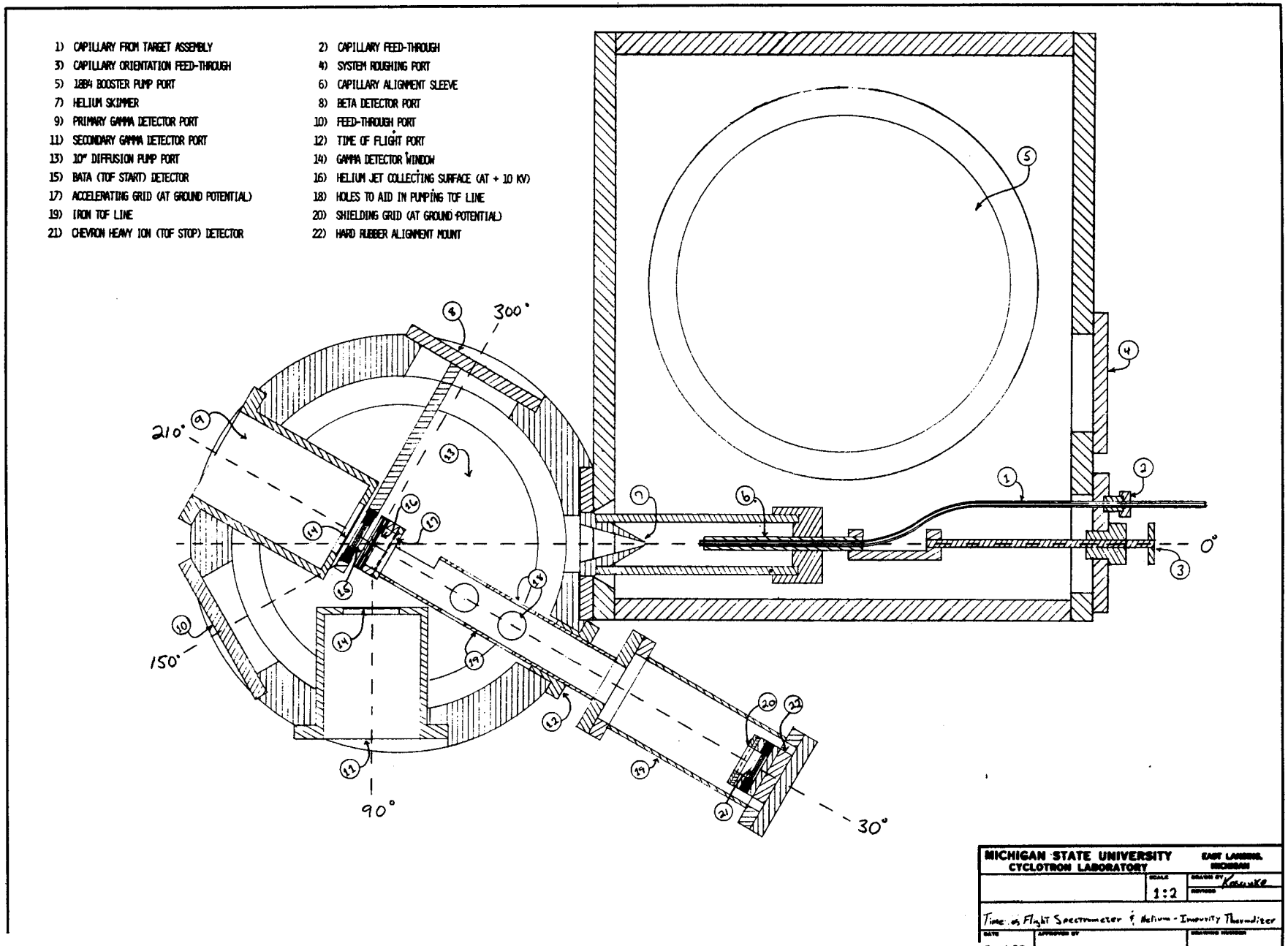

Fig. 1.--The M.S.U. time of flight spectrometer and helium-impurity thermalizer-transport system, presently under construction.

Delayed Coincidence Experiments with Accelerator Beams

R.G.H. Robertson and T. L. Khoo

Techniques for studying the decays of isomeric states with half-lives longer than a few microseconds are well known. Often, however, it is of greater interest to know what transitions populate the isomer from higher excited states. The delayed coincidence method has been applied successfully for cascades through isomers where the half-life does not exceed a few hundred nanoseconds, but severe difficulties due to random coincidences can arise as the coincidence resolving time is made larger to accommodate longer half-lives.

When the isomer can be populated in a nuclear reaction, these problems may be alleviated by pulsing the accelerator beam and observing isomeric decays only during the beam-off intervals, when the background is low. Three types of delayed coincidence experiment can be distinguished. Method 1, in which the beam runs continuously, is the conventional practice and is equivalent to radioactive source experiments. In Method 2 the accelerator beam is pulsed periodically, and delayed coincidences are observed between γ-rays occurring during the beam burst and the isomeric decays occurring in the beam-off periods. Method 3 is a new procedure in which the beam is allowed to run continuously until a γ-ray is detected, whereupon it is interrupted to see whether an isomeric decay follows the 'start' event within a few mean lives. The third method thus consists of event-initiated, aperiodic beam pulsing, and offers some important advantages over the previous techniques. We have applied it to observation of cascades through the 10 μs 53 keV isomer in ^{58}Co,[1] and the 9.5 μs 1333 keV and 9.8 μs 1559 keV isomers in ^{176}Hf.[2]

Presently we are carrying out detailed calculations of the true and chance coincidence rates to be expected for each method as functions of all relevant parameters to permit the optimization of experiments. A number of interesting general results have been found; for example, in a Method 2 experiment it is best to use the shortest possible beam burst width, and a beam-off period of approximately 0.8 mean lives. Method 3 experiments can offer a two-fold improvement in running time for a given statistical accuracy (or permit correspondingly longer-lived isomers to be investigated), and in addition are less sensitive to non-optimum settings of the beam current than Method 2 experiments. They do, however, require more complex electronic and beam-control apparatus. The diagram shows a figure-of-merit (inversely proportional to the time it takes to do an experiment to some specified accuracy) plotted for Methods 2 and 3 as a function of the beam current, which has been normalized to the optimum current for each method. The advantages of Method 3 are evident.

1. R.G.H. Robertson and R. G. Summers-Gill, Can. J. Phys. 49, 1186(1971).

2. T. L. Khoo, J. C. Waddington, R. A. O'Neil, Z. Preibisz, D. G. Burke, and M. W. Johns, Phys. Rev. Letters 28, 1717(1972), and Can. J. Phys., to be published.

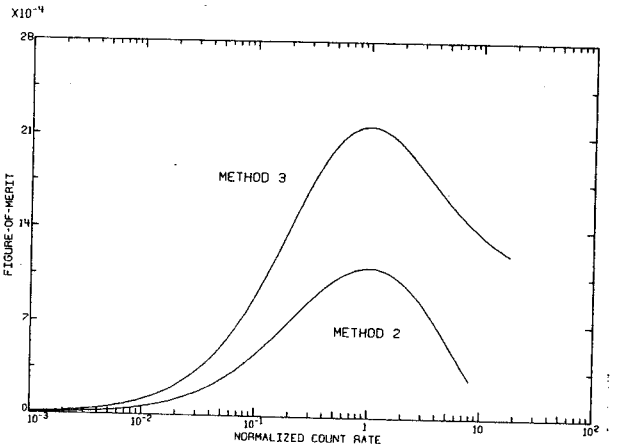

Progress Report on an Automated Plate Scanner

J. A. Nolen, R.G.H. Robertson and D. Show

An automated nulcear track plate scanner is in preliminary stages of operation at MSU. Since there are currently no broad range live focal plane detection systems capable of recording intrinsic line widths ~0.1-0.2 mm without adversely affecting the experimental resolution, the continued use of nuclear emulsions is necessary. The large number of tracks per mm^2 in these narrow peaks also requires the use of thin emulsions (25μm or 10μm) and high resolution scanning optics.

The present scanner design incorporates a monolithic array of silicon photo-diodes in the focal plane of a conventional microscope to obtain an overall resolution of 1-2μm in the detection of nuclear tracks. The scanning is done via a commercial motorized stage which moves the plate in a square wave pattern beneath the microscope objective. In the current simplified mode of operation a single photodiode views a rectangular area 0.6μm x 25μm on the plate oriented parallel to the tracks. Tracks are detected as sharp pulses at the output of a charge sensitive preamp as they move across this slit in a direction perpendicular to its long dimension. Bright field illumination is used so the pulses represent darkening of the detector slit. The signal to noise ratio and signal height reproducibility of this detection system are very good.

With this single channel detector, tracks are discriminated electronically from dirt and scratches by the following criteria: (1) the pulse must exceed a D.C. discriminator level, (2) the pulse must stay above this level for less than a preset time interval, and (3) the pulse must have a rise time less than a preset value. The events which satisfy these criteria during a scan across the plate are scaled in a single channel of a computer or multichannel analyzer. The plate is advanced a distance equal to the length of the diode array after each scan across the band of tracks. The plate advance is accompanied by a channel advance signal to the computer or analyzer. The scanning process is computer independent except for this storage of the data. In the present mode the scans are in 25μm strips which is ideal for the narrowest lines but adjacent channels can be summed when the experimental resolution does not require such narrow strips.

In the figure an automated scan of 20 MeV deuterons tracks in 25μm thick emulsion is compared with a hand scan done in 100μm strips. The track counting efficiency varies by about a factor of two in this spectrum, due mainly to two problems which are currently being worked on. Firstly, the illuminator was a 10 Watt Zr arc lamp which has position and intensity instabilities. This light source will be replaced with a different type. Secondly, the very small optical depth of field causes focussing problems which will ultimately be overcome by a continuous focussing feedback system which is currently being designed.

Even with these problems, however, the preliminary results in this simple mode of operation are promising. Results similar to those shown in the figure have also been obtained with deuterons in 10μm thick emulsion and 25 MeV proton tracks in 25μm emulsion. The scanner is already useful in peak centroid determinations for excitation energy and Q-value measurements as well as for scanning of closely spaced doublets which are very difficult to scan in such fine (25μm) steps by hand.